SOVIET PHYSICS USPEKHI VOLUME 6, NUMBER 2 SEPTEMBER-OCTOBER 1963

TWILIGHT PHENOMENA, THEIR NATURE, AND USE FOR ATMOSPHERIC RESEARCH

G. V. ROZENBERG

CONTENTS

1. INTRODUCTION

THE concept of twilight includes the entire complex of optical phenomena which occur in the atmosphere of a planet when day turns into night. This process is accompanied by striking changes in the illumination—by approximately a factor of one billion under terrestrial conditions—and evokes a complete qualitative realignment of the structure of the energy balance both on the surface of the planet and in the atmosphere surrounding it. The latter, owing to its ability to scatter light, softens this transition so that it occurs not instantaneously but extends over a more or less prolonged period, filled with a whole set of rapidly occurring and amazingly varied phenomena.

Viewed from the outside, through the eyes of a space traveler, the earth appears to be girdled by a broad multicolored twilight penumbra belt continuously covering from 20 to 25 per cent of the earth's surface, depending on the state of the atmosphere. On one side of this belt, on 42—45 per cent of the earth's area, we have daylight, and on the other side, on 32—35 per cent of the earth's surface, nighttime prevails. This means that, on the average, one-quarter of the time humanity lives and works under twilight conditions. In the tropics, where the sun's descent to the horizon is steeper, this time is shorter, about 10—15 per cent, whereas at high latitudes it rises to 30—40 per cent of the duration of the day (white nights), while in polar regions the continuous twilight lasts for weeks in the spring and fall.

Naturally, with the direct effect of twilight on our living conditions being on such a scale, interest in twilight has never abated. This has found its expression not only in religious theories and in the art of all nations, but also in an inexhaustible stream of scientific research. However, real progress in this field of knowledge has always lagged appreciably the study of day or night. One of the reasons for this lag can be readily seen in the complexity and variety of the twilight phenomena and in their sharply pronounced dynamicity, which makes it quite difficult both to set up the experiments and to analyze scientifically their results. Another reason is that twilight is produced essentially in the upper layers of the atmosphere, which have remained unknown and inaccessible to research until most recently.

It has been known for a long time that the course and the character of the twilight phenomena is determined by the optical properties of the atmosphere. This dates back apparently to one of the boldest minds of the eleventh century, the pioneer in experimental optics El Hassan or, in the poor Latin of the middle ages, Alhazen [1]. Later on, we encounter among the scientists engaged in twilight such names as Kepler, the brothers Bernoulli, Maupertuis, d'Alambert, Clausius, and many others. However, the modern explanation of twilight phenomena, as being due to a combination of scattering and attenuation of the sun's light in the earth's atmosphere, was advanced only in 1863 by Bezold [2]. Bezold's paper was published merely eleven years after Brücke discovered the scattering of light, three years after Govey discovered polarization of light by scattering and made it possible to attribute the glow of the daytime sky precisely to the scattering of the sun's light in the earth's

atmosphere, and six years before the remarkable researches by Tyndall, who made this explanation universal (see, for example, [3]). This is convincing evidence of the persistent attention which twilight phenomena have attracted during that time. But the complexity of the phenomena and the lack of information concerning the optical structure of the atmosphere did not permit going beyond most general opinions. Even the development of the theory of molecular scattering of light by Rayleigh and the development of the theory for the scattering of light by spherical particles by Lamb and Mie, events which revolutionized the atmospheric optics of those days, hardly influenced the degree of understanding of the nature of twilight phenomena. This has given rise to a purely empirical "observational" approach to the study of twilight, an approach that found its expression in numerous attempts to relate various characteristics of twilight (the purple light, the position of the neutral points, etc.) with meteorological conditions and in persistent but unsuccessful searches for various twilight "omens" for predicting weather.

Only in the Twenties and Thirties of our century was this slow and essentially purposeless accumulation of observational data replaced by systematic experimental and theoretical studies of the general laws that govern the phenomenon itself. This serious advance toward the disclosure of the actual connection between twilight phenomena and the structure of the atmosphere was brought into being by the beginning of the active mastery of the atmosphere, and in particular, its higher layers, as fields for practical human activity. During those years the conditions existing above 20—30 km, that is, beyond the limits reached directly by flying craft, could be judged exclusively on the basis of data obtained by indirect research methods. It was they that led to a radical review of all our notions concerning the upper layers of the atmosphere. In particular, we are indebted to them for such important discoveries as the existence of the ionosphere, ozone, and sodium layers, the temperature maximum at 50—60 km and minimum near 80 km, and also the discarding of the previously accepted view that the upper atmosphere is a static formation. The development of rocketry, which has made all altitudes accessible not only to measuring instruments but even to humans, has for some time relegated the indirect methods to the background. However, one of the essential results obtained with the aid of rockets and satellites was a confirmation of those general concepts deduced from indirect research on the upper layers of the atmosphere. Many physical parameters of the upper atmosphere are still much easier to investigate by indirect methods than by direct measurements from rockets and satellites. The indirect methods have therefore not lost their value at all, particularly if their relatively low cost is taken into consideration.

Among those indirect methods of investigation of the upper layers of the atmosphere, which have played in their time an appreciable role and which are still important, is the method of twilight sounding, based on a detailed analysis of the course of the twilight. The general idea of the method was expressed already by Alhazen[1], who estimated with its aid the height of the earth's atmosphere as being 52,000 paces—not so far from the truth, for in accordance with modern data less than one thousandths of the air mass is located above this level. In 1923 V. G. Fesenkov [4] revived this idea and recast it in modern form, i.e., formulated it as the inverse problem of the general theory of twilight.

During the last forty years the efforts of many scientists have been devoted to a critical review of various aspects of this problem. Numerous obstacles which have many times shaken confidence in the reliability of the method were disclosed and eliminated, and direct evidence has been obtained that if careful attention is paid to the details of the phenomenon, the data extracted from observations of the twilight sky do correspond to reality. At the same time, extensive material has been accumulated by systematized and purposeful observation, permitting reliable disclosure and quantitative study of the main features of the behavior of twilight.

Thus, by now the purely speculative constructions that have prevailed even recently have been replaced by a theory developed in detail and verified by experiment, providing both a quantitative description of the course of twilight phenomena and a reliable derivation of valuable data concerning the structure and the state of the higher layers of the atmosphere, obtained by observation of the twilight sky. All these results, however, are scattered in many periodicals. It is therefore timely to summarize them and consider them from a common point of view. Inasmuch as the size of a journal article does not permit an exhaustive review of all the papers devoted to twilight phenomena, particularly the work of the earlier period, the author has been forced to confine himself only to an outline of the modern status of the problem. Appreciable space is devoted here to ideas developed by the author for many years in the Atmospheric Optics Laboratory of the Atmospheric Physics Institute of the USSR Academy of Sciences. The development of these ideas was greatly contributed to by familiarity with the material of many years' twilight observations performed by T. G. Megrelishvili at the Abastumani Astrophysical Observatory of the Georgian Academy of Sciences. These notions were discussed many times by the author orally and have been partly expressed in some publications, but this is their first presentation in unified form, and as a consequence more attention is paid to them than to work by others, although the author has tried to review the literature as fully as possible and to present the

readers with a convenient key to it. As usual, an indication that the material is original is the lack of a literature reference in the text.

2. GENERAL PATTERN OF TWILIGHT PHENOMENA

The main factor determining the course of the twilight phenomena is the scattering of sunlight by the earth's atmosphere and the associated attenuation of the sun's direct rays. When the sun is inclined to the horizon, the path covered by its rays through the atmosphere increases and their brightness decreases, and this leads to a reduction in the illumination of the earth's surface both by the sun's direct light and by the light scattered by the atmosphere. Under daytime conditions this dependence of the illumination on the height of the sun is small. But when the sun drops to 5 or 10 degrees above the horizon, the decrease in the illumination becomes greatly accelerated. The onset of accelerated decrease in illumination is indeed the start of the twilight.

At the same time, the relative role of the rapidly attenuating direct rays of the sun in the illumination of the earth's surface begins to decrease. More and more illumination is now produced by the atmosphere itself, permeated by the rays from the setting sun. From the instant of sunset on, this atmosphere is the only source of light. But gradually the earth's shadow rises higher, enclosing an ever increasing part of the atmosphere. The lower layers of the atmosphere, submerged in the earth's shadow, no longer contribute to the brightness of the sky, and the scattered light comes from the higher and higher layers, which are still illuminated by the sun's direct rays. Since the density of the air, and with it the scattering coefficient, rapidly decreases with altitude, the sunlight becomes less and less scattered, the brightness of the sky decreases, and at the same time the illumination of the earth's surface decreases. When the sun drops approximately 14 or 15° below the horizon, the intrinsic glow of the upper layers of the atmosphere and the light from the stars begins to come into play, and the illumination gradually approaches that of nighttime. The transition to nighttime concludes usually when the sun's depth is $\xi = 17—19°$ under the horizon, but sometimes, when the atmosphere's turbidity is high, it extends to 22 or 23°. As a rule, a weak minimum of illumination and sky brightness is observed when the sun drops 20—23° below the horizon [5-7]. Thus, the boundaries of the twilight period are highly diffuse and shift in accordance with atmospheric conditions. The duration of the twilight is determined by the speed with which the sun dips below the horizon, that is, the geographic latitude and the time of the year. The corresponding tables can be obtained, for example, in [8-9].

During the twilight the illumination of the earth's surface changes from approximately $10^4—10^5$ lux in the day to 10^{-4} lux at night. This makes measurements extremely difficult, and relatively few have been made up to now [5,8,10]. In addition, there are a few investigations of twilight illumination of a vertical area of varying orientation [11-16], and also of the illumination of a horizontal area from a limited but rather extensive region of the sky [17-19].

Figure 1 shows the averaged dependence of the illumination E of a horizontal area on the zenith distance of the sun ξ as given by V. E. Sharonov [8]. The ξ-dependence of the illuminations of differently oriented vertical areas are indicated in Fig. 2 [16].

The data of Figs. 1 and 2 pertain to a cloudless summer sky. The presence of snow increases slightly (by 1.5—2 times) the illumination at large depressions of the sun below the horizon, and is hardly manifest in the bright part of the twilight [8]. A much more noticeable influence on the illumination is exerted by the character of the cloudiness [8-16]. As a rule, the presence of clouds causes a decrease in illumination, sometimes (in the case of overcast weather) by one order of magnitude, but hardly affects its dependence on the sun's depression. Detailed tables of twilight illumination are contained in [8-16].

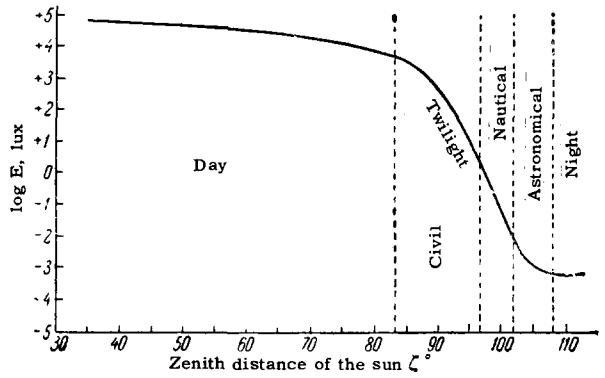

FIG. 1. Averaged dependence of the illumination of a horizontal area on the zenith distance of the sun.

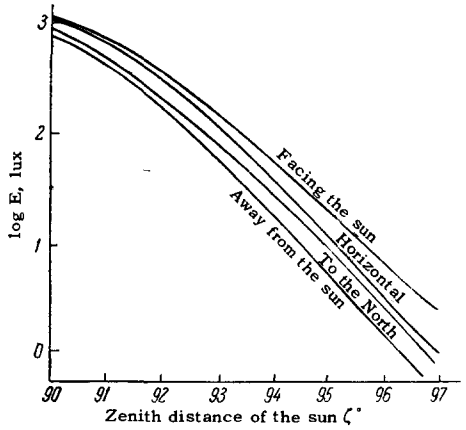

FIG. 2. Comparison of the ζ-dependence of twilight illuminations of differently oriented areas.

Starting from the practical need for estimating the conditions of visibility during different times of the day, a historic tradition has developed of subdividing twilights into three stages, depending on the value of the twilight illumination (see Fig. 1). The brightest part of the twilight, when natural illumination still permits normal activity, including reading, in open places is called "civil twilight." There is no agreed-upon definition of its boundaries, which are related with the sun's depression from 6 to 8° under the horizon. Recently, however, most writers are inclined to use the lower figure. This is followed by "marine" or "nautical" twilight, during which darkness already causes the loss of many details, but silhouettes of large objects, say shorelines, are seen quite clearly. Its limit is assumed to be a depression angle between 6 and 12° under the horizon, and by the end of the nautical twilight it is possible to distinguish clearly only the horizon line. Finally, nautical twilight is followed by "astronomical" twilight, which continues until the sun is depressed 18° below the horizon, that is, until night sets in. During that time the illumination conditions hardly differ from those of nighttime, but the sky is still noticeably illuminated, hindering astronomical measurements. The illumination levels corresponding to the boundaries between the different twilight stages amount in the mean to 2.5 lux at a depression angle $\xi = 6°$ under the horizon, 6×10^{-3} lux at $\xi = 12°$, and 6×10^{-4} lux at $\xi = 18°$[10].

Lunar twilight, which occurs when the moon's disc approaches the horizon, is similar in all respects to solar twilight, but is much paler. The brightness of the lunar illumination fluctuates, depending on the phase of the moon, between 10^{-9} (for a new moon) and 2×10^{-6} (during full moon) of the brightness of illumination produced by the sun in the same position in the sky. Thus, the level of illumination of a high full moon corresponds approximately to the mid-point of solar nautical twilight, and the end of lunar astronomical twilight (again in the case of a full moon) practically coincides with the instant that the moon sets [8]. However, the presence of the moon should affect the brightness of the sky until it submerges under the horizon (in the case of a full moon) to approximately 5—7°. [7]

Let us turn now to the sky and its variations during the course of twilight.

On approaching the horizon, the sun not only loses its brightness, but begins to change color gradually, with the shortwave part of its spectrum becoming suppressed to an increasing degree. The gist of this phenomenon, qualitatively explained as long ago as 1840 by Forbes, is that the spectral dependence of atmospheric transparency, which generally speaking increases with increasing wavelength, becomes particularly noticeable when the path of the sun's rays through the atmosphere lengthens. At the same time, the sky also begins to change color. In the sun's vicinity it assumes yellowish and orange tones, and on the part of the horizon opposite the sun a pale strip appears, with a weakly pronounced range of colors.

By the instant of sunset, when the sun already has assumed a dark red color, a bright afterglow belt appears, the color of which changes from orange-yellow at the bottom to greenish-blue at the top. Located above it is a round bright almost uncolored glow. During the same time, on the opposite horizon, a bluish-gray dim segment of the earth's shadow, surrounded by a pink belt (the "belt of Venus") begins to rise slowly.

As the sun drops deeper under the horizon, the coloring of the sky on the sun's side becomes saturated; at the horizon itself the sky turns dense red, while at the top of the glow over the sun, at some 20—25° above the horizon, a rapidly spreading pink spot appears, the so-called "purple light," which reaches maximum development when the sun's depth under the horizon is about 4—5°. The clouds and mountain peaks are flooded with scarlet and purple tones, and if the clouds or the high mountains are behind the solar horizon, then their shadows stretch over the brightly colored sky, from horizon to horizon, in the form of pronounced radial strips ("Buddha's rays"). At that time the earth's shadow rapidly moves onto the sky; its outlines spread out, and its pink border becomes washed out and pales.

At the end of the civil twilight, the purple light dims, the clouds become darker, their silhouettes appear sharply against the background of the fading sky, and only at the horizon, in the place where the sun has set, is a bright colored segment of the afterglow left. It, too, gradually decreases, pales, and by the start of the astronomical twilight it turns into a greenish-whitish narrow strip. At the end of the astronomical twilight this strip also disappears and night sets in. However, according to some data [20], a weak glow of the atmosphere due to scattering (apparently multiple) of the sun's light, remains even during the night, and is called "nighttime twilight." It is concentrated in a narrow segment at the horizon and moves together with the sun in azimuth during the entire night. Its height above the sun reaches 40—55°, and in the case of larger depressions of the sun under the horizon it disappears. Inasmuch as this glow is very weak and the zodiacal light and particularly the glow from the earth's atmosphere proper are superimposed on it, the nighttime twilight has not yet been investigated, and even its very existence has not been reliably confirmed.

The picture described here (many details of which have been left out, see for example, [21-25]) must be regarded only as typical of clear weather. Actually, the character of the course of the twilight is subject to great variations. With increased turbidity of the air the colors of the afterglow are usually pale, particularly near the horizon, where only a weak brown

color appears instead of red and orange tones [23]. Frequently, as was already noted by N. I. Kucherov [23], simultaneous twilight phenomena develop differently in different parts of the sky. Each twilight has its own non-repeating individuality, and this can be regarded as one of the most characteristic features of twilight.

Compared with the relatively static day, twilight develops before us as an impetuous process, a study of which in time and in space, by photometric, spectral, and polarization methods, uncovers a way toward a regular investigation of the optical structure of the atmosphere and its variations, at different levels separately. This is precisely the main difference between twilight research on the atmosphere and studies made during the day, when the relatively small range of variation sharply limits the resolving power of integral optical methods and makes them of little use from the point of view of recognizing the optical structure of the atmosphere itself (see [3,26]).

3. SPECTROPHOTOMETRY OF THE TWILIGHT SKY

Direct measurements of the brightness of the cloudless twilight sky are quite numerous [3,4,6,7,11, 16-20,26-82]. The total number of twilights for which the changes in the brightness of the sky have been measured as functions of the zenith distance ζ of the sun and of the zenith distance z of the sighted point and its azimuth A relative to the vertical of the sun reaches to several thousand. It must be borne in mind that the measurements themselves entail great difficulties: the tremendous range of brightness variation; the extreme weakness of glow when the depression of the sun under the horizon is large, calling for the use of light receivers with very high sensitivity; the speed of the processes, which does not permit the use of accumulating receiving systems (such as photographic plates) with prolonged exposures; and finally the need for working under field conditions and while waiting, sometimes for quite a long time, for favorable meterological conditions. Therefore most measurements performed up to the middle Forties of our century have been made visually, without the use of optical filters. Many investigations, however [38,40,41, 44,47,48], and particularly the extensive research by T. G. Megrelishvili [53,57] have shown that the character of variation of the sky's brightness as a function of ζ differs greatly for different wavelengths, a fact that manifests itself, in particular, in that play of colors which is so characteristic of the afterglow.

At the same time, T. G. Megrelishvili called attention to the fact that similar variations of the spectral composition can cause serious errors in measurements made in large wavelength intervals [57]. This has induced most of the later researchers [16,26, 59,65-73,78-82] to change to measurements with filters, aided by the development of highly sensitive light receivers—photocells and photomultipliers, which have practically completely replaced visual photometry. Thus, extensive material has been accumulated in recent years, not only on the brightness but also on the spectral composition of the light of the twilight sky. The overwhelming majority of these measurements pertain to the zenith, and only a few of them pertain to other regions of the sky—the vicinity of the North Star [6,29], some points of the solar vertical [37,63,65,69,78,81,82], the afterglow segment, and the "purple light" [20,42,43,45,61,77]. In addition, many measurements have been made to determine the brightness pattern of the twilight sky [7,16,35,60,61,75].

Most frequently the photometry of the twilight sky was aimed only at ascertaining the variation of its brightness with ζ. The researchers therefore confined themselves to relative measurements. Absolute determinations were made only by a few workers [4,7,16,27,28-30,32,33,45,59,75,81,82], and some of these were unsufficiently reliable.

Notice must first be taken of the very good agreement between individual measurements. The brightness of the twilight sky measured by different workers, at equal values of ζ and in the same sighting direction (but not too close to the horizon), which varied by a factor of 10^7—10^8 during the course of the twilight, differed in the short-wave region of the visible spectrum (and also in measurements without filters) by not more than 3—5 times. Approximately similar differences were obtained also in measurements made by one and the same worker on different days (see, for example, [74]). Incidentally, these differences increased sharply in the long-wave region of the spectrum. All the observers unanimously note also that away from the horizon the brightness of the twilight sky is practically independent of the weather at the point of observation. In particular, the brightness of the sky, measured through gaps in clouds, turns out to be the same as during perfectly clear weather.

W. Brunner [7] averaged the measurement data obtained prior to 1935 (without filters) and plotted an average curve of sky brightness at the zenith from $\zeta = 30°$ to $\zeta = 140°$, as shown in Fig. 3. The latest measurements fit this curve well (see, for example, [16]). Figure 4 shows analogous curves, obtained by E. V. Ashburn [59], but with optical filters. Interference filters at effective wavelengths $\lambda_{eff} = 0.44$, 0.52, and 0.59μ had a transmission band with half-width 105 Å; the effective half-width of the transmission band at $\lambda_{eff} = 0.75\mu$ was 0.23μ.

Even Brunner [7] called attention to the characteristic bend in the curve near the limit of the astronomical twilight ($\zeta \cong 102$—$104°$) and advanced the hypothesis that it may be due to the superposition of a relatively constant brightness from the intrinsic glow of the atmosphere's higher layers on the variable brightness of the scattered light from the sun.

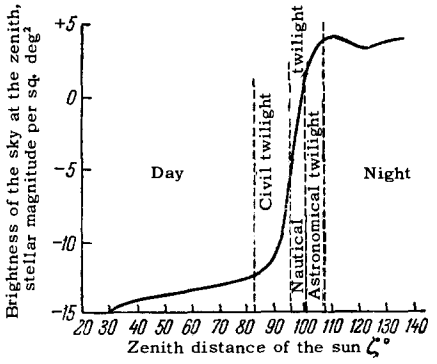

FIG. 3. Brightness of the sky at the zenith as a function of the zenith distance of the sun.

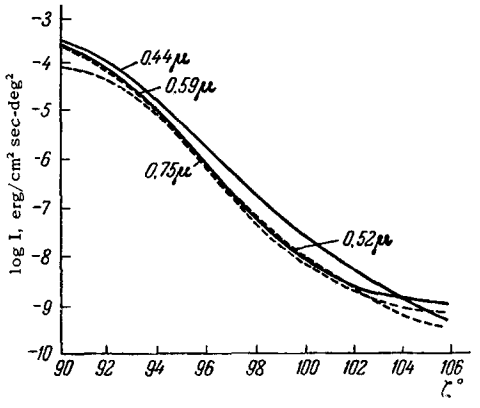

FIG. 4. Brightness of the sky at the zenith in different parts of the spectrum as a function of the zenith distance of the sun.

Indeed, subtraction of the corresponding brightness of the night sky from the brightness of the twilight sky practically eliminates this bend [7,50]. Moreover, we see from Fig. 4 that with increasing wavelength, that is, on going over to those regions of the spectrum where the brightness of the scattered light is smaller and the brightness of the sky light is larger, this bend shifts clearly toward smaller values of ζ (see [44,67]).

This gives grounds for assuming that the variations in the course of this part of the curve are caused primarily by variations in the atmosphere's own glow [7]. The latter, however, does not exclude variations in the intensity of the sun's light scattered by the atmosphere, including multiply scattered light.

Further, Fig. 3 discloses clearly a minimum near $\zeta = 123-125°$, which coincides approximately with the minimum of illumination on the earth's surface, as noted by P. P. Feofilov [5]. This minimum in the near-twilight course of the brightness of the night sky was observed also by N. B. Divari [6]. They all give grounds for assuming that it is due to features of the diurnal variation of the night sky itself.

Let us turn now to the distribution of the brightness over the sky. During the day, with increasing ζ, the minimum brightness of the sky gradually approaches the zenith, and simultaneously moves away from the sun. This continues also during the bright part of the civil twilight [83]. The minimum reaches the zenith only when total darkness sets in. During the entire twilight it remains somewhat shifted relative to the zenith along the sun's counter-vertical. This is illustrated in Fig. 5, which shows the motion along the vertical and counter-vertical of the sun of the points of constant brightness with varying sun's zenith distance (from data by K. Graff [35]). In Fig. 6, borrowed from [16], are shown the relative changes in the brightness of the sky along the sun's vertical and counter-vertical at different zenith distances of the sun. Es-

FIG. 5. Displacement of points with a given sky brightness along the vertical and counter-vertical of the sun with variation of the sun's zenith distance.

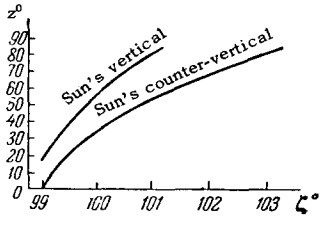

FIG. 6. Relative variations of the sky brightness along the sun's vertical and counter-vertical at different zenith distances of the sun. a) Without filter, λ_{eff} = 4600 Å; b) λ_{eff} = 4350 Å; c) λ_{eff} = 5275 Å; d) λ_{eff} = 6350 Å.

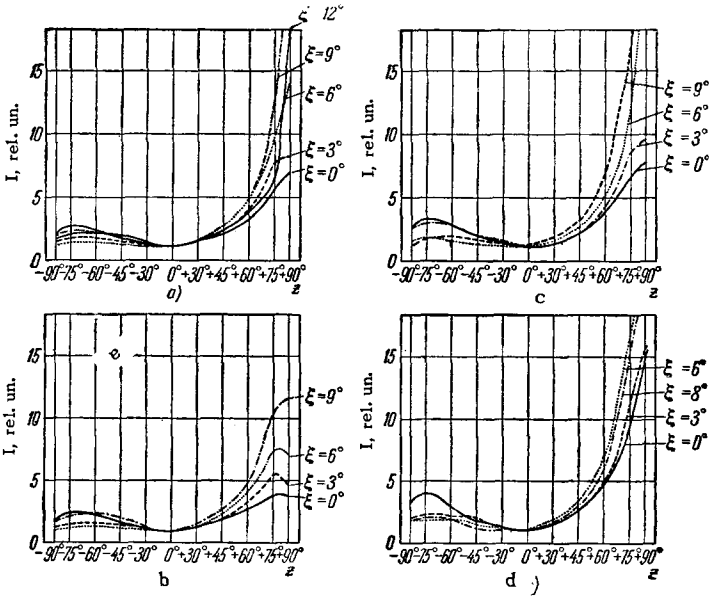

sentially, the aggregate of the curves shown in Fig. 6 represents a quantitative illustration of the twilight pattern described qualitatively in Sec. 2.

What is most striking is that during the twilight the brightness of the sky is concentrated in relatively small afterglow segments near the sun's horizon, and the dimensions of this segment decrease rapidly with increasing ζ [45]. For comparison we give a map of isophots of the solar side of the twilight sky, calculated by N. M. Shtaude [84] with allowance for only single molecular scattering of the light (Fig. 7). Returning to Fig. 6, we also call attention to the fact that the dimensions in the brightness of the afterglow segment depend appreciably on the wavelength, and this dependence varies with ζ. Further, the maxima of the brightness are observed not at the horizon itself, as was suggested by Hulbert [45], but considerably higher. Figure 8 shows the dependence of the brightness of the sky in the afterglow segment, averaged over a series of measurements, for ζ = 6—11°, on the zenith distance z of the sighting point, as given by O. B. Vasil'ev [85], and also the dependence of the position of maximum brightness and of the sky brightness at the maximum on the zenith distance of the sun. The measurements were by photography with a broadband filter. However, as is clear from Fig. 6, the position and magnitude of the maximum should depend on the wavelength. This is illustrated in Fig. 9, which was graciously furnished at our request by A. Kh. Darchiya, on the basis of data of her spectrographic study of the afterglow segment [77]. Figure 9 pertains to a zenith distance of the sun ζ = 90°. However, an analogous pattern occurs also for other zenith distances up to ζ = 94°. It is noted here that the horizon is frequently overcast by a continuous haze, which hides the lower part of the afterglow segment. In this case the position of the brightness maximum no longer depends on the wavelength and is located approximately near z = 83—85°, which does not change with changing ζ. In other words, the distribution of the brightness near the horizon itself depends in this case only on the altitude structure of the haze. The appreciable spread in the points of

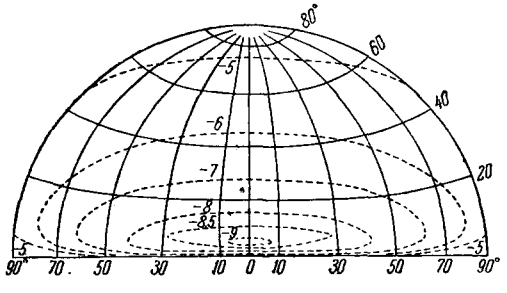

FIG. 7. Isophots of solar part of the twilight sky at ζ = 96°, calculated with allowance for single molecular scattering only (the numbers on the isophots denote the brightness in stellar magnitude).

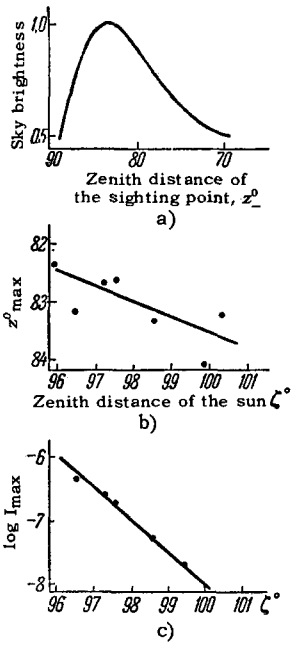

FIG. 8. Distribution of the brightness in the afterglow segment along the solar vertical (a) and the dependence of the zenith distance z_{max} of the brightness maximum (b) and the value of the maximum brightness I_{max} (c) on the zenith distance of the sun.

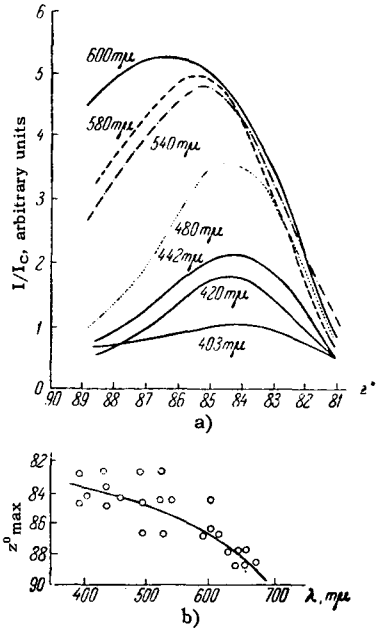

FIG. 9. Distribution of brightness in the afterglow segment along the solar vertical for different portions of the spectrum (a) and dependence of the zenith distance z_{max} of the maximum brightness on the wavelength (b) for ζ = 90°.

Fig. 9b, as well as of the data obtained by other authors on the region of the sky near the horizon, is naturally explained by the variable turbidity of the lower layers of the atmosphere.

Measurements of the brightness of the twilight sky along different almucantars [60,61,75] show that the changes in the brightness in azimuth occur monotonically and much more slowly than in the vertical. Investigation of the changes in the sky brightness at large ξ (at the nighttime boundary) at different azimuths near the horizon was carried out by N. B. Divari [61].

One of the essential results in the study of the twilight sky was the conclusion that the phenomenon

has the same main outlines in all parts of the sky; this is evidence that the conditions of its formation are identical. There is, however, a noticeable regular and quite appreciable phase shift: twilight in the sun's vertical is delayed compared with the sun's counter-vertical. Therefore, when we talk of the twilight sky, we cannot classify twilights by stages only on the basis of the change in the sun's zenith distance, that is, simultaneously for the entire sky, as in Sec. 2 (see Fig. 1). A classification based on the illumination of the earth's surface more or less corresponds to conditions prevailing for the zenith (see Fig. 3), but is not suitable for other regions of the sky. It is therefore necessary to have a classification of twilight which is individual for each point of the sky (see Secs. 8 and 10).

Further, although in principle the phenomenon has a similar course for all points of the sky, many details of this course turn out to depend on the position of the sighting point. This is the result of the variability of the relative role of different factors in the dependence on the geometrical circumstances. Therefore it is precisely these differences in the details that become most essential when twilight observations are used to study the optical structure of the atmosphere.

Differences in the character of the dependences of the sky brightness on the zenith distance of the sun in different parts of the solar meridian appear clearly already in Fig. 6. They are shown most illustratively in Figs. 10a and b, graciously furnished the author by T. G. Megrelishvili. Figure 10a shows the dependence of the sky brightness I at $\lambda_{eff} = 0.52\mu$ on the zenith distance of the sun, obtained by Megrelishvili for one evening in simultaneous measurements at three points of the solar meridian: in the zenith ($z = 0$), at $z = +70°$ (in the sun's vertical), and at $z = -70°$ (in the counter-vertical). In Fig. 10b the same sky brightness is shown as a function of the height H of the earth's geometrical shadow in the sighting direction. What is striking is first of all the increase in the slope of the I(H) curves with increasing distance from the sighting point to the sun, and the sharp excess in the sky brightness in the sun's counter-vertical over its brightness in the zenith and in the solar vertical for one and the same height of the earth's geometrical shadow, when the latter rises more than approximately 50—60 km above the earth. As was first noted by V. G. Fesenkov, this is the obvious result of superposition of effects due to the secondary scattering of the sun's light, and points a way toward their experimental study. In fact, the brightness of the secondarily scattered light for a given zenith distance of the sun depends relatively little on the sighting direction. At the same time, the height of the earth's shadow is much larger in the counter-vertical of the sun than in the vertical, and

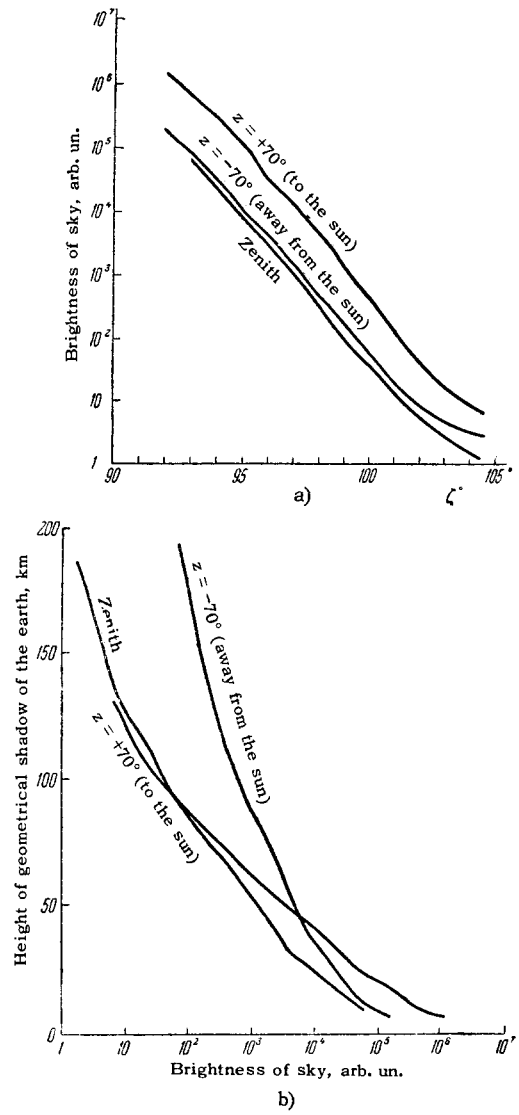

FIG. 10. Simultaneous plots of the brightness of the sky in three sighting directions against the zenith distance of the sun (a) and against the height of the geometrical shadow of the earth in the sighting direction (b).

accordingly the brightness of the singly-scattered light is much smaller.

Further, it is clearly seen in Fig. 10 that along with differences in the regular character there are also noticeable individual variations in the curves, which incidentally change strongly from day to day. These disturbances in the smoothness of the curves, which are quite characteristic of twilight, reflect, as we shall show later on, singularities in the optical structure of the atmosphere (including its upper layers), and their variability is patently due to the variability of the atmospheric conditions, and partially its horizontal inhomogeneity. In this connection we recall that all workers have noted strong variations in the intensity of the "purple light" with a pronounced maximum in its brightness during the fall,

and sharp intensification following powerful volcanic eruptions.

Let us turn now to a more detailed examination of the color variations of the twilight sky. The first and most pronounced symptom of the onset of twilight is the reddening of the sky, which always takes place, but is pronounced to different degrees in different regions of the sky, depending on the meteorological conditions. P. Grunner [20] and C. Dorno [27] carried out photometry of the "purple sky" in different parts of the sky and have found that when the sun dips to approximately $\xi = 4—4.5°$, the progressing reddening of the sky is replaced by a bluish tint. Later on F. Link [38] called attention to the fact that the sky turns blue also in the zenith with increasing depression of the sun below the horizon. Assuming that this change to blue is caused by an increase in the secondary scattering, he attempted to estimate, on the basis of his experiments with optical filters, the relative intensity of the secondarily scattered light. This attempt, however, was based on primitive considerations, which were not applicable to the real atmosphere. This was shown, in particular, by I. A. Khvostnikov, E. N. Magid, and A. A. Shubin [47], who confirmed the fact that the twilight sky turns blue and have established that this effect does not reduce to the appearance of a factor of the form λ^{-4}, as essentially assumed by F. Link. We shall show later on (Secs. 9 and 10) that the actual cause of the sky turning blue is entirely different.

Systematic investigations of the color of the twilight sky were started in 1942 by T. G. Megrelishvili [53,57] and are continued by her to this very day [78]. These investigations have disclosed that when the sun dips below under the horizon to $\xi = 9—11°$, the turning blue at the zenith is again replaced by reddening. Figure 11 shows the dependence of the color exponent of the twilight sky at the zenith on the average distance of the sun, averaged over the seasons and obtained by numerous measurements in 1945 [57]. The ordinates represent here the color exponent CE, defined as

$$CE_{\lambda_2}^{\lambda_1} = -2.5 \ln \frac{I(\lambda_1)}{I(\lambda_2)} = -1.08 \ln \frac{I(\lambda_1)}{I(\lambda_2)}, \qquad (1)$$

where $\lambda_1 = 379$ mμ and $\lambda_2 = 527$ mμ. The measurements were made with light filters, but, since the spectral sensitivity of the instrument on the whole was not investigated, the results are expressed in relative units. This manifests itself in an uncertainty that is constant for all the measurements in the multiplier of the color exponent. Later on analogous results were obtained by other investigators [63,70,73,81,82,86], and in particular for a large set of various wavelengths, reaching to 1μ.

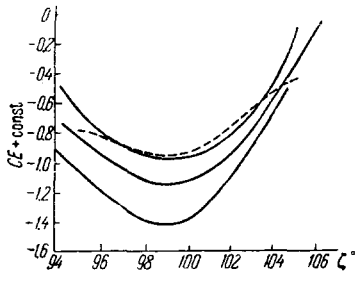

FIG. 11. Variation of the color of the sky at the zenith as a function of ζ (for large ξ) – averaged curves.

Figure 12 shows the variation with ζ of the color exponents for several pairs of wavelengths in the sighting direction A = 0, z = 70°, as measured by F. Volz and R. Goody [81] during two twilights. Figures 11 and 12 indicate first of all that the reddening of the sky at the zenith at $\zeta \gtrsim 90—100°$ is a regular phenomenon, and that by the end of the twilight the sky is as a rule much redder than at the instant of its maximum reddening at the sun's depression angles near $\xi = 4—5°$ (at z = 70°, A = 0 the reddening begins later, namely at $\zeta \gtrsim 102—103°$; see Fig. 12). This phenomenon, however, is subject to very strong variations, both seasonal (Fig. 11), which offer direct evidence of the influence of meteorological conditions, and from day to day. For individual days, the dependence of the color exponent on ζ usually has a more complicated character than on the averaged curves. Examples can be seen in Figs. 12 and 13, which were constructed [86] on the basis of measurements performed in 1958 in Crimea [79], with filters having $\lambda_{eff} = 448$ and 528 mμ [26]. Comparison of Fig. 11 with Fig. 4 immediately discloses the gist of the reddening of the sky at $\zeta \gtrsim 100°$ at the zenith and at $\zeta \gtrsim 103°$ at the solar horizon. At approximately the same angles of the sun's depression below the horizon (which are different for different wave-lengths), the decrease in the sky brightness slows down in the long-wave portion of the spectrum, whereas in the short-wave portion the brightness continued to decrease persistently as before. In the next chapters we shall discuss in detail the possible physical reasons of this phenomenon. Here we merely note that it concerns the spectrum part beyond the Chapuis ozone absorption bands, namely the 0.7—1μ region.

The fact that the absorption of light by atmospheric ozone influences the color of the sky has been known for a long time. It was first observed by Chapuis [87], who even proposed that the presence of ozone is

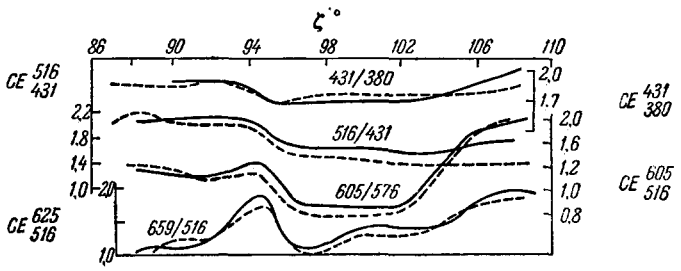

FIG. 12. Variations of the color of the sky in the sun's vertical at a zenith distance in the sighting directions z = 70°, as a function of ζ – individual curves for two days (solid and dashed lines).

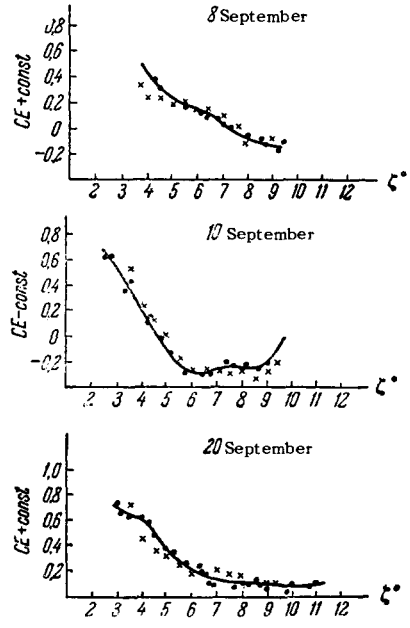

FIG. 13. Variation of the color of the sky at the zenith as a function of ζ – curves for individual days. ● – observations, × – calculation.

wholly responsible for the blueness of the daylight sky. As applied to twilight, the role of the ozone was clearly pointed out as long ago as 1935 by J. Gauzit [88], who described in detail the general form of the twilight-sky spectrum. The question was later on discussed by E. Hulburt [89]. Colorometric investigations by M. Gadsden [71] have confirmed qualitatively the appreciable influence of absorption of light by atmospheric ozone on the color of the twilight sky. Finally, N. B. Divari [73], on the basis of thorough measurements with light filters, disclosed quantitatively the Chapuis bands in the twilight-sky light.

Figure 14 shows the spectral variations of the twilight-sky brightness at the point A = 0, z = 70° for ζ = 90° as calculated by F. Volz and R. Goody [82] for two models of the atmosphere—purely molecular (1) and one containing aerosol (2), as well as the result of their measurements for two days (curves 3 and 4). Analogous curves can be found in the work of

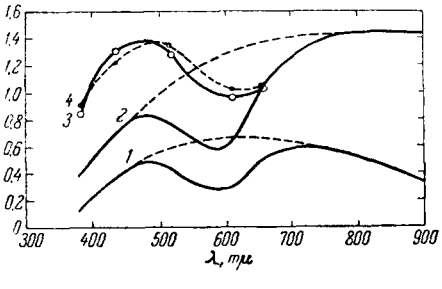

FIG. 14. Theoretical (1 and 2) and experimental (3 and 4) data on the spectral variation of the relative sky brightness at z = 70° and A = 0°. Dashed curves – without allowance for the absorption of light in the ozone layer.

N. B. Divari [73], and also derived from the observations of F. Link and A. Ljunghall [16] (see also [67]). Goody and Volz have shown that by measuring the brightness defect of the twilight sky in the region of the Chapuis bands it is possible to determine the total content of the ozone in the atmosphere, in spite of the fact that the procedure proposed by them is quite crude, as noted by the authors themselves.

We have dealt so far exclusively with observations by means of optical filters. This is due not at all to the absence of twilight spectra (see, for example [40,90]) but to the fact that these spectra, obtained in large numbers and by many observers, have served as a rule only to determine the atmosphere's own glow (auroras, night sky), but were not considered from the point of view of the analysis of the behavior of the background against which this glow appears as a function of ζ and of the sighting direction. In addition, these spectra were the results of long photographic exposures, which is essentially tantamount to averaging over large intervals of variation of the zenith distance of the sun. Because of this, the most abundant material on the spectroscopy of the twilight sky turned out to be actually useless for deduction of the laws governing the twilight sky itself. An exception is the extensive series of investigations of so-called "twilight flashes" of emission from the night sky, on which we shall dwell briefly below. Of importance to us here are only the special studies of the character and variation of the spectra of the twilight sky at the stage where the glow of the atmosphere itself does not yet play any role.

Recently A. Kh. Darchiya [77] published a series of twilight-sky spectra pertaining to this stage. The spectra were likewise obtained photographically, but with short exposures, at the cost of confining oneself to very small $\xi = \zeta - 90°$ and to the brightest region of the sky, namely the dawn segment near the horizon.

The spectra disclose an extreme variety, which is quite natural, since we are dealing with measurements near the horizon itself, when even insignificant variations in the atmospheric extinction in the troposphere region manifest themselves in strongly exaggerated form. We have therefore chosen for illustration only two series of relatively quiet spectra and have smoothed them out somewhat in order to eliminate the insufficiently reliable singularities (Fig. 15). However, in order to emphasize the variability of the spectra, we chose cases with essentially different character of variation of the brightness and of the wave-length, to illustrate the variations of the spectra with the zenith distance of the sun ζ and with the zenith distance of the same point z. We note that all the measurements were carried out in units of daytime illumination of a horizontal white screen, the spectrum of which, generally speaking, differs essentially from the spectrum of the sun, owing to the presence of scattered radiation from the daytime sky

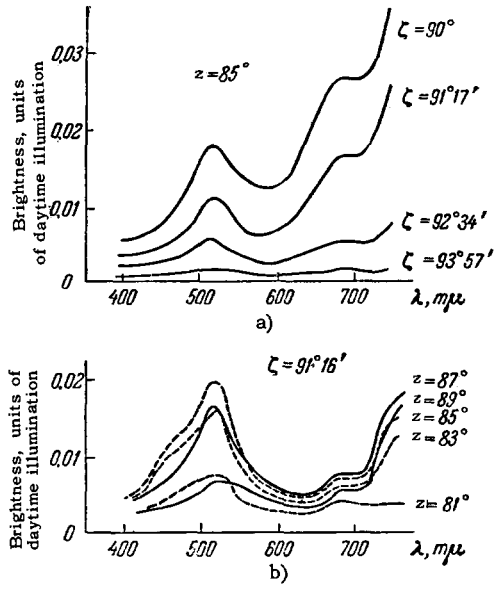

FIG. 15. Examples of spectral variations of the sky brightness in the dawn segment. a) For different zenith distances of the sun, ζ; b) for different zenith distances of the sighting point, z.

(see, for example, [91]). This involves, in particular, an appreciable underestimate of the intensity of the short-wave part of the spectrum, which furthermore progresses rapidly with decreasing wavelength. It must be assumed that the highly pronounced nature of the brightness maximum near $\lambda = 500$ mμ is to a certain degree the consequence of such a choice of units, whereby the decrease in intensity toward the short waves becomes more acute. At the same time, the spectra display clearly the Chapuis ozone absorption bands between 500 and 700 mμ, which vary strongly from day to day. The left edge of this band indeed forms the long-wave slope of the green maximum of the brightness (see Fig. 14). What is further striking is the variability of the long wave slope of the spectrum—beyond the Chapuis band—which obviously owes its origin to variations in the transparency of the lower layers of the atmosphere.

Recently a group of members of the Atmospheric-optics Laboratory of the Institute of Atmospheric Physics (A. Ya. Driving, O. A. Zigel', I. M. Mikhaĭlin, G. V. Rozenberg, G. D. Turkin) obtained spectra of the twilight sky in the zenith by means of an automatic-recording spectrometer with a diffraction grating, up to sun zenith distances $\zeta = 100°$. Owing to the weak glow of the twilight sky, the measurements were made with a wide target, causing the spectral resolution to be 70 Å. The spectrum scanning time amounted to one minute.

Figures 16a and b show some of the spectra obtained by us, in absolute units and in sun brightness units. (The instrument was calibrated against a wide

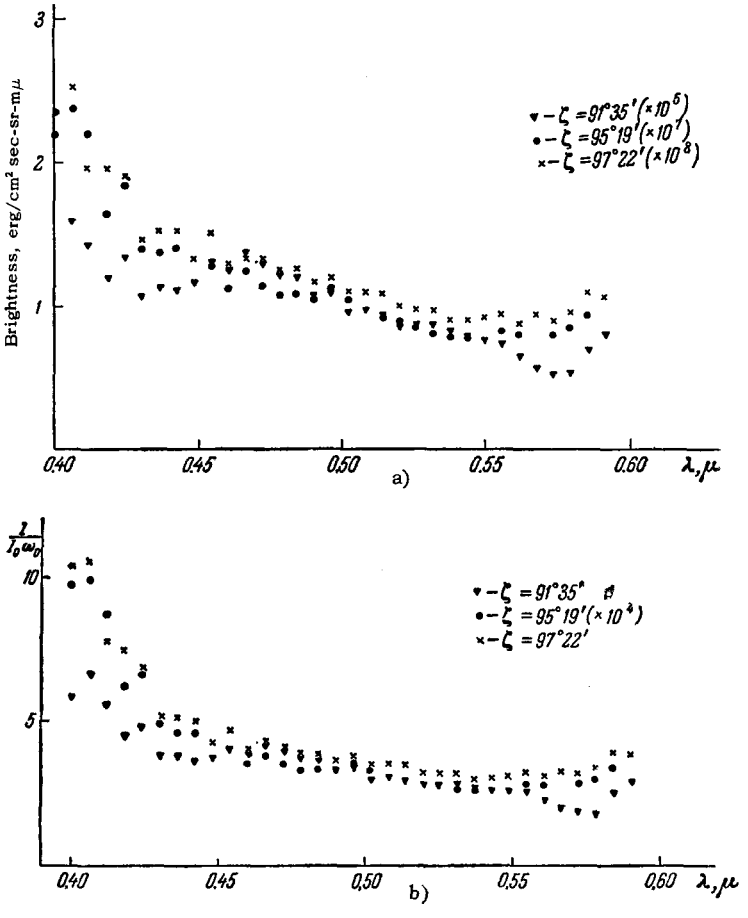

FIG. 16. Spectra of the light from the twilight sky in the zenith for different ζ, in absolute units (a) and in units of solar brightness (b).

screen illuminated by the sun, and the illumination of the screen by the scattered light from the sky was eliminated by the "sun-shadow" method, corrections being also introduced for the spectral transparency of the atmosphere in accordance with the so-called Bouguer long method.)

Attention must be called to the difference between the spectra shown in Figs. 16, 14, and 15, which reflects the variation in the color of the twilight sky with increasing zenith distance z of the sighting direction.

In 1933 V. Slipher [92] first noticed an intensification in the nighttime emission of the ionized nitrogen N_2^+ (of the negative band system) during atmospheric twilight. Three years later H. Garrigue noticed that when the sun dips 9° below the horizon, the red oxygen line $\lambda = 6300$ Å appears in the spectrum of the twilight sky and becomes weaker with increasing zenith distance of the sun. In the same year V. I. Chernyaev and M. F. Vuks [40] found in the twilight-sky spectrum the sodium-D doublet, which occurs when the earth's shadow reaches a height of 50—60 km, and which attenuates noticeably with increasing height of the earth's shadow. Later on, twilight flashes and flashes of other emissions of the night sky were observed, namely the Ni 5200 Å line [94], the atmospheric system of O_2 bands [95,96], the OH band [96], the CaII H and K lines [97], and also the resonant lines of lithium and helium [98]. All these twilight glows are characterized by two circumstances: 1) they appear against the continuous background of the spectrum of the scattered light of the twilight sky when the brightness of the latter becomes already sufficient to mask the weaker emissions of the atmosphere's own glow, and 2) their intensity decreases with depression of the sun below the horizon. We cannot enter here into a discussion concerning the origin of these glows (see, for example, [99,100]), and we shall stop only to discuss the glow of atmospheric sodium, which has played a noticeable role in the development of a twilight method of investigation of the atmosphere.

The problem of the twilight flash of the sodium resonant line has been the subject of an extensive literature (see [100-118] and others). At the present time there is no doubt that it is due to resonant fluorescence of sodium vapor, which forms a sufficiently clearly pronounced layer in the upper atmosphere and is illuminated by the rays of the rising or setting sun. At small depressions of the latter behind the horizon, this fluorescence is drowned out by the bright scattered light of the sky. Then as the zenith distance of the sun increases and the brightness of the twilight sky decreases, the fluorescence becomes observable and is itself finally attenuated when the sodium layer submerges in the shadow of the sun. However, this simple pattern is spoiled by the attenuation of the direct rays of the sun as they

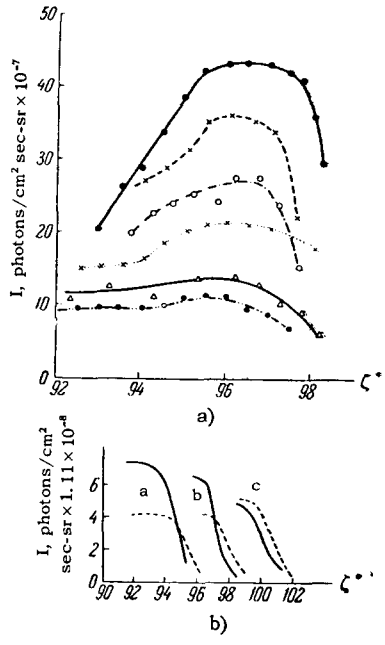

FIG. 17. Plot of the intensity of the resonant lines of sodium against the zenith distance of the sun for different days (a) and different sighting directions for two different days (b).

penetrate into the layer of sodium, which reduces the illumination of the latter at small depressions of the sun below the horizon. As a result, the intensity I of the twilight glow of atmospheric sodium plotted against the zenith distance of the sun exhibits a typical "plateau," the extent of which depends on the optical thickness and the structure of the layer and also on the sighting direction. This is clearly seen on Figs. 17a and b [107]. What is striking is the phase shift occurring upon change in the sighting direction, and also the essential differences in the courses of the curves and in the absolute values of the brightness during different days and for different azimuths. In addition, the ratio of the intensities of the two components of the doublet also changes with changing ζ.

A detailed quantitative analysis of the twilight flash of the D doublet of atomic sodium has shown that the latter is present in the atmosphere in the form of a clearly pronounced layer with a concentration maximum near 70—90 km, and its amount, together with the height of the layer, is highly variable and subject, in particular, to strong seasonal variations [116,118]. Examples of the altitude distribution of the sodium during different days are shown in Fig. 18a. The total content of sodium in a column 1 cm^2 in cross section fluctuates from 2×10^9 to 2×10^{10} atoms. There are serious grounds for assuming that the sodium layer has a cloud-like structure.

Owing to the rapid increase in the scattering coefficient, and consequently also in the optical thickness of the atmosphere, one should expect the character of the twilight phenomena to change noticeably on going into the ultraviolet region of the spectrum. For the time being, however, we have no obser-

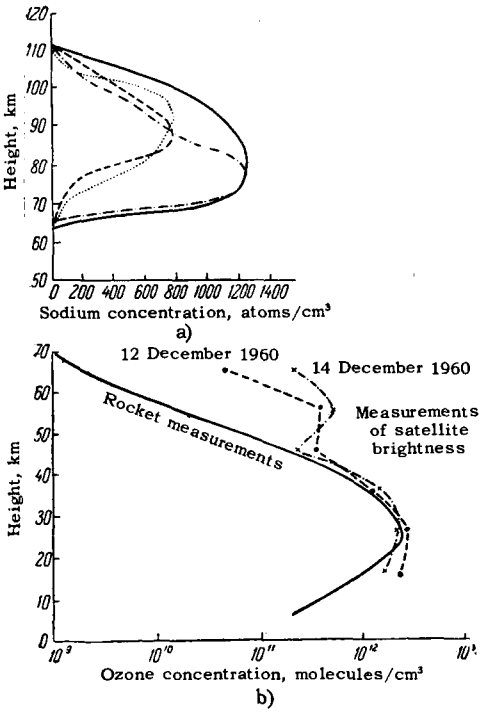

FIG. 18. a) Examples of the altitude distribution of atomic sodium during different days. b) Average altitude distribution of ozone according to data of rocket measurements and distributions for two days according to measurements of brightness of an artificial earth satellite.

vational data. An exception is the region near $\lambda = 0.3\mu$, that is, the region of the long-wave slope of the large ozone absorption band (the Hartley band). As is well known, the latter extends farther into the ultraviolet until it overlaps the absorption bands of oxygen in the Schumann region of the spectrum, as a result of which the lower layers of the atmosphere are completely shielded against the penetration of ultraviolet radiation with $\lambda \lesssim 30\mu$ from the sun. We also recall that the ozone, like the sodium, is present in the atmosphere in the form of a clearly pronounced but strongly smeared layer (Fig. 18b), with a concentration maximum at an altitude of approximately 25 km [119]. The total amount of ozone in the earth's atmosphere is approximately 0.3 cm and fluctuates approximately between 0.2 and 0.4 cm (the quantity of ozone is customarily expressed in terms of the thickness of the layer that the ozone would occupy were it separated in pure form and reduced to 0°C and 760 mm Hg).

Increased interest in the $\lambda = 0.3\mu$ region of the spectrum is due essentially to the tendency to employ twilight phenomena for a determination of the altitude distribution of the ozone—all the information concerning the latter was essentially obtained in this manner before rocket flight became feasible. The scope of the article does not enable us to review the extensive literature devoted to this problem [120].

We are interested here only in that unique character which is acquired by the twilight phenomena in the given region of the spectrum as a result of the large optical thickness of the atmosphere and the presence of a light-absorbing ozone layer located at relatively high altitudes. We have in mind the inversion effect, observed in 1929 by F. Götz [121], and also the related anomalous-transparency effect, discovered in 1936 by S. F. Rodionov, E. N. Pavlova, and N. N. Stupnikov [122], and which, like the inversion effect, is now described even in textbooks. In both cases we are dealing with behavior of the color exponent $CE_{\lambda_2}^{\lambda_1}$, upon variation of the sun's zenith distance, for a pair of wavelengths on the long-wave slope of the Hartley band.

According to Bouguer's law, the intensity of the sun's rays penetrating through the layer of ozone towards the earth should decrease monotonically with increasing zenith distance of the sun, namely

$$I(h) = I_0 e^{-m\tau'(h)}, \qquad (2)$$

where $\tau'(h) = \int_h^\infty k(h)\,dh$ is the optical thickness of the air in a vertical direction above a level h, the total vertical optical thickness of the air being $\tau^* = \tau'(h) + \tau(h)$, where $\tau(h) = \int_0^h k\,dh$ is the optical thickness of the air in the upward vertical direction from sea level to a height h, $k(h) = \alpha(h) + \sigma(h)$ is the extinction coefficient of air, α and σ are its absorption and scattering coefficients, and $m(\zeta)$ is the so-called air mass along the path of the light ray, equal to the ratio of the optical thickness along its path and the optical thickness in a vertical direction for the same altitude difference.

Inasmuch as in the vicinity of $\lambda = 0.3\mu$ both the ozone absorption (α) and the molecular scattering (σ) increase on advancing into the short-wave part of the spectrum, τ' also increases with decreasing wavelength. Therefore, if $\lambda_1 > \lambda_2$, then $\tau'(\lambda_1) < \tau'(\lambda_2)$ and the color exponent, which is given by formula (1)

$$CE_{\lambda_2}^{\lambda_1} = 2.5m\,[\tau'(\lambda_1) - \tau'(\lambda_2)], \qquad (3)$$

should decrease monotonically with increasing m, that is, with increasing ζ.

If we now aim a measuring instrument at the zenith and assume that the scattering of the sun's direct rays occurs essentially in the lower densest layers of the atmosphere, that is, after the sun's rays have penetrated the ozone layer, then we should expect $CE_{\lambda_2}^{\lambda_1}$ for the scattered light also to decrease monotonically with increasing ζ. Götz has observed, however, [121] that actually at a certain value of ζ, which varies from day to day, the monotonic de-

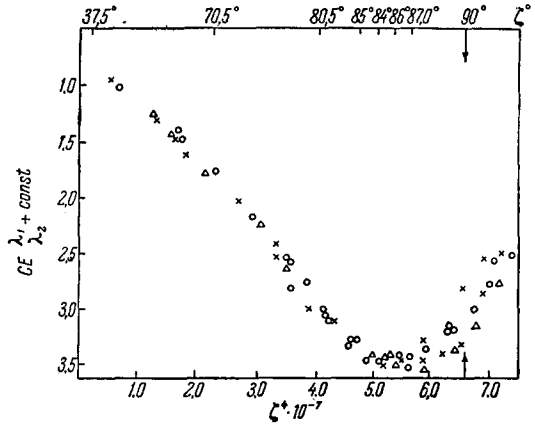

FIG. 19. Examples of experimental $CE^{\lambda_1}_{\lambda_2}(\zeta)$ curves obtained from zenith observations ("inversion curves"). It is traditional to mark the abscissas in units of $\zeta^4 \times 10^{-7}$. Different symbols correspond to different pairs of wavelengths. All curves have been reduced to a single value of CE at small ζ.

crease in the $CE^{\lambda_1}_{\lambda_2}$ is replaced by an increase (Fig. 19). This phenomenon has been called the inversion effect, and the plot of $CE^{\lambda_1}_{\lambda_2}(\zeta)$ is customarily called the inversion curve.

The position of the minimum on the inversion curve depends on the choice of the pair of wavelengths, and with decreasing λ_2 and constant λ_1 the minimum shifts regularly toward smaller ζ. In addition, the position of the minimum, together with the entire course of the inversion curve, depends essentially on the total content of ozone in the atmosphere—an increase in the ozone content shifts the inversion curve also toward smaller ζ. Finally, the character of the inversion curve is quite variable and is frequently essentially different for different pairs of wavelengths; cases are observed when the inversion effect is completely missing.

S. F. Rodionov, E. N. Pavlova, and N. N. Stupnikov [122] observed an analogous phenomenon also in the case when a measuring instrument is aimed directly at the sun, that is, when formula (3) should hold true without any qualifications (Fig. 20). The authors have called this the "anomalous transparency effect," on the basis of the fact that if Bouguer's law is valid the effect can be due only to a relative increase in the atmospheric transparency (that is, a decrease in σ) for λ_2 as compared with its transparency for λ_1 ($\lambda_2 < \lambda_1$). We shall return to the explanation of this effect later. We shall merely note here, as shown by Götz, that the inversion effect can be explained without this hypothesis. To explain this effect it is sufficient to forego the assumption that the sun's direct rays are scattered only below the ozone layer.

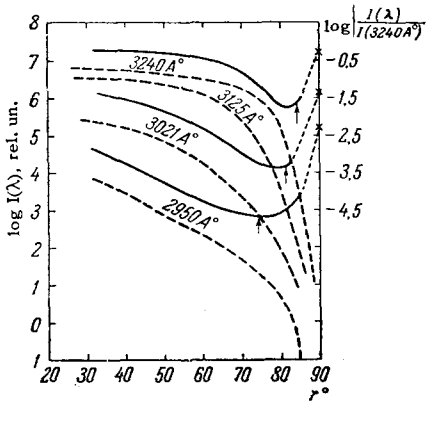

FIG. 20. Dependence of log I on ζ and the "anomalous transparency effect" (instrument aimed at the sun).

In fact, if the instrument is aimed at the zenith, then the light scattered in the rarefied atmosphere above the ozone layer and passing vertically through the ozone layer also strikes the instrument (Fig. 21). So long as the sun is high above the horizon, scattering in the lower layers of the atmosphere predominates, so that Eq. (3) holds true. But when the sun approaches the horizon, the increase in m and the corresponding increase in the absorption of the sun's direct rays by the ozone layer cause the principal role to be assumed by the light scattered above the ozone layer, since the absorption of this light by the ozone layer does not depend on the zenith distance of the sun. This transition occurs at sun's zenith distances that are the larger, the smaller the absorption, that is, the smaller the wavelength, and this leads to the inversion effect.

This explanation, supplemented with an account of the structure of the ozone layer, is indeed the basis of the method proposed by Götz to determine by means of the inversion curves the altitude dependence of α and consequently also of the ozone concentration [120].

The character of the twilight phenomena in the oxygen and water-vapor absorption bands, and also in the infrared region of the spectrum with $\lambda > 1\mu$, has not been investigated at all.

4. POLARIMETRY OF THE TWILIGHT SKY

Supplementary and perfectly independent information on the course of the twilight can be obtained by measuring the polarization of the light from the twilight sky.

The initial measurements [27,34,42,123-129] pertained predominantly to the positions of the so-called neutral parts, that is, those points of the sky where the polarization vanishes.

FIG. 21. Explanation of the inversion effect, after Götz.

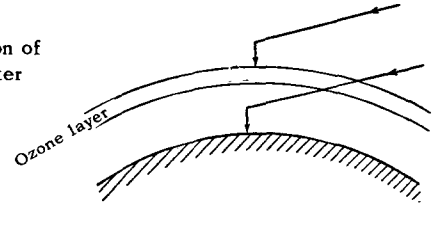

Although the positions of these points relative to the sun and to the antisolar point are relatively stable during the daytime (see, for example, [130,131]) and depend essentially on the meteorological conditions, they begin to display an intensified mobility during twilight. Their behavior in the solar and antisolar verticals becomes entirely different. This is a reflection of the difference in the illumination conditions of the dark and light horizons of the sky during twilight hours and, apparently, primarily a manifestation of the differences in contributions of multiple scattering from different regions of the twilight sky to its brightness (cf. [131,132]). At the same time, data on the observation of the neutral points offer evidence of increased sensitivity of the polarization of the light from the sky to variability in atmospheric conditions.

In addition to the positions of the neutral points, the degree of polarization in different parts of the sky was also measured, but these measurements were confined only to the bright part of the twilight, up to $\zeta = 95—96°$.

The main results consisted here in the fact that the degree of polarization of the twilight-sky light first increased with increasing ζ, and then decreased. In particular, for the zenith the polarization maximum was reached at $\zeta = 92—94°$, with the degree of polarization assuming in the mean a value $p = 0.7—0.8$.

The main purpose of all the foregoing polarization investigations of the twilight sky was to find a direct connection with the weather and to facilitate weather forecasting. For reasons that will become clear in what follows, however, these searches were not crowned with success. The first to suggest the use of polarization measurements for the analysis of the course of the twilight phenomena themselves, and also for the study of the structure of the upper layers of the atmosphere and the processes occurring in them, was I. A. Khvostnikov. Therefore the measurements carried out during many years by Khvostnikov and his co-workers were concentrated on the near-zenith region of the sky, where these polarization effects were most clearly pronounced and, as it seemed at that time, were simplest to interpret. We note that the later investigators, with a few exceptions, also adhered to this tradition, and consequently the data on the polarization in other regions of the sky are practically nil.

The first measurements [133] made on Mount Elbruss in the summer of 1936 have shown that starting with $\zeta \cong 97°$ the degree of polarization p decreases rather rapidly, and the region of ζ approximately between 98 and 102°, in which the p vs. ζ curves have one or two deep minima, are especially singled out. At the same time, a single curve was obtained, covering the entire dark part of the twilight up to the nightime boundary and having an exceedingly deep and broad polarization minimum ($p = 0.15$) at $\zeta \cong 106.5°$.

If the depression of the sun is converted into height of the earth's shadow at the zenith, and if account is taken of the fact that the effective height at which scattering occurs during the twilight lies some 20 km above the height of the geometrical shadow (see below), then it turns out that the positions of the minima correspond to effective scattering heights on the order of 100 and 300 km. The existence of more or less clearly pronounced minima of variable form in the indicated altitude ranges was confirmed also by subsequent measurements of I. A. Khvostnikov [134]. The fact that these heights correspond approximately to the locations of the E and F layers of the ionosphere have enabled Khvostnikov to advance the suggestion [133,134] that the degree of depolarization of the light from the twilight sky is connected in some manner with the degree of ionization of the upper layers of the atmosphere, and that polarization measurements during the time of twilight can yield a direct "cross section" of the ionosphere.

In 1939 polarization measurements of the twilight sky were performed in Crimea by two methods (visual and photoelectric), simultaneously with measurements of the critical frequencies and the heights of radiowave reflection from the E and F layers [135]. The optical measurements were carried out, without filters, in a wide spectral band, limited only by the sensitivity limits of the light receivers. The curves obtained turned out to be quite varied (Figs. 22a and b), thus evidencing the deep differences in the conditions of twilight formation on different days. They share, however, the same features as noted in [133,134], namely the existence of minima at effective heights of the earth's shadow near 80 and 250—290 km, or a strong general fall-off in the degree of polarization with increasing ζ. The same features were also clearly pronounced in measurements of the polarization of the twilight sky near Moscow, carried out in the summer of 1940 with the aid of a photographic procedure [49,50].

In the earlier measurements, the degree of polarization was determined from the intensities of two mutually-perpendicularly polarized components, the orientations of the planes of polarization being maintained constant during the twilight (one of them either followed the sun or coincided with the position of the sun's vertical averaged for the twilight). In this case, however, the measurements were with the aid of three polarization prisms, turned 60° relative to one another. This made it possible to determine both the polarization direction and its true value. Some of the obtained plots of p against the effective height of the scattering layer are shown

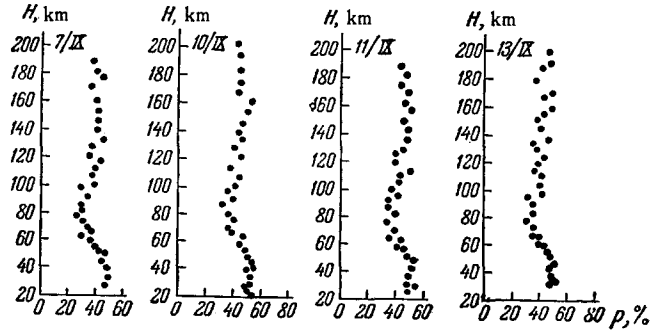

FIG. 22. Examples of the dependences of the degree of polarization of the light from the zenith of the twilight sky on the effective height of the scattering layer. a) Visual measurements; b) photoelectric measurements; c) photographic measurements.

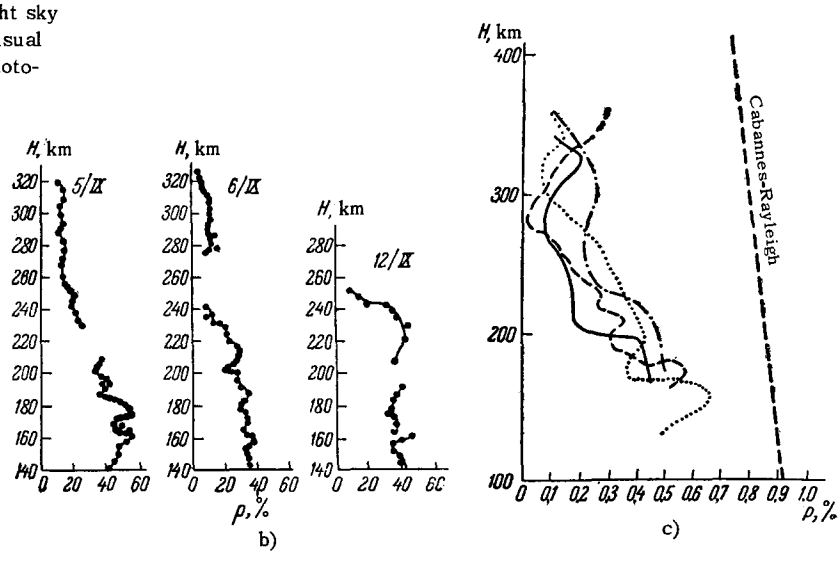

in Fig. 22c, which shows also for comparison the p(h) dependence expected for single molecular scattering.

A correlation was found between the depolarization for effective scattering heights h ≅ 80 km (as well as for h ≅ 270—300 km) and the critical frequencies for the corresponding atmospheric layers, viz., the depth of the minimum increases and the minimum degree of polarization decreases with increasing critical frequency [50,135-137]. The possible causes of this correlation will be discussed in Sec. 10, although it must be noted that the very fact of its existence needs confirmation, and its character needs investigation.

Returning to Fig. 22, attention must be called to two other circumstances. First, during the course of the twilight the degree of polarization is much less than would be expected from the single molecular scattering alone. Second, random short-duration variations of polarization are observed, covering very small intervals of zenith distances or shadow heights. These two circumstances will also be discussed later on, and it will be shown that the second of these is a purely temporal effect. Finally, the increase in polarization at $\xi \gtrsim 107°$ is worthy of attention.

The polarization of light from the zenith region of the twilight sky was subsequently measured many times and, unlike the measurements already described, predominantly with the aid of light filters [3,26,67,70,78-80] or spectrophotographically [138]. In the main features, these measurements have confirmed the general pattern explained by the observations of I. A. Khvostnikov and his co-workers. By way of an example, Fig. 23 shows two plots of p against ζ, pertaining to the zenith. The dashed

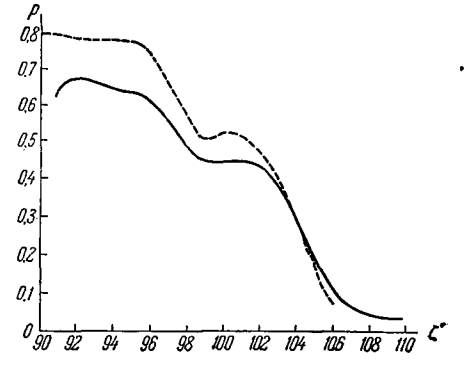

FIG. 23. Examples of averaged dependences of the degree of polarization of light from the zenith twilight sky on the zenith distance of the sun.

curve was obtained by R. Robley [138] visually, and the continuous one by J. Dave and K. Ramanathan [67] photoelectrically (spectral interval 4000—5700 Å). In both cases the results were averaged over several days, so that random (including short-duration) variations were erased. We note that averaging over different groups of measurements or for different spectral intervals leads to different curves [67].

As far as we know, the polarization of light from the twilight sky at points other than the zenith was measured only by T. G. Megrelishvili and by J. Dave and K. Ramanathan [67]. Figure 24 shows a comparicon of p vs. ζ curves, averaged for several days, for three points of the solar meridian with zenith distances z = 0 and ±30° (the minus sign pertains to the sun's counter-vertical). The measurements were made in the spectral interval 4350—4850 Å. In practice the intensities of two mutually-perpendicular polarized components were measured, one component ($I_{\parallel}$) corresponding to the oscillations of the electric vector of the light wave in the plane of the solar meridian. Figure 25 shows the variation of the intensities of both components (averaged over several observation days) with the zenith distance of the sun. It is easy to see that the weaker component $I_{\parallel}$ reaches its limiting (nighttime) value much earlier than the stronger component $I_{\perp}$, for which the electrical vector oscillates perpendicularly to the scattering plane. The inflection in the $I_{\parallel}(\zeta)$ curve begins already at $\zeta = 103.5°$, whereas on the $I_{\perp}(\zeta)$ curve it does not occur until $\zeta = 105°$. This explains the nature of the polarization fall-off in the interval from 103—104° to 107—108°, corresponding to effective scattering heights from 160—200 to 300—350 km (see Figs. 22 and 23). This fall-off in the $p(\zeta)$ plot will be discussed below.

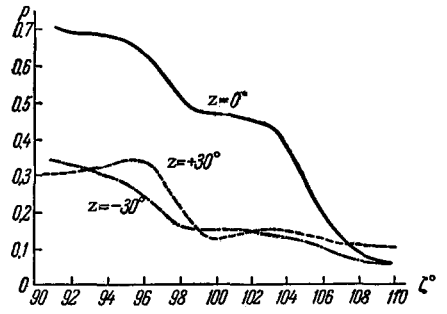

FIG. 24. Averaged p vs. ζ curves for different sighting directions.

Let us turn now to the variability of $p(\zeta)$ with the light wavelength. Figure 26a shows $p(\zeta)$ curves obtained spectrographically for one of the days by R. Robley [138]. For comparison, Fig. 26b shows analogous results obtained by N. B. Divari [75] by measurements with light filters (averaged for two days).

Attention must be paid first of all to the essential difference in the course of the curves for different wavelengths. The reasons for these variations will be discussed in Secs. 8—10. We shall merely note here that they imply that the detailed analysis of data obtained from measurements in broad spectral intervals is not fully valid. It must also be noted that the minimum of polarization at $\zeta \cong 97$—101° and its falloff at $\zeta \gtrsim 102$—103° are differently manifest for different wavelengths and experience

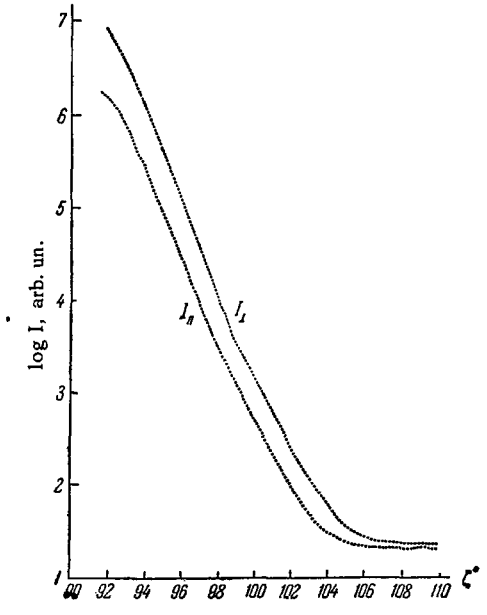

FIG. 25. Averaged ζ-dependence of the logarithms of the intensities of two alternately polarized-light components from the zenith of the twilight sky.

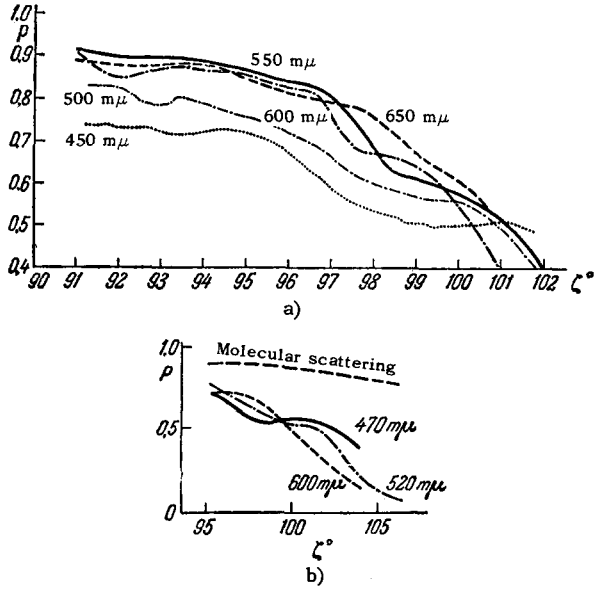

FIG. 26. Plots of $p(\zeta)$ for different spectral intervals. a) Photographic photometry of the spectra of the twilight sky; b) photoelectric measurements with light filters.

noticeable shifts along the axis of the sun's zenith distances. Further, when $\zeta \gtrsim 100°$, the light from the sky is much more strongly polarized in the short-wave region than in the yellow-red part of the spectrum.

N. B. Divari [70] observed a correlation between the atmospheric transparency and the degree of polarization for close wavelengths at $\zeta \cong 99—100°$, whereas for other ζ the correlation becomes worse. We note, however, that the statistics covered only seven or eight days and that the transparency was determined during a different time (daytime) and with different light filters, making the correlation analysis insufficiently convincing.

Almost all the measurements of the polarization of the light from the zenith region of the twilight sky were made, as already mentioned, by determining the intensities of light passing through an analyzer (polaroid or a polarization prism) set in two mutually-perpendicular positions. It has been assumed beforehand that the scattered light from the sky is always polarized either strictly in the scattering plane, or strictly perpendicular to it. It therefore became necessary to make a special check on this assumption, all the more since there were known cases when this assumption was certainly not satisfied both during the day and during the time of total eclipses of the sun, when the conditions of atmospheric illumination are analogous in many respects to twilight conditions.

The first to measure the positions of the plane of polarization of the light from the zenith region of the twilight sky was G. V. Rozenberg [49,50,137]. The result obtained was unexpected. It turned out that the position of the plane of polarization is subject to appreciable variations. Its deviations from the meridian of the sun, occurring at $\zeta \gtrsim 104°$, are considerable, −20—30° and even more.

Later on, N. B. Divari [70] carried out analogous measurements but with light filters, and found that when $\zeta \lesssim 100°$ the deviations of the plane of polarization from the sun's vertical, if they exist at all, are small and have a random character. This was confirmed by measurements of G. V. Rozenberg and N. K. Turikova [26,79] with light filters for relatively small ζ ($92° < \zeta < 102°$). However, when $\zeta \gtrsim 101°$, according to Divari, the deviations of the plane of polarization begin to increase, and when the sun's zenith distance is $\zeta = 103—104°$ they reach noticeable values, on the order of 10° and more, which differ for different wavelengths. Unfortunately, Divari's measurements extend only to $\zeta = 105°$, corresponding to an effective scattering altitude of approximately 220 km. Thus, the strong deviation of the plane of polarization relative to the scattering plane, observed by G. V. Rozenberg at large ζ, has still not been confirmed by subsequent measurements. We add that the accuracy of the measurements of the deviation of the scattering plane at large ζ is low, owing to the smallness of the degree of polarization (Figs. 22 and 23). This calls for a cautious approach to the values obtained in [49,50] for its magnitude. In addition, one cannot exclude the fact that such large deviations of the plane of polarization are due to some specific meteorological conditions (for example, strong horizontal inhomogeneity of the atmosphere, or silver clouds) or some effects of the glow from the night sky. In any case, repeated measurements are called for here, if possible using light filters or spectroscopy. At the same time, the quantitative data concerning the degree of polarization of the light from the twilight sky at $\zeta \gtrsim 104°$, obtained without account of possible rotations of the plane of polarization, are still under doubt.

5. GEOMETRY OF SUN'S RAYS AND THEIR ATTENUATION ON THEIR PATH THROUGH THE ATMOSPHERE

Let us turn now to the theory of twilight phenomena.

On penetrating the earth's atmosphere, the sun's rays experience both attenuation and scattering. The relation between these two phenomena determines, in final analysis, the entire set of optical phenomena observed in the sky during the bright time of the day, including twilight. In principle the total pattern of the twilight phenomena could be obtained by solving the radiation transport equation with suitable boundary conditions. However, no general methods have yet been developed for solving this equation for the three-dimensional problems of the type applying to twilight conditions. Even if they were to exist, they would make it possible to determine the pattern of the twilight sky only if the optical structure of the atmosphere is known beforehand. Yet the greatest interest attaches to precisely the opposite picture, namely the determination of the highly variable structure of the atmosphere from the pattern of the twilight sky. Therefore the principal aim of twilight theory, at any rate in its present state, is to clarify the main laws governing twilight phenomena and to separate the most essential factors that govern their course. It is obvious that this is possible only by constructing a simplified model of the phenomenon and subsequently refining it from the point of view of the influence of various extraneous circumstances. It is not enough here that the main features of such a model merely reflect actuality sufficiently well. It is also necessary that the method of its analysis not go outside the framework of the transport equation and, in final analysis, that it lead to its solution. Such a method can be a successive tracing of the fate of each light beam through all its vicissitudes as it wanders through the atmosphere. Owing to the vertical inhomogeneity of the atmosphere and its

spherical form, a decisive role is assumed in this case by the geometrical factors, which are further complicated by the requirement that they be expressed in the observer's own coordinate frame.

It is necessary to know first precisely where a specified sighting direction meets with a sun's ray characterized by definite perigee altitude (in particular, the boundary of the earth's shadow), and also how this point of encounter moves with varying zenith distance of the sun or sighting direction. This problem was solved many times without account of refraction [39,50,139] and also with its account for different assumptions concerning the structure of the atmosphere [4,38,140-150], and even with account of the geoid form [131]. However, the results in the cited references are represented either in the form of tables, sometimes excessively detailed and convenient only for the solution of particular problems but not for a qualitative analysis of the course of the phenomena, or else in the form of cumbersome formulas not amenable to practical analysis. The formulas become much simpler and assume a form more convenient for the analysis of twilight phenomena if one resorts to approximating the earth's sphere in the vicinity of the point of observation by means of a cylinder whose generatrices are perpendicular to the sun's rays. The approximation obtained in this manner is fully satisfactory in an extensive region of the sky near the zenith, and over the entire extent of the sun's meridian.

We first neglect the sun's angular dimensions and assume that the sun's rays illuminating the earth's sphere are strictly parallel. In exactly the same way, we disregard refraction for the time being, all the more since it turns out to be perfectly inessential to many of the most important problems, as will be shown below. Then the earth's geometrical shadow will be a circular cylinder of radius R (the earth's radius) and its generatrices will be the sun's rays tangent to the earth's sphere (the irregularities of the latter will be also neglected here for the time being, as well as the deviations of the true figure of the earth from spherical form.)

Because of the spherical symmetry of the atmosphere, all the rays that bypass the earth's surface at identical height above the terminator, that is, that have identical perigee height y, are under identical conditions. Therefore the entire aggregate of the sun's rays must be regarded as a one-parameter family, classified in accord with the value of y. If the ray does not bypass the earth's sphere but strikes its surface, that is, if it lies inside the cylinder whose continuation is the earth's shadow, we ascribe to it a negative value of the perigee "height," −y. By the latter we mean the largest dip of the continuation of the ray inside the earth's sphere below the terminator. We now obtain in the cylindrical approximation, for an observer standing on the earth's surface, and for a height h of intersection of the sighting line with the sun's ray with perigee equal to y, the approximate expression

$$h = Rv\gamma\left[1 + \frac{v}{2}\gamma\,\mathrm{tg}^2 z\,(1 - \gamma\sin^2 A)\right], \qquad (4)^*$$

where z and A are the zenith distance and the azimuth of the line of sight

$$v = 1 - \sin\zeta + \frac{y}{R}, \qquad (5)$$

$$\gamma = \frac{\cos z}{\cos\psi} \qquad (6)$$

and

$$\cos\psi = \cos z\sin\zeta - \sin z\cos\zeta\cos A, \qquad (7)$$

where in the sun's meridian we have

$$\cos\psi = \sin(\zeta - z), \qquad (8)$$

z being assumed positive in the vertical and negative in the counter-vertical of the sun. Expression (4) gives satisfactory accuracy under the condition

$$4v\gamma\,\mathrm{tg}^2 z\sin^2 A \leqslant 1,$$

and a correction term in the square brackets is essential only for large z, owing to the smallness of v. In addition, (4) can be generalized without difficulty to the case when the observer is at an arbitrary height L, provided $L \ll R$.

If we denote by H the height of the geometrical shadow of the earth (y = 0),

$$H = R\gamma(1 - \sin\zeta), \qquad (9)$$

and put

$$\eta = y\gamma, \qquad (10)$$

then expression (4) assumes the form

$$h = (H + \eta)\left[1 + \frac{v}{2}\gamma\,\mathrm{tg}^2 z\,(1 - \gamma\sin^2 A)\right], \qquad (11)$$

that is, in an extensive near-zenith region of the sky we have with good accuracy

$$h = H + \eta. \qquad (12)$$

In particular, for the zenith we have

$$H_0 = \frac{R(1 - \sin\zeta)}{\sin\zeta}, \quad \eta_0 = \frac{y}{\sin\zeta}, \qquad (13)$$

and since under twilight conditions $\xi = \zeta - 90° \ll 1$, we have

$$H_0 \cong R\frac{\xi^2}{2}, \quad \eta_0 = y. \qquad (14)$$

In the same approximation, the zenith distances ζ' of the sun and z′ of the line of sight at the point where the latter intersects the sun's ray, are determined by the relations

$$\cos z' = \cos z + \frac{v}{\cos\psi}, \quad \cos\zeta' = \cos\zeta + \frac{v\cos\varphi}{\cos\psi}, \qquad (15)$$

where φ is the scattering angle and

$$\cos\varphi = \cos z\cos\zeta + \sin z\sin\zeta\cos A. \qquad (16)$$

*tg = tan.

Let us turn now to an approximate account of refraction. The latter, as is well known, is determined by the altitude variation of the refractive index n of the air, that is, by the structure of the gas component of the atmosphere. It is therefore subject to rather noticeable variations and different values have been calculated for it by different authors using different models of the atmosphere. However, so long as we deal with a determination of the heights of the sun's ray trajectory, aimed at an analysis of twilight phenomena, these discrepancies, as well as all possible variations of the refraction, can be neglected. It is likewise possible to neglect its dependence on the wavelength. Rozenberg has shown [152] that the dispersion $\Delta\nu$ of the angle of refraction ν can in first approximation be written in the form

$$\Delta\nu = \frac{\Delta n}{n-1}\nu, \qquad (17)$$

from which it follows that under atmospheric conditions $\Delta\nu$ is approximately two orders of magnitude smaller than ν for the visible range of the spectrum, that is, it does not exceed one or two minutes. This permits the refraction effects to be approximately evaluated from V. G. Fesenkov's calculations [150] for the model of the atmosphere given in Allen's tables [153], as applied to $\lambda = 0.5\mu$.

First of all, the angle ν_ζ of astronomical refraction at the perigee of the beam decreases rapidly with increasing perigee height y as a result of the decrease of the earth density with altitude. If we use the results of V. G. Fesenkov [150], we find that the dependence of ν_ζ on y is satisfactorily approximated by the expression

$$\nu_\zeta = 0.013e^{-0.16y}, \qquad (18)$$

where y is in kilometers and ν_ζ in radians. The error of such an approximation amounts to approximately 5 per cent, that is, it does not exceed the uncertainty due to variations of the atmospheric conditions, and is at any rate negligible from the point of view of an analysis of twilight phenomena.

It follows immediately from (19) that when $y \gtrsim 15$ km refraction phenomena become so weak, that they hardly influence the trajectory of the sun's ray inside the earth's atmosphere, although they are still quite noticeable, for example, during the formation of the earth's shadow on the moon's surface in eclipses, and even in the illumination of high-orbit artificial satellites such as "Echo." When $y \lesssim 15$ km, the sun's rays bend noticeably toward the earth's surface, but their curvature becomes appreciable only near perigee, where it barely influences the height of the trajectory of the sun's ray. Thus, an account of the refraction variation of the heights of the sun's rays is essential only beyond their perigee and when $y \lesssim 15$ km. This is clearly seen in Fig. 27, which shows the path of the sun's

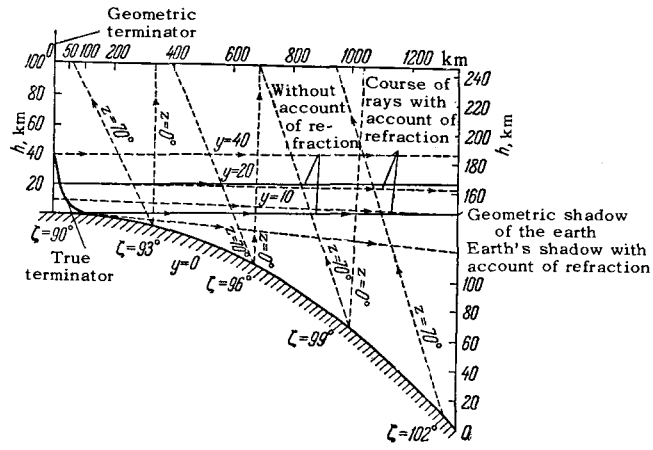

FIG. 27. Path of sun's rays with different perigee, with and without allowance for refraction.

rays with allowance for refraction (dashed) and without it (solid lines), based on calculations for one of the probable models of the atmosphere [81]. It also shows the sighting directions corresponding to z = 0 and 70° and A = 0°, for observers situated at points with different zenith distances of the sun (we call attention to the fact that the vertical scale is five times larger than the horizontal one).

One of the consequences of the bending of the sun's rays is the shift of the true terminator away from its position in the absence of refraction ("geometrical terminator"). Because of the dependence of ν_ζ on y, the shift of the terminator also depends on y. This is also illustrated by Fig. 27, from which it is seen that when $y \gtrsim 15$ km this shift can be neglected.

Along the path to the geometrical terminator, the true ray lies somewhat above the ray drawn without account of refraction, but inside the earth's atmosphere the difference in height remains practically constant and does not exceed 2–2.5 km for y = 0 and approximately 1.5 km for y = 5 km. (We notice that this difference increases sharply if we neglect the shift displacement of the terminator.) Further, although noticeable differences in the character of the variation of the rays do arise in the vicinity of the terminator, their height difference remains negligibly small as before. The true and straight-line rays begin to diverge rapidly behind the true terminator, and it is no longer possible to neglect the difference in the heights of their intersections with the sighting line. Here, too, we can replace the true ray by a straight line with the same perigee height y but with a different zenith distance $\zeta - 2\nu_\zeta$. Thus, in the first rather crude approximation we can replace the true ray by the schematized one (Fig. 28), and the error in the location of the ray above the earth's surface will not exceed 2.5 km for y = 0 and will decrease rapidly with increasing y, remaining always negative.

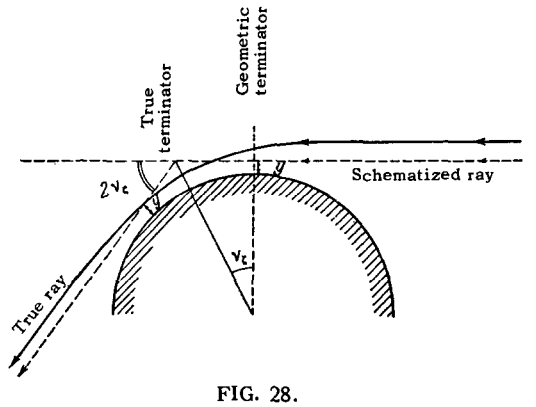

FIG. 28.

Owing to the smallness of ν_ζ, we can determine the refraction shift of the height h of the intersection of the line of sight with the ray having a perigee altitude y by using the first two terms of the expansion of (4) in powers of $2\nu_\zeta$. For the near-zenith regions of the sky, where refraction of the line of sight can be neglected, this leads to the expression

$$\Delta h \cong 2\nu_\zeta \gamma R \cos\zeta'. \tag{19}$$

There is one other refraction effect that must be taken into consideration. Owing to the dependence of the refraction angle ν_ζ on y, the sun's rays bypass the terminator and cease to be parallel, diverging in fanlike fashion. This changes illumination of the atmosphere (atmospheric extinction can be left aside for the time being). Since this refractive divergence is significant only at large distances from the terminator, we can assume as before that the rays are straight and diverge away from the terminator at angles $\zeta - 2\nu_\zeta(y)$. Taking into account Eq. (18) and the fact that R ≅ 6370 km, this leads immediately to an expression E = ME$_0$, for illumination by the sun's straight rays, where

$$M = [1 - 27e^{-0.16y}\cos\zeta']^{-1}, \tag{20}$$

E_0 is the illumination by the sun's straight rays beyond the limits of the atmosphere and [as in the case of (19)] cos ζ' is defined not by (15) but by the expression

$$\cos\zeta' \cong \cos\zeta + \frac{v\cos\varphi}{\cos\psi} - 2\nu_\zeta \sin\zeta. \tag{21}$$

Expression (20) hardly differs from the more rigorous expression previously obtained by F. Link [145-147], which calls for cumbersome calculations. It is very important that the decrease in illumination due to the refraction divergence remains appreciable (for sufficiently large cos ζ') up to values of y noticeably exceeding 15 km, namely to y = 30–40 km. This is illustrated by Fig. 29, which shows a plot of E/E_0 vs. y for different ζ, z, and A. It is striking that the effect varies quite noticeably with ζ, but depends relatively little on z and A.

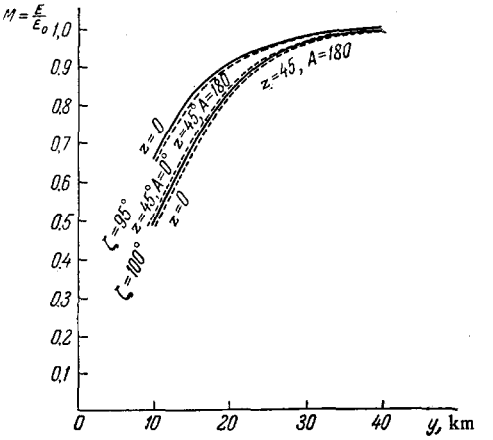

FIG. 29. Variation of M for different z, ζ, and A.

To take into account extinction we can, within the limits of validity of Bouguer's law, use expression (2). For this, however, we must know the dependence of the air mass m on the zenith distance z and, generally speaking, on the height h, with particular interest attaching under twilight conditions to cases when z is close to 90°.

For a horizontally homogeneous spherical atmosphere with arbitrary vertical structure, elementary calculation leads to

$$m(z, L) = \frac{\int_L^\infty k(h)\sec z'(h, L)\,dh}{\int_L^\infty k(h)\,dh} = \overline{\sec z'}, \tag{22}$$

where z′ is the zenith distance of the ray at height h, if its zenith distance is equal to z at the point of observation, which is situated at height L < h, while the bar over sec z′ denotes averaging. For a homogeneous thin spherical layer at a height h we have

$$\cos z' = \sqrt{\cos^2 z + 2w}, \tag{23}$$

where w = (h − L)/(R + L). Thus, for a homogeneous thin spherical layer with z ≲ 75° we have

$$m \cong \sec z - w\sec^3 z, \tag{24}$$

where for z ≲ 60° we can confine ourselves to the first terms. The same expression remains in force also for an arbitrary vertical structure of the atmosphere if w is replaced by its mean integral value, which depends on the character of this structure (this was first pointed out by N. M. Shtaude [154]). In particular, if k(h) = k exp (−h/H), where H is the optical thickness of the homogeneous atmosphere, then w = H/(R + L).

Theoretical calculations by different workers [145-148,150] have shown that m(z) is practically independent of L (this, of course, is the consequence of the previously stipulated assumption that H de-

pends little on the height). Actually, of course, the variations of the temperature stratification, unavoidable horizontal inhomogeneities of the atmosphere which manifest themselves pronouncedly in the scales of hundreds and even thousands of kilometers that are characteristic of the twilight phenomena, and the presence of aerosol layers (as well as ozone and sodium layers), all lead to a rather noticeable dependence of $\overline{w}$ on z, L, and the time. The value of m becomes particularly sensitive to variations of the optical structure of the atmosphere at $z > 75°$, when formula (24) is no longer applicable and different models of the atmosphere begin to lead to values of m which differ appreciably from one another (say by five whole units at $z = 89°$[155]). No less serious discrepancies are obtained also when the measured values of m for large z are compared with one another and with the theoretical calculations. All this makes a reliable calculation of m rather hopeless when z is close to 90°. Obviously, m should be experimentally determined in each specific case. However, for an analysis of various kinds of twilight effects it is advantageous to use some averaged function m(z), which can be assumed the same for all $L \ll R$. To this end, the author of these lines has proposed the empirical formula

$$m = (\cos z + 0{,}025e^{-11\cos z})^{-1}, \qquad (25)$$

which gives results that differ relatively little from the calculation data of Bemporad, and also of F. Link and L. Neužil, and which agree well with the calculations of V. G. Fesenkov [150] for $z = 90°$.

All the foregoing is valid only if Bouguer's law holds. In the case of scattering media with low absorption ($\alpha \ll \sigma$), this law may be violated by multiple scattering effects [157], which become more noticeable the larger the optical thickness of the layer τ, the angle of incidence of the rays ζ, and the solid angle ω limiting the field of view of the instrument. If $\tau \sec \zeta \gtrsim 5$ and $\omega \geq \omega_0$ (ω_0 is the aperture angle illuminating the layer of the light beam), then the ratio of the scattered and direct light fluxes Φ_s and Φ_d as measured by an instrument aimed at the sun will be [157]

$$\frac{\Phi_s}{\Phi_d} = \frac{\omega}{\pi} \cdot \frac{g^2(\zeta)\, e^{\tau \sec \zeta}\, l}{\sec \zeta\, (1-A)\,\tau + l}, \qquad (26)$$

where l is a constant that depends on the form of the scattering indicatrix ($l = 4/3$ for molecular scattering), $g(\zeta)$ a function that does not differ much from unity and depends also on the form of the scattering indicatrix, and A the albedo of the underlying surface. In the case of a spherical layer of large radius, $\sec \zeta$ can be approximately replaced by $m(\zeta)$. It is easy to see that when $\omega = \omega_0 \cong 9 \times 10^{-5}$ (the sun's angular dimensions), this ratio reaches 10 per cent for the following values of m, depending on τ (the limits correspond to the principal variations of the albedo of the earth's surface):

τ	0,3	0,4	1,0
m	39—40	28,5—30	10,6—11,2

Inasmuch as $m \leq 40$ for an observer on earth, there should be no noticeable deviations from the Bouguer's law in the long-wave region of the spectrum $\lambda \gtrsim 0.5$, where $\tau \lesssim 0.25$ in clear weather. However, for $0.4\mu \lesssim \lambda \leq 0.5\mu$, the brightness of the haze at the horizon should become comparable with the brightness of the setting sun even in clear weather, and in the ultraviolet region, near $\lambda \cong 0.3\mu$, where $\tau \cong 1$, the brightness of the haze already begins to exceed noticeably the brightness of the sun when $\zeta \gtrsim 86—87°$. (In particular, this explains why we observe indeed a "green ray" and not a blue one at the instant of the rise or setting of a celestial body, as is expressly manifest on photographs of Venus obtained in the direct vicinity of the horizon [158].) For the sun's rays that bypass the earth's surface with a perigee height y, deviations from Bouguer's law will be already unnoticeable if y is greater than approximately 1 km for $\lambda = 0.7\mu$, 7.5 km for $\lambda = 0.5\mu$, 13 km for $\lambda = 0.4\mu$, and 18 km for $\lambda = 0.3\mu$. As will be shown below, this fully ensures the applicability of Bouguer's law to calculations of the brightness of the twilight sky when the sun is behind the horizon.

At the same time, relation (26) enables us to explain the above-described anomalous transparency by attributing it just to a violation of Bouguer's law due to multiple scattering [159]. If we take into account the absorption of light in the ozone layer, then the light flux measured by an instrument aimed at the sun with $\omega > \omega_0$ is proportional to

$$\Phi \sim \frac{\omega}{\pi} g(\zeta) \frac{l}{(1-A)\,\tau + l} \left[g(\zeta) \cos \zeta e^{-(\tau_0+\tau')m_0} + \frac{\tau'}{2} e^{-\tau_0 s(\tau_0)} \left(1 - \frac{m_0}{2}\tau'\right) \right] + e^{-(\tau_0+\tau')m_0 - \tau m}, \qquad (27)$$

where τ_0, τ, and τ' are optical thicknesses of the ozone, subozone, and superozone air layers, respectively, m_0 and m are the air masses in the direction of the sun for the ozone layer and for the atmosphere below it, and $s(\tau_0) = 1 - \tau_0 \exp(-\tau_0) \times \mathrm{Ei}(-\tau_0)$.

Inasmuch as the altitude of the ozone layer is about 30 km we have $\tau' \cong 10^{-2}\tau$, with $1 \lesssim \tau \lesssim 1.4$ and $10^{-2} \lesssim \tau_0 \lesssim 5$ in the vicinity of $\lambda = 0.3\mu$, and $l = 4/3$ because molecular scattering predominates. The first term in the square brackets of (27) takes into account multiple scattering under the ozone layer, the second allows for single scattering above

this layer with subsequent multiple scattering in the lower layers of the atmosphere, while the last term takes into account the direct light from the sun.

It is easy to see that for small ζ (that is, small m and m_0), the last term predominates. But for sufficiently large ζ and not too small τ_0 the principal role is assumed by the second term (the first is always smaller than either the third or the second), that is, the decrease in Φ with increasing ζ becomes incomparably slower than exponential and occurs the sooner the larger τ_0, causing reversal of the plot $CE_{\lambda_2}^{\lambda_1}$ against ζ. The arrows on Fig. 20 show the positions of the minimum of $CE_{\lambda_2}^{\lambda_1}$ as calculated by formula (27) with allowance for the spectral variation of τ and τ_0, while the crosses show the values of $CE_{\lambda_2}^{\lambda_1}$ expected from (27) for $\zeta = 90°$. We see that the agreement with the observation data is perfectly satisfactory.

An analogous result was obtained independently and by a different method by G. P. Gushchin [160], who confirmed experimentally, in particular, the shift of the minimum of $CE_{\lambda_2}^{\lambda_1}$ with increasing ω, which follows from (27).

The anomalous transparency effect should also be observed in the region of the spectrum where τ_0 is negligibly small but τ is still sufficiently large. In this case it is a direct result of the fact that the larger τ (that is, the smaller λ), the smaller the values of ζ for which Bouguer's law is violated. This violation is the result of the transfer of the predominant role from the last term in (27) to the first term (the second term vanishes as $\tau_0 \to 0$) and occurs at considerably larger ζ than in the ozone absorption region. The anomalous transparency effect and the inversion effect thus have a common explanation, as expected from their similarity [161].

In fact, if the instrument is not aimed at the sun (say at the zenith), then expression (27) assumes the form [159]

$$\Phi \sim \frac{\omega}{\pi} g(z) \frac{l}{(1-A)\tau + l} \left[g(\zeta) \cos\zeta e^{-(\tau_0+\tau')m_0} + \frac{\tau'}{2} e^{-\tau_0 s(\tau_0)} \left(1 - \frac{m_0}{2}\tau'\right)\right], \quad (28)$$

where z is the zenith distance of the sighting direction. For small ζ, the first term in the square brackets predominates and Φ decreases exponentially with increasing m_0. For large ζ, however, the predominant role shifts from the first term to the second, which depends only little on ζ; the larger τ_0 the sooner this occurs, thus explaining the inversion effect. We note that in Götz's theory account is taken only of single scattering, which corresponds to replacing in (28) the factor

$$\frac{g(z)}{\pi} \frac{l}{(1-A)\tau + l} g(\zeta)\cos\zeta$$

by

$$\frac{f(\varphi)}{4\pi} m(z) \frac{e^{-m(z)\tau} - e^{-m(\zeta)\tau}}{m(\zeta) - m(z)}$$

[see formula (42) below] and the term

$$\frac{g(z)}{\pi} \frac{l}{(1-A)\tau + l} \frac{\tau'}{2} e^{-\tau_0 s(\tau_0)} \left(1 - \frac{m_0}{2}\tau'\right)$$

by

$$\frac{f(\varphi)}{4\pi} m(z) \tau' e^{-m(z)\tau_0},$$

where $f(\varphi)$ is the scattering indicatrix. In either variant, the relations presented are valid only for a sharply outlined thin layer of ozone. Since the ozone layer is actually greatly spread-out in altitude, it is necessary to include in the theory the altitude distribution of the ozone concentration. Such a theory was developed by several authors in connection with the ozone measurement problem [120] but with account of single scattering only, a procedure which we regard as invalid.

There is also every reason for assuming that the so-called selective transparency of the atmosphere, observed by S. F. Rodionov and his coworkers [162,163,20] and used by Rodionov [161] to explain the anomalous transparency effect, is actually a fictitious result of an incautious interpretation of the observational data, namely the use of Bouguer's law without allowance for its possible violation due to multiple scattering.

6. TWILIGHT ILLUMINATION OF THE ATMOSPHERE

If the atmosphere is spherically symmetrical then, subject to the stipulations that follow from the preceding section, the influence of extinction on its illumination is described by a factor of the form

$$T = e^{-m_e \tau'(h)}, \quad (29)$$

where $\tau'(h)$ is the optical thickness of the atmosphere above the level and m_e is a certain effective air mass, which depend on the position of the illuminated volume.

In particular, for a beam penetrating through the atmosphere, we have $m_e = 2m(\pi/2)$, that is, according to (25) we have $m_e = 80$ and $\tau'(h) = \tau'(y)$.

Calculations of the function $T(y) = \exp[-2m(\pi/2)\tau'(y)]$ for different λ were undertaken by various authors, who started from different assumptions concerning the altitude and spectral variations of the scattering and absorption coefficients σ and $\dot{\alpha}$ of atmospheric air. In particular, a large number of calculations were carried out for $\lambda = 589$ mμ in connection with the problem of the twilight flash of glow of atmospheric sodium [101,107,108,164,etc.] under the assumption of purely molecular scattering of the light by the atmosphere. As applied to the theory of twilight phenomena,

similar calculations for different wavelengths and different models of the atmosphere were made at various times by V. G. Fesenkov [4,150], E. Hulburt [45], E. A. Polyakova [165], N. M. Shtaude [84], F. Link and his co-workers [145-147,156], F. Volz and R. Goody [81], etc., with the contribution of the aerosol to the attenuation of the light by the earth's atmosphere neglected everywhere except in [165,150,81]. Furthermore, in [145-147,150,156] account was taken of the refraction variation of the path of the light beam, while the refraction divergence effect is allowed for in [145-147,156,81]. Figure 30 shows the functions T(y) for different wavelengths, as obtained by V. G. Fesenkov [150] under the assumption that 1) σ is proportional to the air density, 2) the air-density altitude distribution is standard, and 3) the dependence of the vertical transparency of the atmosphere on the wavelength is standard, in accordance with [153]. Analogous curves for T(y), obtained under different assumptions concerning the optical structure of the atmosphere, differ noticeably from those in Fig. 30 mostly in their wavelength dependence. (By way of an example, Fig. 30 shows the function T(y) for λ = 589 mμ, calculated by J. Dufay under the assumption of pure molecular scattering.) It is significant that in all cases the function T(y) is monotonic, similar in form to the volt-ampere characteristic of a radio tube, with a clearly pronounced linear portion and with a point of inflection located near T = 0.4. The form of the curves depends little on the wavelength, which affects principally the displacement of the curve along the y axis, so that displacement toward the short-wave portion of the spectrum corresponds (in the absence of selective absorption) to a shift of the curve toward larger y. It is easy to see that an analogous result is obtained for any sensible assumption concerning the optical structure of the cloudless atmosphere, and even strong turbidity of the lower layers of the atmosphere will affect the general course of the curves little, distorting them (namely, reducing the already small values of T) in the region of small y only, where the atmosphere is practically opaque.

Inasmuch as m_e does not depend in practice on either y or λ, the position y_n of the point of inflection of the T(y) curve is determined in accordance with (29) by the condition

$$m_e k(y_n) = -K(y_n), \tag{30}$$

where

$$K = -\frac{d \ln k}{dh}. \tag{31}$$

In particular, if K does not depend on h in the vicinity of y_n, then

$$\tau'(y_n) = \frac{1}{m_e} \text{ and } T(y_n) = e^{-1}.$$

Figure 31 shows lines of equal τ' as functions of the height and wavelength for a purely molecular atmosphere [166]. Using Fig. 31 or its analog for the real atmosphere, we can readily obtain the value of y_n corresponding to any m_e. If K does not depend on the height and if we neglect refraction, we get

$$y_n(m_e) = y_n(m_e = 80) - \frac{1}{K} \ln \frac{80}{m_e}, \tag{32}$$

that is, a reduction in m_e leads to a displacement of the T(y) curves on Fig. 30 toward smaller y, while the existence of an opaque earth's surface is manifest at small m_e only in the fact that the part of the T(y) curves corresponding to y < 0 is cut off.

Expanding T(y) in a series about the point of inflection and retaining the first two terms of the expansion (the third vanishes and the fourth makes no essential improvement), we find that in the absence of selectively-absorbing or cloud layers the function T(y) can be approximated with satisfactory accuracy by the expression [50,137]

$$T(y) = \begin{cases} 0 \quad \text{for} \quad y \leqslant y_n - \frac{1}{K}, \\ e^{-1}[1 + K(y - y_n)] \quad \text{for} \\ y_n - \frac{1}{K} \leqslant y \leqslant y_n + \frac{e-1}{K}, \\ 1 \quad \text{for} \quad y \geqslant y_n + \frac{e-1}{K}. \end{cases} \tag{33}$$

Figure 32 shows an example of such an approximation for λ = 0.7μ, from among the cases given in Fig. 30.

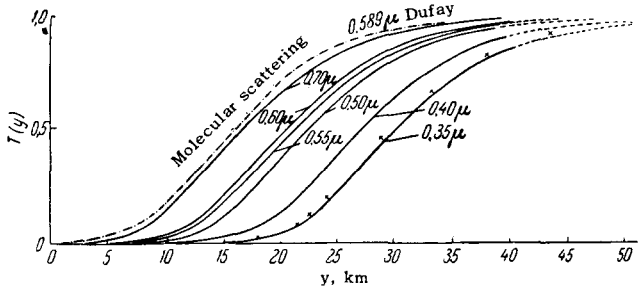

FIG. 30. Plots of $T = \exp[-2m(\pi/2)\tau'(y)]$ against y for different λ, after V. G. Fesenkov.[150]

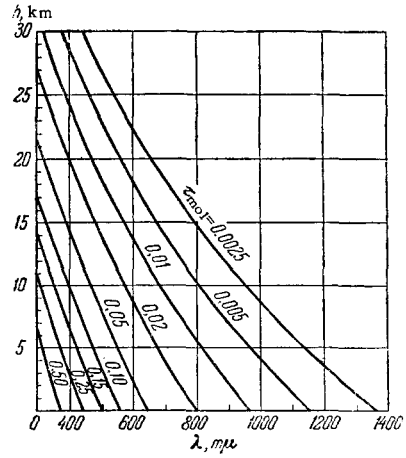

FIG. 31. Vertical optical thickness of pure air as a function of the height and wavelength.

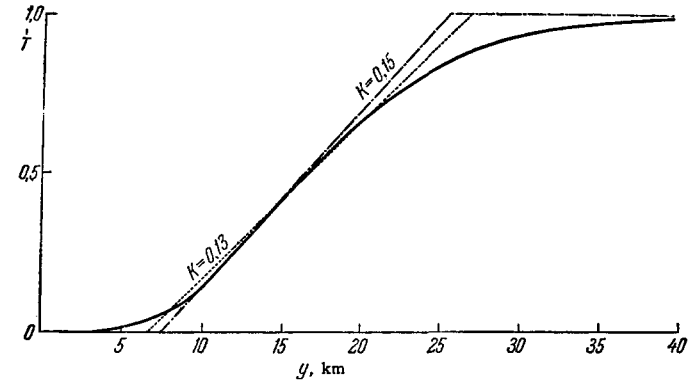

FIG. 32. Approximation of the T(y) curve.

It is seen from (30)—(33) that the form of the function T(y) remains relatively insensitive to the atmospheric conditions and to changes of the wavelength, inasmuch as they do not influence k. On the other hand, the location of the point of inflection does depend strongly on these conditions, since it is determined primarily by the value of k. Figure 33 shows the spectral variations of $y_n(\lambda)$ for $k \sim \lambda^{-4}$ (molecular scattering), $k \sim \lambda^{-1}$, and $k \sim \lambda^{-1.6}$, and also for the cases calculated by V. G. Fesenkov [150] and J. Dufay [164]. In particular, for the model of the atmosphere considered by V. G. Fesenkov [150] we have approximately $y_n = 12.5(1 - 2 \log \lambda)$ km, where λ is in microns.

For what follows it is essential to investigate also the behavior of the function $T(h) \exp[-m(z)\tau(h)]$, where the second factor takes into account the attenuation of the light along the path from the volume illuminated by the sun to the observer on earth. Recognizing that $\tau(h) = \tau^* - \tau'(h)$, where τ^* is the total vertical optical thickness of the atmosphere, we obtain

$$T(h)\, e^{-m(z)\tau(h)} = e^{-m(z)\tau^*} T_c(h), \qquad (34)$$

where

$$T_c(h) = T(h)\, e^{m(z)\tau'(h)}. \qquad (35)$$

Writing down $T_c(h)$ again in the form (29), we find that if the illuminated volume is located on the sun's ray ahead of its perigee, then $m_e = m(\zeta' < \pi/2) - m(z)$, and if it is located behind the true perigee

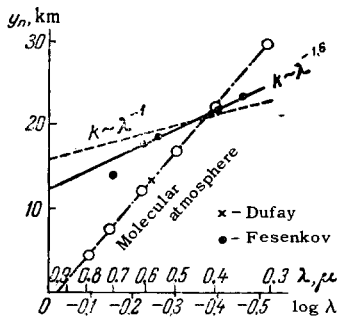

FIG. 33. Height of the point of inflection y_n of the T(y) curve vs. log λ for different optical states of the atmosphere.

of the ray, then, following the recommendation of N. M. Shtaude [167,168] we can write $m_e = 2m(\pi/2) - m(\pi - \zeta) - m(z)$. Here, however, we can no longer neglect refraction and use (32), so that the calculations are quite complicated. However, if $m(z) \ll m(\zeta)$ and if γ differs little from 1, as is true for the extensive near-zenith region of the sky, we obtain relatively simple approximate relations for the dependence of the height h_n of the location of the point of inflection of the function $T_c(h)$ on ζ. According to (9)—(11), $h_n = H + \gamma y_n$ without account of reflection, and if the illuminated volume is located ahead of the perigee of the sun's ray, then $H = 0$. Under the foregoing limitations, an account of refraction leads to the relations

$$\tau'(h_n) \cong \frac{1}{m(\zeta) - m(z)} \left[1 + \left(\frac{1}{1 - \frac{m(z)}{m(\zeta)}} + \frac{K}{p} \right)^{-2} \right], \qquad (36)$$

if the illuminated volume is located ahead of the true perigee, and

$$\tau'(y_n) \cong \frac{m(\zeta)\left(2\frac{p^2}{K} - 2\frac{p}{K} + 1\right)e^{-2KH} + 80}{\left| m(\zeta)\left(1 - \frac{p}{K}\right)e^{-KH} - 80 \right|^2}, \qquad (37)$$

if it is located behind the true perigee, where

$$p \cong m_\zeta \left[\frac{1}{R} \frac{\cos\varphi}{\cos\psi} - 0.002 e^{-0.16 y_n} \right]. \qquad (38)$$

If we now use Fig. 31, then we obtain for a purely molecular atmosphere the plots of y_n vs. $\xi = \zeta - \pi/2$ shown in Fig. 34. The corresponding plots of h_n against ξ are shown in Fig. 35. Attention must be called to the fact that the perigee of the sun's ray illuminating the point of inflection of the function $T_c(h)$ breaks away from the earth's surface even before sunset, and the shorter the wavelength the sooner this takes place, so that when $\xi \cong 0.07$ (that is, $\zeta \cong 94°$) y_n reaches a maximum value and no longer changes with increasing ζ. A consequence of this is the characteristic inflection of the curves in the region $h_n \cong 20$ km and $\zeta \cong 94°$, shown in Fig. 35.

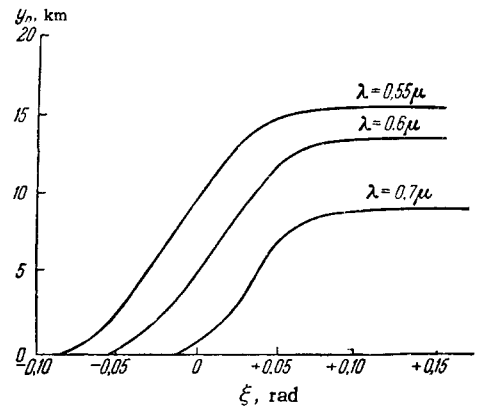

FIG. 34. The functions $y_n(\xi)$ for different λ for a molecular atmosphere.

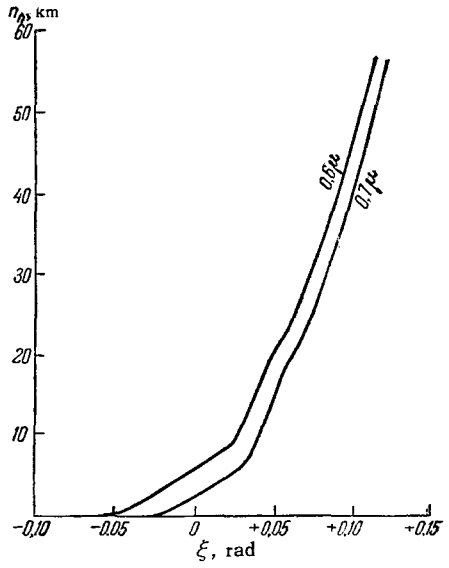

FIG. 35. The functions $h_n(\xi)$ for different λ for a molecular atmosphere.

No less important is the fact that the maximum value of y_n increases rapidly with decreasing λ, and exerts a decisive influence on the color of the twilight sky.

The illumination of the atmosphere at a point with coordinates (z, A, h) is in accordance with (21) and (29) equal to

$$E(z, A, h, \zeta, \lambda) = M(z, A, h, \zeta) \times T(z, A, h, \zeta, \lambda) I_0 \omega_0, \quad (39)$$

where I_0 is the brightness of the sun and ω_0 its angular dimension. The corresponding calculations were carried out by different authors under different assumptions concerning the structure of the atmosphere. Figure 36 shows plots of E(h) borrowed from [81], for different $\xi = \zeta - 90°$ and for three wavelengths, at $z = 70°$ for a pure molecular atmosphere. It is clearly seen that when $\xi > 2-3°$ refraction effects are significant only in the long-wave region of the spectrum, where y_n is small and h_n is located in the vicinity of the earth's geometrical shadow (the shaded areas correspond to regions of

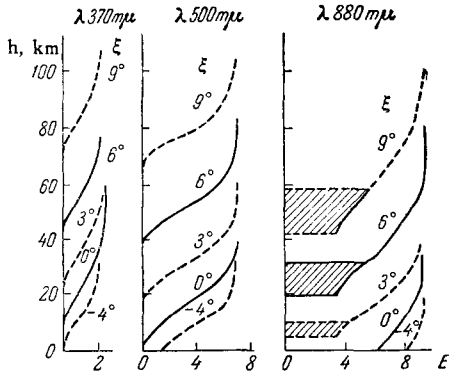

FIG. 36. The functions T(h) for $z = 70°$ and different ξ, for a pure atmosphere at different values of λ.

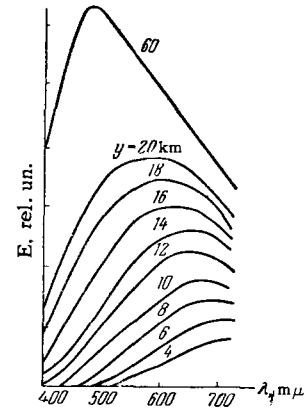

FIG. 37. Variation of the spectrum of the sun's direct rays as a function of y.

the atmosphere located below the geometrical shadow and illuminated as a result of refraction).

It is also easy to see that the sharp variations in T(y) on the one hand, and in $y_n(\lambda)$ on the other, cause appreciable changes in E as a function of λ for a given h, that is, in the spectral composition of the light illuminating the atmosphere. Figure 37 shows by way of example plots of $E(\lambda)$ beyond the limits of the atmosphere for different y and for a purely molecular atmosphere, without account of the influence of the ozone [45]. Notice must be taken of the rapidly progressing reddening of the sun's light with decreasing y.

In conclusion let us note that in the vicinity of the selective absorption of the substances contained in the atmosphere in the form of more or less pronounced layers, this form of the function $T_c(y)$ is greatly modified. However, if the illuminated volume is located under the absorbing layer, the function $T_c(y)$ can be approximated even in this case, albeit with a much larger error, by expressions of the form (33), but with different coefficients. By way of an example Fig. 38 shows plots of $T_c(y)$, borrowed from [107], pertaining to $\lambda = 0.589\mu$ and calculated under the assumption that the scattering of light has a purely molecular character and that the altitude distribution of the ozone concentration is Gaussian with a maximum at an altitude h_0, a half-width t_0, and a total ozone content c_0.

7. BRIGHTNESS OF THE TWILIGHT SKY. THE TWILIGHT LAYER

On the basis of the geometrical picture of the illumination of the atmosphere by the sun's rays, we can calculate the brightness of the twilight sky, taking into account for the time being only single scattering of the direct sunlight and neglecting effects of the self illumination of the atmosphere. This problem was first formulated and solved in a crudely schematic form by P. Grunner [139]. We shall not stop to retrace his reasoning, but present a general formulation of the problem, deduced from papers of V. G. Fesenkov [4,31,37,149,169], N. M.

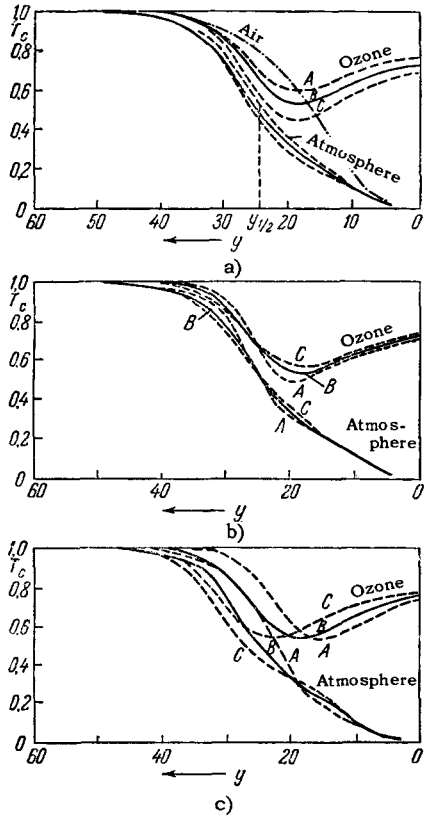

FIG. 38. Plot of the transparency of ozone and of pure air containing ozone, for a ray passing through the entire thickness of the atmosphere, against the height of its perigee y. a) Effect of the total content of ozone: $A-c_0 = 2$ mm, $B-c_0 = 2.5$ mm, $C-c_0 = 3$ mm; b) effect of half-width of ozone layer: $A-t_0 = 12.4$ km, $B-t_0 = 15.6$ km, $C-t_0 = 18.8$ km; c) effect of height of the ozone layer: $A-h_0 = 19$ km, $B-h_0 = 23$ km, $C-h_0 = 27$ km.

Shtaude [39,54,55,84,167,168,170], F. Link [51,52,141,171-174], and G. V. Rozenberg [50,86,137]. We confine ourselves here to equations for the brightness of the sky. Generalization of these relations, needed to take into account the polarization effects, can be made without difficulty by formal transition to the matrix form and by replacing the intensities with the Stokes parameters [50,86,137].

The intensity of the light scattered in the direction of the observer by a volume element dV situated at the point with coordinates (z, A, h) is equal to

$$dI = D(h, \varphi) E \frac{dV}{l^2 d\omega}, \qquad (40)$$

where

$$D(h, \varphi) = \frac{1}{4\pi} \sigma(h) f(h, \varphi),$$

f is the scattering function, l the distance from observer to the scattering volume element, and $d\omega = dV/l^2 dl$ the solid angle at which the observer sees the volume dV. Along the path to the observer, this light experiences additional attenuation, taken into account by the factor $\exp[-m(z)\,\tau(h)]$. Integrating along the entire line of sight and taking into account (34), (39), and the relation $dl = m(z')\,dh$, we find that the brightness of the sky in the direction (z, A) is equal to

$$I(z, A, \zeta, \lambda) = I_0(\lambda)\,\omega_0 e^{-m(z)\tau^*(\lambda)} \int_0^\infty D(h, \varphi) \times \left| M[(h, \zeta, z, A)\, T_c(h, \zeta, A, \lambda, z)\, m(z)\, dh. \right.$$

In particular, in the absence of absorption ($k = \sigma$) and for $\zeta < 90°$ (that is, $M = 1$), assuming $f(\varphi)$ to be independent of h and confining ourselves to not too large z and ζ [so that refraction can be neglected and we can put $m(z') = m(z)$ and $m(\zeta') = m(\zeta)$], we get

$$I = I_0 \omega_0 \frac{f(\varphi)}{4\pi} m(z) \frac{e^{-m(z)\tau^*} - e^{-m(\zeta)\tau^*}}{m(\zeta) - m(z)}, \qquad (42)$$

that is, we arrive at a well known formula, which describes the brightness pattern of the daytime sky without account of multiple-scattering effects (see, for example, [148,166]).

In order to make formula (41) amenable to interpretation under twilight conditions, we must now use an analysis of the geometrical picture and the properties of the function T_C, as was done in the preceding sections.

We first recognize that, as shown by the analysis, the character of the dependence of the product MT_C on y does not differ in practice from the character of the function $T_C(y)$, and the presence of the factor M causes only some change in the value of y_n, increasing it by 1 or 2 km. We have seen further that the function T (and consequently also MT_C) can be written with sufficient accuracy in the form $T(y, \zeta, z, A, \lambda) = T[y - y_n(\zeta, z, A, \lambda)]$, and if we use an approximation of the form (33), then

$$MT_c = \begin{cases} 0 & y \leqslant a(\zeta, z, A, \lambda), \\ \frac{y-a}{b} & a \leqslant y \leqslant a+b, \\ 1 & y \geqslant a+b, \end{cases} \qquad (43)$$

where in the general case b = const and $y_n = a + cb$ (c = const), while in the absence of selective absorption

$$b \cong \frac{e}{K}, \quad y_n \cong a + \frac{1}{K} \cong a + \frac{b}{e}.$$

If, finally, we take into account the mutually unique relationship between h and y for given ζ, z, and A, then we can rewrite (41) in the form

$$I(z, A, \zeta, \lambda) = I(\lambda)\,\omega_0 P^m(\lambda)\, m \int_0^\infty D[h, \varphi(z, A, \zeta), \lambda] \times T_c[y(h), \zeta, z, A, \lambda]\, dh = I(\lambda)\,\omega_0 P^m(\lambda)\, m \int_0^\infty D[h(y), \times \varphi(z, A, \zeta), \lambda]\, T_c[y - y_n(\zeta, z, A, \lambda)] \frac{dh}{dy} dy, \qquad (44)$$

where $P(\lambda) = e^{-\tau^*(\lambda)}$ is the vertical transparency of the atmosphere, m stands for m(z), and it is assumed that z is not too large, so that the h-dependence of m can be neglected.

In the approximation(43), expression (44) assumes the form

$$I(z, A, \zeta, \lambda) = I_0(\lambda)\omega_0 P^m(\lambda) m \times \left\{ \int_a^{a+b} D[h(y), \varphi(\zeta, z, A), \lambda] \frac{dh}{dy}(y-a)\,dy + \tau'_p[h(a+b)] \right\}, \quad (45)$$

where

$$\tau'_p(h) = \int_h^\infty D(h)\,dh. \quad (46)$$

We assume first that the geometric shadow boundary H is lifted sufficiently high, so that the influence of refraction, and consequently also the value of y_n, does not depend on ζ, z, and A. Then, using (12), we obtain in place of (44)

$$I(z, A, \zeta, \lambda) = I_0(\lambda)\omega_0 P^m(\lambda) m \int_0^\infty D(H+\eta, \varphi, \lambda) T_c\left(\frac{\eta}{\gamma}, \lambda\right) d\eta. \quad (47)$$

It is important that the integrand is a product of two factors, of which one (D) depends only on the structure of the high layers of the atmosphere at the level $H + \eta$ and decreases rapidly with altitude, while the second (T_c) depends on the structure of the lower layers of the atmosphere at the level y_n only, and increases rapidly in the interval $a \le y \le a + b$. Since both factors are essentially positive, their product should have a maximum at some $\eta = \eta_m$, and the pronouncedness of the maximum depends on the logarithmic gradient of D at the altitude $H + \eta$, that is, on $K(h + \eta)$, and on dT_c/dy at the level y_n, that is, on $K(y_n)$. Figure 39 shows the case $\gamma = 1$, $K(H + \eta) = 0.1$, $K(y_n) = 0.15$, and $T(y)$ corresponds to the data of V. G. Fesenkov for $\lambda = 0.4\mu$ (see Fig. 30). The shaded region corresponds to the product DT_c, the area of which is proportional to the brightness of the twilight sky for a given H and for $\gamma = 1$.

The same figure shows the linear approximation of $T_c(y)$ and the area DT_{approx} corresponding to it: we see that the latter differs only insignificantly from the area of DT_c.

Figures 40 and 41 show the corresponding plots of DT_c against h for different ζ and λ, with $z = 70°$, for a purely molecular atmosphere [81,82]. We note that in the long-wave region of the spectrum, owing to the smallness of y_n, the curves are bounded from below by the geometrical shadow of the earth, which is appreciably shifted downward by refraction (shaded region).

It follows from Figs. 39—41 that the lion's share of the light received by the earth observer is due to scattering of light in a relatively thin so-called "twilight layer." Its half width is close to 20 km. The lower layers of the air are in the shadow and hardly scatter any light, while the upper layers hardly scatter any because of the relatively low density of the air. This circumstance was first noted by V. G. Fesenkov [31], and was used by him [37,169] and by N. M. Shtaude [39,54,55,84,168,170] as the basis for an approximate theory of twilight phenomena (see also [45,50,81]). As the sun dips below the horizon, that is, as H increases, the twilight layer rises higher and higher (see Figs. 40 and 41), changing relatively little in outline and scanning, as it were, the upper layers of the atmosphere. This circumstance was indeed used by V. G. Fesenkov [31,37,69] and N. M. Shtaude [84,168, etc.] to justify the method they developed for twilight sounding of the atmosphere (see below).

The position of the maximum brightness of the twilight layer can be readily obtained by resorting to the approximation (43) and assuming that $K = K(H)$ is constant in the region of the twilight

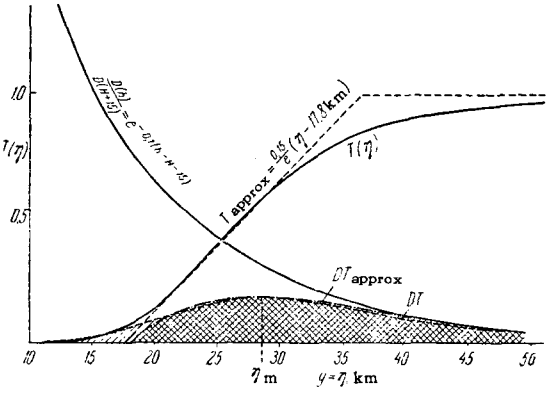

FIG. 39. Plot of DT against η for $\gamma = 1$, $K(y) = 0.15$, and $K(H + \eta) = 0.10$ with $\lambda = 0.4\ \mu$.

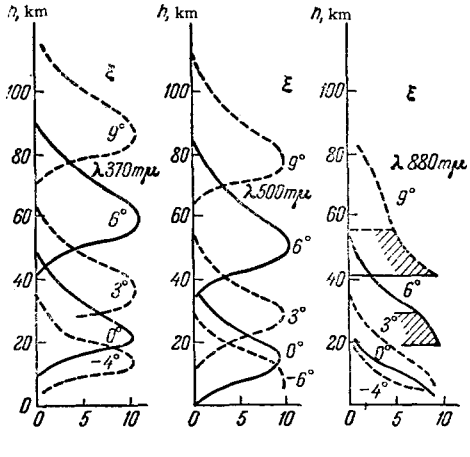

FIG. 40. Altitude profiles of the twilight layer for $z = 70°$ and for different parts of the spectrum at different ξ.

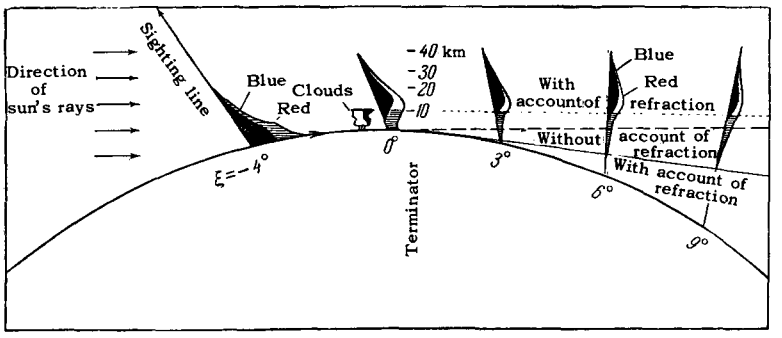

FIG. 41. Altitude profiles of the twilight layer for $z = 70°$ and for two regions of the spectrum at different ξ.

layer. Then the first integral in the curly brackets of (45) is transformed into

$$\frac{D[h(a)]}{\gamma b}\int_0^{\gamma b} e^{-Kx}x\,dx, \tag{48}$$

from which we get for the maximum of the integrand

$$\eta_{max}=\gamma y_n+\begin{cases}\dfrac{1}{K(H)}-\dfrac{1}{K(y)} & K(H)\geqslant e^{-1}K(y),\\ \dfrac{e^{-1}}{K(y)} & K(H)\leqslant e^{-1}K(y).\end{cases} \tag{49}$$

Since y_n increases rapidly with decreasing λ, the height of the brightness maximum $h_m = H + \eta_m$ increases on going into the shortwave region of the spectrum (see Fig. 40). In addition, however, η_m increases rapidly with decreasing K, that is, the position of the maximum depends essentially on the structure of the atmosphere. With decreasing K, the half-width of the maximum also increases rapidly, and consequently at the small values of K observed in the high layers of the atmosphere, the very concept of the twilight layer becomes less definite.

Returning to Fig. 40, we can readily see that the twilight layer drops down on the earth's surface much later than the sunrise, and that the shorter the wavelength, that is, the greater the optical density of the atmosphere, the later this occurs. The first to call attention to this circumstance was N. M. Shtaude [168], who indicated that the start of the twilight must be taken to be precisely the instant when the maximum brightness of the twilight layer breaks away from the surface of the earth.

8. EFFECTIVE BOUNDARY OF THE EARTH'S SHADOW AND ITS DEPENDENCE ON THE STRUCTURE OF THE ATMOSPHERE. PHASES OF TWILIGHT

The notion of effective boundary of the earth's shadow was introduced by G. V. Rozenberg [50,86,137] and in indirect form by N. M. Shtaude [84]. Since $T_c(y)$ is essentially a monotonic function and since D and T are essentially positive, the integral in (44) can be rewritten in the form

$$\int_0^\infty D[h,\varphi,\lambda]\,T[y(h),\zeta,z,A,\lambda]\,dh = \int_{\overline{H}(\zeta,z,A,\lambda)}^{\infty} D(h,\varphi,\lambda)\,dh=\tau'_p(\overline{H}), \tag{50}$$

where $\overline{H}$ is some still unknown height, which plays the role of the effective height of the earth's shadow (see Fig. 42). This makes formula (44) exceedingly simple:

$$I(z,A,\zeta,\lambda)=I_0(\lambda)\,\omega_0\,P^m(\lambda)m\tau'_p(\overline{H}), \tag{51}$$

and the entire complexity of the problem is transferred to the determination of the height $\overline{H}$ as a function of ζ, z, A, λ, and the state of the atmosphere. The finite dimensions of the sun's disc angular radius ν, neglecting refraction distortion, is then taken into account by merely replacing ζ by $\zeta + 8\nu/3\pi$ in the argument of the function $\overline{H}(\zeta)$, as can be readily demonstrated.

Obviously the quantity $\overline{H} = H + \overline{\eta}$ depends for given ζ, z, A, and λ on the structure of the atmosphere both in the region where the sighting direction crosses the twilight layer, and in the region of the terminator.

If the real functions D(h) can be approximated in the vicinity of h_n [more accurately, in the height interval from $H + \gamma a$ to $H + \gamma(a + b)$] and in the vicinity of the perigee y_n by exponentials with logarithmic gradients $K(h_n)$ and $K(y_n)$ respectively, then the following approximate relation holds for not too large values of z:

$$\overline{H}=h_n+\frac{1}{24}[K(y_n)-K(h_n)]\,b^2\left(\frac{dh}{dy}\right)^2_{h_n}. \tag{52}$$

It is easy to see that the height $\overline{H}$ is located in the vicinity of h_n, and also that the difference in heights $\overline{H} - h_n$ is relatively insensitive to variations of $K(h_n)$, and does not exceed 2—5 km in the absence of cloud layers. The most essential influence is exerted on $\overline{H}$ by variations of λ, with $(d\overline{H}/d\lambda) \cong (dy_n/d\lambda)$, which leads, say for the case considered by V. G. Fesenkov (see Fig. 30), to $(d\overline{H}/d\lambda) \cong -\gamma(25/\lambda)$ km/μ.

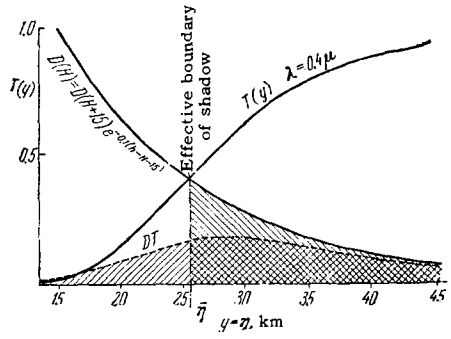

FIG. 42. Illustrating the concept of effective boundary of the earth's shadow.

Appreciable deviations can be expected only when the height a becomes negative, that is, when $T(y=0) \neq 0$, or when $T(y) = 0$ with $y < a + \Delta$ and $T(y)$ is again described by formula (43) when $y > a + \Delta$; the latter can occur in the presence of high clouds in the vicinity of the terminator. An approximate examination in both cases leads to the expression

$$\overline{H'} = h_n + \frac{\gamma\Delta^2}{2b} + \frac{1}{24}\left[K(y_n)b^2 - \left(1+\frac{2\Delta}{b}\right)K(h_n)(b-\Delta)^2\right]\left(\frac{dh}{dy}\right)^2_{y_n}. \quad (53)$$

Another reason for appreciable deviations may be the presence of a cloud layer in the vicinity of h_n. If a layer with optical thickness τ_c is characterized by an altitude distribution of its scattering ability in the form $\sigma_c = \tau_c\delta(h - h_c)$, where $\delta(h - h_c)$ is the delta function and $h_c = H + \eta_c$ is the height of the layer, then we have approximately

$$\overline{H} = h_n + [K(y_n) - K(h_n)]\frac{\gamma^2 b^2}{24} - \frac{\tau_c}{K(h_n)\,b}\left[\frac{\eta_c}{\gamma} - \begin{cases}(a+b) & \text{for } h_c > \overline{h}\\ a & \text{for } h_c < \overline{h}\end{cases}\right]. \quad (54)$$

In other words, $\overline{\eta}$ is in practice insensitive to the presence of the layer, so long as $y_c \gtrsim (a + b)$, and then, as ζ increases, $\overline{\eta}$ begins to grow, until the equality $\overline{\eta} = \eta_c$ is reached for a certain value of ζ and is maintained over the extent of some interval of variation of ζ (that is, of decrease in η_c), after which η becomes larger than η_c and again increases, returning to its initial position when $\eta_c = \gamma a$.

Finally, it follows from (42) that under daytime conditions

$$\tau'_p(\overline{H}) = \frac{1 - e^{-\Delta m\tau^*}}{\Delta m},$$

where $\Delta m = m(\zeta) - m(z)$, from which we get approximately

$$\overline{H} \cong \frac{\Delta m\tau^*}{2K}\left(1 - \frac{\Delta m\tau^*}{12}\right). \quad (55)$$

It is obvious that so long as $\Delta m < 0$ we have $\overline{H} = 0$, but when $\Delta m > 0$ the value of $\overline{H}$ increases approximately in proportion to Δm; the larger τ^* and the smaller K, the faster the increase.

Figure 43 shows the behavior of $\overline{H}$ and $\overline{\eta}$ during the day and the bright stage of the twilight, for a purely molecular atmosphere (the calculations were made in accordance with formulas (55) and (53), respectively, with h_n calculated for the twilight from (36) and (37) as a function of ζ). As the sun moves to the horizon, starting with a certain value of ζ (which depends on z), $\overline{H}$ begins to increase slowly, and the smaller τ^* the slower this increase. The growth of $\overline{H}$ then accelerates at a rate that increases with τ^*, and as the sun inclines toward the horizon, the point of inflection y_n of the transparency curve $T_c(y)$ begins to rise above the earth's surface (see Fig. 34). In this entire interval of ζ, the equality $\overline{H} = \overline{\eta}$ is maintained, since $H = 0$. Further, when the sighting direction is behind the true perigee of the ray passing at the altitude $\overline{H}$, the increase in $\overline{H}$ becomes more intense, owing to the rise of the geometrical shadow of the earth, which at first is slow and then accelerates gradually, inasmuch as $\overline{H} = \overline{H} + \overline{\eta}$ from that instant on. However, near $\zeta \cong 94°$ (see Fig. 35) the increase in $\overline{H}$ is slowed down for a short time because y_n, together with $\overline{\eta}$, reaches its maximum value, and further increase in $\overline{H}$ is due only to the dependence of H on ζ.

Inasmuch as according to (49) the brightness of the sky is proportional to $\tau'_p(\overline{H})$, its variaton with ζ, z, A, and λ will reflect directly the dependence of $\overline{H}$ on these quantities. And since we have seen that the dependence of $\overline{H}$ on ζ also exhibits an essentially different sensitivity to different effects in different regions of the spectrum and for different sighting directions, this means that at one and the same instant of time the course of the twilight phenomena will also be different for different λ, z, and A. Consequently, inasmuch as we are dealing with the picture of the twilight sky, we can

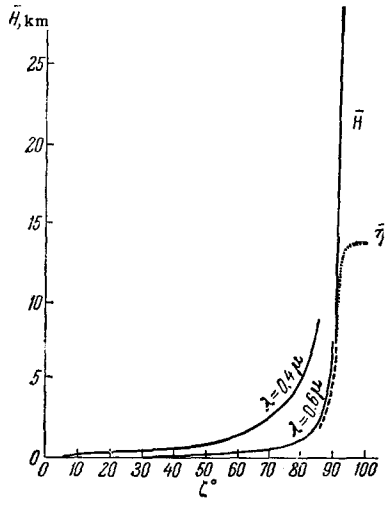

FIG. 43. Plot of the height $\overline{H}$ of the effective boundary of the earth's shadow at the zenith vs. ζ.

no longer have a single subdivision of twilight into phases of time or of the quantity ζ, which is uniquely related with the time, for the entire sky as a whole, as was done in Sec. 2.

The boundaries between the twilight phases should be determined separately for each sighting direction and for each wavelength, and the sensible choice of a single parameter for the determination is just the height $\overline{H}$ of the earth's effective shadow.

We have seen that $\overline{H}$ varies very little as the sun moves over the sky during the day. The changeover to twilight, that is, to a rapid decrease in the sky brightness, is connected with a rapid increase in $\overline{H}$ as the sun approaches the horizon. It is seen from Fig. 43 (see also Figs. 1 and 3) that the changeover from daytime to twilight is very diffuse and cannot be clearly defined. Therefore the criterion of the onset of twilight can be chosen only arbitrarily. By way of such a criterion let us propose the instant when $y_n = 0$, that is, when the point of inflection is at sea level (see Fig. 34), which is practically the same as the criterion proposed by N. M. Shtaude, that is, the instant when the brightness maximum of the twilight sky breaks away from sea level (see Fig. 40).

In addition, the value of y_n stabilizes at a certain value of ζ, different for different points of the sky but approximately the same for all wavelengths outside the selective-absorption band (for the zenith near $\zeta = 94°$); the further increase in $\overline{H}$ ceases to depend on the refraction effect and is determined only by the rising of the geometrical shadow of the earth, that is, the relation $\overline{H} \cong H + \gamma y_n$ becomes valid. From that instant on, the twilight can be regarded as fully established in the given portion of the sky.

Thus, we arrive at a sufficiently clear cut distinction between two phases of twilight:

1. Semitwilight, corresponding to the period between daytime and the establishment of twilight for a given section of sky, that is, the time interval during which $0 \leq y_n(\lambda) < y_{n\max}$.

2. Total twilight, which begins in the given portion of the sky at the instant when twilight is established, that is, the instant when $y_n = y_{n\max}$.

However, if we turn to the observational data, we see that for a certain value of ζ, different for different parts of the sky ($\zeta \cong 100°$ at the zenith) and for different regions of the spectrum, the character of any twilight phenomena changes radically. This allows us to single out a third and last phase of twilight.

3. Deep twilight, when, as will be shown below, the decisive role is assumed by the multiple scattering of light in the earth's atmosphere, and also the atmosphere's own glow and the other light of the night sky.

Deep twilight terminates in the transition to nighttime, and again this transition occurs at different times in different parts of the sky and in different regions of the spectrum (for more details see Sec. 10).

Owing to the essential differences in the course of the semitwilight for different parts of the spectrum, that is, owing to the strong dependence of $\overline{H}$ on λ during the semitwilight period, a dependence which varies with ζ, semitwilight is characterized by a rapid change in the color of the sky, that is, by the phenomena usually grouped under the designation sunset. In other words, sunset is the aggregate of the simultaneous but different stages of development of semitwilight in a given section of the sky at all wavelengths (the term semitwilight is therefore best retained only for relatively narrow spectral intervals). In addition, for the sake of tradition, it is advantageous to retain the name sunset for the most illuminated segment of the sky above the horizon near the sun. This is justified to the extent that in this segment the twilight phenomena come into play in the most pronounced form and remain there much longer than in other parts of the sky, continuing even after deep twilight has already set in on the opposite side of the horizon or even in the zenith.

Of all the quantities characterizing the course of twilight, the one most investigated is perhaps the logarithmic brightness gradient of the twilight sky

$$q = -\frac{d \ln I}{dH} = -\frac{d \ln I}{d\zeta}\frac{d\zeta}{dH}. \qquad (56)$$

It follows from (51) that

$$q = \frac{D(\overline{H})}{\tau_p'(\overline{H})}\frac{d\overline{H}}{dH}, \qquad (57)$$

and in the case when D depends exponentially on h, we have $D(\overline{H})/\tau_p'(H) = K(\overline{H})$ in the vicinity of h_n. On the other hand, if we start with the concept of the twilight layer, then, as shown by N. M. Shtaude [39,170] (the same result was obtained earlier by somewhat different methods by V. G. Fesenkov [31,169] and F. Link [141,171,174]), $q = K(h_{max})[dh_{max}/dH]$. In view of the smallness of $d\overline{H}/dH$ and dh_{max}/dH during the period of the total twilight, both formulas lead to results that are close. Thus, if we assume in the first approximation $d\overline{H}/dH = 1$, then $q = K(H)$ and the knowledge of q from measurements of $I(\zeta)$ enables us to determine approximately the value of $d \ln \tau_p'/dH$ at the level $\overline{H}$. It is precisely this circumstance that has prompted many authors to measure the dependence of q on H ([46,49,50,57], and others). Particularly numerous measurements were made for many years at the Abastumani Observatory by T. G. Megrelishvili. Figure 44a shows $q(\overline{H})$ plots which she obtained simultaneously in three portions of the spectrum for two sighting directions ($z = 0$ and $A = 0$, $z = 70°$). Analogous

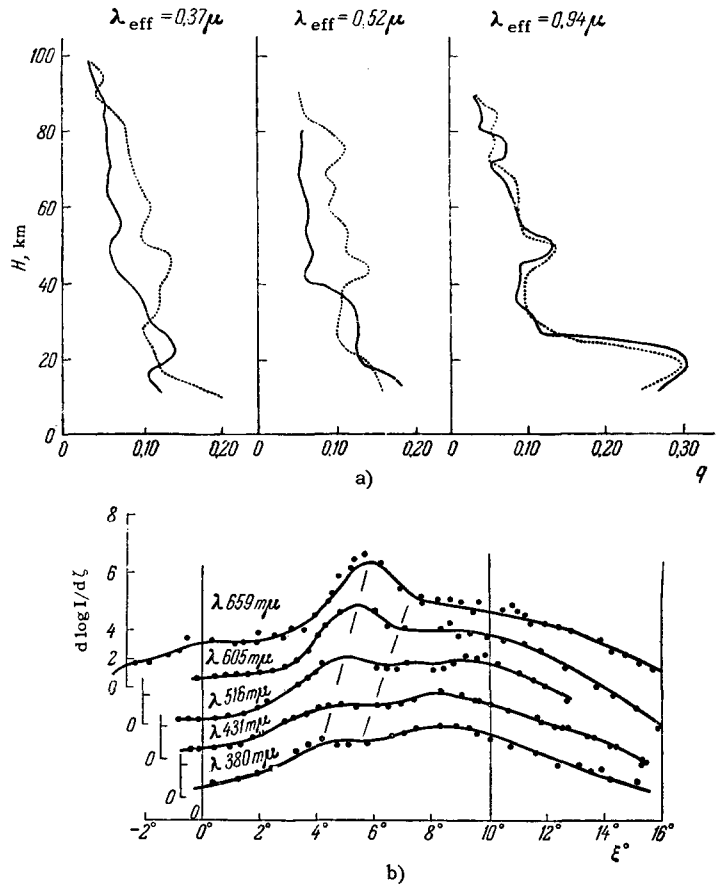

FIG. 44. a) Typical plots of q(H) in three regions of the spectrum, as measured by T. G. Megrelishvili for $z = 0$ (continuous lines) and $z = 70°$ (dashes). b) Plots of $-d \ln I/d\zeta$ for one of the days and for different wavelengths, as measured by F. Volz and R. Goody.

relationships were obtained for one of the days and for a series of wavelengths by F. Volz and R. Goody [81], as shown in Fig. 44b.

The most striking is the extreme variability of $q(H)$ both from day to day and on going from certain values of z and λ to others. Further, attention should be paid to the rather capricious course of the $q(H)$ curves, which exhibit a variety of small-scale bends, the reality of the existence of which was demonstrated by E. Bigg [68], who used an instrument intended for direct registration of $d \ln I/dt = -q\, dH/dt$. Finally, notice should be taken of many peculiarities of $q(H)$, observed more or less systematically, although with essential variations. First among them is the maximum at $H \cong 5$—20 km, which becomes more sharply pronounced and increases with increasing λ, and in the interval of heights H from ~ 30 to 100 km the value of q amounts to merely a few hundredths of a reciprocal kilometer. Then we have the rapid decrease in q for $H \gtrsim 150$ km, with q reaching values measured in thousandths of a reciprocal kilometer [50].

Let us dwell first on the maximum of q at $H \cong 20$ km. E. Bigg [68] interpreted this maximum as evidence for the existence of an aerosol layer at high altitudes near 20 km. T. G. Megrelishvili [72] and F. Volz and R. Goody [81] have shown that such an interpretation is inconsistent both because it is incorrect to identify $\overline{H}$ or h_{max} with H, as is done by Bigg, and from considerations connected with the resolution of the twilight method of sounding the atmosphere (see below). At the same time, there are no reasons for ascribing this maximum to the fluorescence of the atmosphere, as is done by T. G. Megrelishvili [69,72]. In particular, F. Volz and R. Goody [81] have shown by direct calculation that the corresponding maximum should occur also in a purely molecular atmosphere. The reason for its occurrence can be readily explained by means of the previously given analysis of the behavior of $\overline{H}$ as a function of ζ. In fact, so long as the sun is under the horizon, that is, so long as $H = 0$, we have $d\overline{H}/d\zeta = d\overline{\eta}/d\zeta$, and, as is evident from Figs. 43, 34, and 35, at this stage $d\overline{\eta}/d\zeta$ increases monotonically. When the sun drops behind the horizon, $d\overline{H}/d\zeta = (dH/d\zeta) + (d\overline{\eta}/d\zeta)$, and $d\overline{\eta}/d\zeta$ first remains practically constant (see Fig. 34), and $dH/d\zeta \cong R\gamma\xi$ increases rapidly. But on the border of total twilight (that is, for the zenith at $\zeta \cong 94°$ and $H \cong 20$ km), $d\overline{\eta}/d\zeta$ begins to decrease rapidly (see Figs. 34 and 43), so that $d\overline{H}/d\zeta$ decreases sharply (compare with Fig. 35), causing the appearance of a maximum in the dependence of $d\overline{H}/dH$ on ζ, and consequently in $q(\zeta)$.

Let us consider now the behavior of $q(H)$ when at a certain height h_c there is a delta-like layer with optical thickness τ_c. We have seen above that

with increasing H the effective boundary of the shadow first tends in accelerated fashion in a direction toward the layer (which corresponds to a decrease in q), and then moves away together with the layer (that is, q increases), and finally, breaking away from the layer, it overtakes its usual position (which is again accompanied by a decrease in q). The process described covers a time interval corresponding to a displacement of the boundary of the geometrical shadow H by a distance 2b, which is approximately equal to 40 km. In other words, the presence of a delta-like layer is manifest on the curve of the dependence of q(H) in the form of a z-shaped bend, which covers an altitude interval on the order of 40 km, with the location of the layer corresponding approximately to the central part of this bend, which has not experienced any disturbance.

The described picture is clearly seen on Fig. 45, which shows the results of the calculated values of q(H) as obtained by T. G. Megrelishvili [72] for a standard atmosphere (curve 1), for the same atmosphere and a layer with double the scattering ability occupying the height interval from 60 to 70 km (curve 2), and also for an atmosphere which contains in addition a second identical layer located 5 km below the first (curve 3).

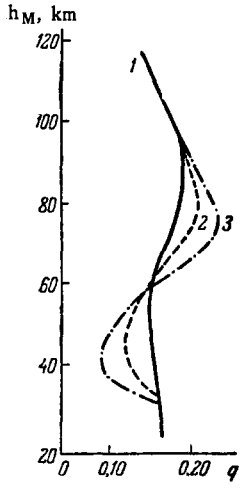

FIG. 45. Plot of q(H) for a standard molecular atmosphere (1) and for an atmosphere with one (2) and two (3) additional scattering layers.

Analogous calculations with similar results were made by Volz and Goody [81]. Quantitatively the behavior of q(H) for a delta-function layer during the period of total twilight in the near-zenith region of the sky is approximately described by the relation

$$q(H)=\frac{q_0(H)+\frac{\tau_c}{\tau'_p(\overline{H}_0)}\left(\frac{dT}{dy}\right)_{\frac{h_c-H}{\gamma}}}{1+\frac{\tau_c}{\tau'_p(\overline{H}_0)}T\left(\frac{h_c-H}{\gamma}\right)}, \qquad (58)$$

where $q_0(H)$ and $\tau'_p(\overline{H}_0)$ are the values of the corresponding quantities for the same H in the absence of a layer.

Thus, no matter how thin the layer, its presence is manifest in the plots of q(H) or $q(\zeta)$ in the form of a widely smeared perturbation. It is therefore impossible to resolve with the aid of these curves atmospheric altitude-structure details separated by distances smaller than approximately the extent of the penumbra that is, on the order of 20 km. We note that failure to take into account the real resolving power of the twilight-sounding method in some other cases [44,48,58,64] has also led to an erroneous treatment of the twilight observation data.

It follows from the foregoing that the small-scale irregularities both in the q(H) curves and in the p(H) curves, where p is the degree of polarization (see Fig. 22), do not reflect the structure of the atmosphere at all, but are merely a temporal effect, which is a manifestation of the instability of the atmosphere, and primarily, as shown by analysis, a manifestation of the variability of the scattering coefficient D in the region contained in the penumbra, a region with heights on the order of $\overline{H}$, with optical thickness τ^*, covering essentially the lower layers of the atmosphere (see [26]); it is also the result movement of the cloud masses in the terminator region along the terminator (that is, perpendicular to the rays of the sun). The presence and motion of clouds, and also the presence of mountain masses in the region of the terminator, can influence the value of y_n and consequently also $\overline{H}$, only if $h\sigma > a$, as pointed out already by E. A. Polyakova [165]. In particular, the presence of clouds or mountains becomes felt, especially in the long-wave region of the spectrum, when the sun is at the horizon and consequently the value of a decreases and becomes even negative. This leads to the appearance of the so-called "Buddha's rays," which represent essentially shadows of clouds or mountains blocking the sun's direct rays (predominantly long-wave, hence their color).

In conclusion we note that the correlation between the small-scale irregularities on the q(H), $q(\zeta)$, p(H), and $p(\zeta)$ curves, obtained in different regions of the sky for the same values of $\overline{H}$ or ζ, makes it possible, as a rule, to establish their nature, which is different in different cases. In addition, observations made on high mountains or on high-altitude airplanes should weaken considerably the influence of many causes of these irregularities (primarily the variability of the lower layers of the atmosphere [26]).

9. COLOR OF THE TWILIGHT SKY

The variability of its coloring is one of the most characteristic features of the twilight sky, and descriptions and measurements of this variability have been the subject of many investigations (see Secs. 2 and 3). The question of the theoretical de-

scription of the color of the sky and of its connection with the structure of the atmosphere as a function of ζ and z was first formulated in clear-cut form by R. Grunner [175]. However, his mathematical analysis pointed only to the general causes of the occurrence of the sunset coloring, but did not disclose in explicit form the roles of the individual factors. For particular models of the atmosphere, as applied to the sunset segments, such an analysis was carried out by direct calculations by E. A. Polyakova [165]. It followed also indirectly from the researches of N. M. Shtaude [64,168]. Finally, N. B. Divari [73], and later F. Volz and R. Goody [81], have carried out numerical calculations of the spectral variation of the brightness of the twilight sky, and also of its color exponent (1) for several pairs of values of λ_1 and λ_2, as a function of ζ for z = 70°, making various assumptions concerning the structure of the atmosphere. We note in passing that the foregoing investigations have disclosed the utter inconsistency of many attempts of purely speculative explanations of the coloring of the twilight sky (see, for example, [25]).

In general form, the connection between the coloring of the twilight sky and the structure of the atmosphere can be obtained in illustrative fashion by using the concept of the effective height of the earth's shadow [86]. In order to disclose more clearly the physical nature of the phenomena, let us consider the brightness of the sky for two wavelengths λ_1 and λ_2 such that $\overline{\eta}(\lambda_1) > \overline{\eta}(\lambda_2)$, and let us rewrite (51) for them in the form

$$I(\lambda_1) = I_0(\lambda_1)\,\omega_0\,P^m(\lambda_1)\,m\tau'_p[\overline{H}(\lambda_1), \lambda_1], \tag{59}$$

$$I(\lambda_2) = I_0(\lambda_2)\,\omega_0\,P^m(\lambda_2)\,m\tau'_p[\overline{H}(\lambda_1), \lambda_2] + \int_{\overline{H}(\lambda_2)}^{\overline{H}(\lambda_1)} D(h, \lambda_2)\,dh, \tag{60}$$

The meaning of (60) is obvious from Fig. 46. The first term in the curly brackets takes into account the scattering of light in that region of a sighting cone, which is situated above $\overline{H}(\lambda_1)$ and sends to the observer light of wavelengths λ_1 and λ_2 [see (57)]. In Fig. 46 this region is doubly hatched. If the effective shadow boundaries $\overline{H}(\lambda_1)$ and $\overline{H}(\lambda_2)$ were to coincide, then the difference between (59) and (60) would reduce only to the spectral variation of the scattering coefficient in the region $h > \overline{H}$, and also to the spectral dependence of the quantities I_0 and P. However, owing to the dispersion of the effective heights of the earth's shadow, an additional volume of sighting cone appears (singly hatched in Fig. 46), in which only light of wavelength λ_2 is scattered (for λ_1 this volume is in the effective shadow). The excess light of wavelength λ_2 formed by scattering in the region between $\overline{H}(\lambda_1)$ and $\overline{H}(\lambda_2)$ is taken into account by the second term in the curly brackets of (60). Because of the rapid decrease in the scattering coefficient with height, the relative contribution of this excess light to the total brightness of the sky depends to a great degree on the logarithmic gradient K of the scattering coefficient in the height interval between $\overline{H}(\lambda_1)$ and $\overline{H}(\lambda_2)$.

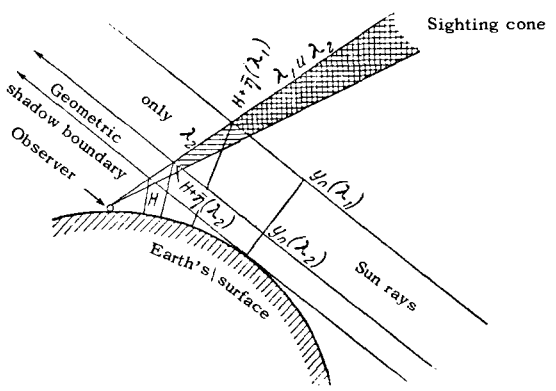

FIG. 46. Illustrating the effect of the dispersion of the effective heights on the color of the sky.

For a quantitative investigation of this effect we take logarithms of (51). Expanding $\ln \tau'_p[\overline{H}(\lambda_2), \lambda_2]$ in powers of $\Delta\overline{\eta} = \overline{\eta}(\lambda_1) - \overline{\eta}(\lambda_2)$ $(\Delta\overline{\eta} > 0)$, we confine ourselves to the third term of the expansion.

Substituting then the obtained expression in (1), we find that

$$CE^{\lambda_1}_{\lambda_2} = C^{\lambda_1}_{\lambda_2} + 1{,}08\left\{Q[\overline{H}(\lambda_1), \lambda_2]\,\Delta\overline{\eta} - \frac{1}{2}\left(\frac{dQ(\lambda_2)}{dh}\right)_{\overline{H}(\lambda_1)}(\Delta\overline{\eta})^2\right\}, \tag{61}$$

where

$$Q = -\frac{d\ln\tau'_p(h, \lambda)}{dh} \tag{62}$$

and

$$C^{\lambda_1}_{\lambda_2}(\overline{H}) = 1{,}08\left\{\ln\frac{I_0(\lambda_2)}{I_0(\lambda_1)} - m[\tau^*(\lambda_2) - \tau^*(\lambda_1)] + \ln\frac{\tau'_p[\overline{H}(\lambda_1), \lambda_2]}{\tau'_p[H(\lambda_1), \lambda_1]}\right\}. \tag{63}$$

At noon, when the sun is high above the horizon, $\overline{H}$ is practically equal to 0 over the entire visible range of the spectrum, that is, $\Delta\overline{\eta} = 0$ and $CE^{\lambda_1}_{\lambda_2} = C^{\lambda_1}_{\lambda_2}$ $(\overline{H} = 0)$. If the composition of the atmosphere does not change with height, then $C^{\lambda_1}_{\lambda_2}$ is independent of $\overline{H}$, and consequently of ζ. But in this case, as the sun approaches the horizon, $\overline{\eta}(\lambda)$ begins to increase, first slowly and then at an ever faster rate. At the same time, the $\Delta\overline{\eta}$ for any pair of wavelengths (see Figs. 34, 35, and 43) increase. This process has, however, an essentially uneven character. At first the increase of $\overline{\eta}$ is noticeable only in the short-wave part of the spectrum and extends only gradually into its long-wave part. In other words, the dispersion of the effective height first occurs and progresses only in the violet-blue region of the spectrum, and only with increasing ζ does it cover the orange-red region. When $\zeta = 80°$, in

particular, $\overline{H}(\lambda = 0.4\mu)$ already reaches 7—8 km whereas $\overline{H}(\lambda = 0.6\mu)$ is still at the 1—1.5 km level. When the sun has completely inclined to the horizon, $\overline{H}(\lambda = 0.4\mu)$ rises high into the stratosphere, while $\overline{H}(\lambda = 0.6\mu)$ barely reaches 5—6 km. This is precisely the explanation of the purple coloring of the snow-covered mountain tops (the so-called "blazing of the Alps"), which are still illuminated by the rays of the setting sun (but by only long-wave ones!), and also the purple color assumed more and more by the high clouds.

The development of the dispersion of $\overline{H}(\lambda)$ and its penetration into the long-wave region of the spectrum continues also during the entire period of the semitwilight and is responsible for the characteristic color changes of the sky of that time, that is, the sunset. If we confine ourselves as before to only a pair of wavelengths λ_1 and λ_2, then $\Delta\overline{\eta}$ increases monotonically during the semitwilight, that is, the sky reddens continuously until total twilight sets in, when $\Delta\overline{\eta}$ reaches its limiting value $\Delta\overline{\eta}_{\lim} \cong \gamma\Delta y_n$ (see Fig. 34). Simultaneously, the color exponent of the twilight sky

$$CE_{\lambda_2}^{\lambda_1} = C_{\lambda_2}^{\lambda_1} + 1.08\gamma\Delta y_n \left\{Q - \frac{\gamma}{2}\frac{dQ}{dh}\Delta y_n\right\} \qquad (64)$$

also reaches its limiting value.

One might expect that the color exponent of the sky should not change with further increase in ζ. This is not so, however, for an entirely different factor comes into play now.

In the preceding section we have seen that $d\overline{\eta}/dH \ll 1$ or $d\overline{H}/dH \cong 1$, that is, $q(h) \cong Q(h)$, during the time of total twilight if $dK/d\overline{H}$ is small. On the other hand, we have seen that during total twilight the value of $q(h)$ decreases generally speaking with increasing h (see Fig. 44). According to (64) this should lead to a decrease in $CE_{\lambda_2}^{\lambda_1}$, that is, the twilight sky should become more blue. This means that on the border of the total twilight the process of reddening of the sky is replaced by the sky turning blue, a process whose course should reflect the altitude variations of Q. This uncovers a possibility unusual in atmospheric optics, that of a direct quantitative experimental verification of the considerations developed above.

In fact, if we measure simultaneously the variation of ln I with ζ for λ_1 and λ_2, then $CE_{\lambda_2}^{\lambda_1}(\zeta)$ can be determined in two ways—directly from formula (1) and from formula (61), if we use the dependence of $\ln I(\lambda_2)$ on ζ, determine from it $q(\zeta, \lambda_2)$ and $dq(\zeta, \lambda_2)/dH$, and equate them to $Q(\zeta; \lambda_2)$ and $dQ(\zeta, \lambda_2)/dH$, respectively. We can then in first approximation put $C_{\lambda_2}^{\lambda_1} = \text{const}$ (which corresponds to an invariant composition of the atmosphere, while the value of $\Delta\overline{\eta}$ can be either determined from the values of $CE_{\lambda_2}^{\lambda_1}$ for two arbitrarily chosen values of ζ, or by using theoretical estimates of this quantity, for example on the basis of Figs. 30 and 33.

Such a verification was made in two variants. First the function $q(H)$ as measured by many authors was averaged and then the value of Δy_n was obtained (using calculations for the molecular atmosphere), making it possible to calculate from (64) the dependence of $CE_{\lambda_2}^{\lambda_1} - C_{\lambda_2}^{\lambda_1}$ on ζ for $z = 0$.

The results of the calculations are represented in Fig. 47 by a continuous curve, arbitrarily shifted relative to the ordinate axis [86]. The points on the same figure show the measured values of $CE_{\lambda_2}^{\lambda_1}$ (for the same pair of wavelengths), as obtained by T. G. Megrelishvili[53,57], also accurate to within a constant, and averaged over the spring period. There is a strikingly good agreement between the curves in the ζ interval from 94 to 99 or 100° and a sharp discrepancy for $\zeta \gtrsim 100°$ (to which we shall return). We note that in other seasons the agreement is worse, something that can easily be attributed to the increased turbidity of the atmosphere, since the presence of aerosol was disregarded in the theoretical calculations.

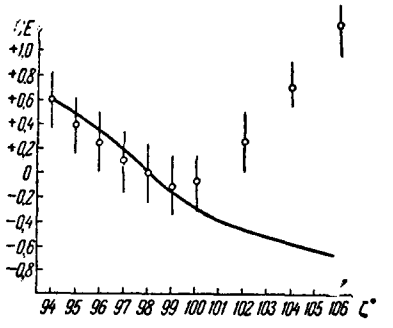

FIG. 47. Comparison of the calculated and measured $CE_{\lambda_2}^{\lambda_1}(\zeta)$ (averaged data).

We next used [86] the measured brightness of the twilight sky at the zenith in two parts of the spectrum ($\lambda = 0.44$ and 0.54μ) for three different twilights [79,26]. The corresponding variations of $CE_{\lambda_2}^{\lambda_1}$ are shown in Fig. 13 by the continuous lines drawn through the points. The crosses in the same figure show the values of $CE_{\lambda_2}^{\lambda_1}$ calculated from (62), with Δy_n obtained from Fig. 33 for the atmosphere considered by V. G. Fesenkov. (All the calculations of $CE_{\lambda_2}^{\lambda_1}$ were accurate to within a constant.) We see that for individual days the agreement is much better than for the averaged curves.

Finally, again starting from values of Δy_n for the molecular atmosphere and the averaged $q(h)$, we calculated the dependence of the quantity

$$\Delta CE = CE_{0.53\mu}^{\lambda_1}(\zeta = 98°20') - CE_{0.53\mu}^{\lambda_1}(\zeta = 95°20')$$

on λ_1 without account of the ozone absorption in the Chapuis band. It is represented in Fig. 48 by a continuous line. The same figure shows (with indication of the errors) the results of measurements by various authors (but in this case the unknown con-

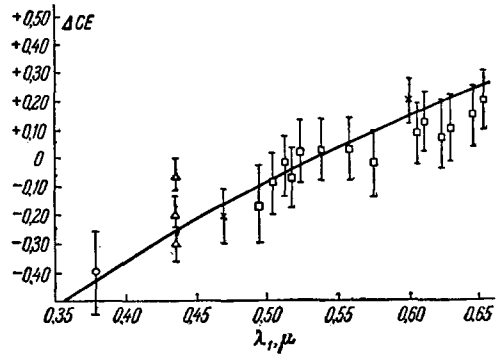

FIG. 48. Comparison of the calculated (solid line) and measured dependence of ΔCE on λ_1. Circle – [53]; triangle – Fig. 28; cross – [70]; square – [90].

stants have been eliminated and absolute values are compared). We see that with the exception of the Chapuis band ($\lambda \gtrsim 0.5\mu$), the theoretical curve duplicates accurately the variation of $CE_{\lambda_2}^{\lambda_1}$ with λ_1.

It follows from the foregoing comparisons that the main factor that determines the change of colors in the twilight sky during the periods of semitwilight and full twilight is indeed the dispersion of the effective height of the earth's shadow, in conjunction with the altitude variations of the logarithmic gradient of the optical thickness of the atmosphere. In addition, it is clear from Fig. 47 that on going to deep twilight the main role is assumed by other effects, which again cause the reddening of the sky (see the next section).

Turning to the gamut of colors of the twilight sky as a function of z and A for constant ζ, we must first recall that during one and the same instant of time the twilights at different points of the sky are at different phases, and that a variation occurs not only in H (and consequently Q), but also in γ and y_n. Therefore for a given ζ the distributions of the brightness and of the color exponent along the sun's meridian duplicate their ζ-dependences at constant z and A, but in a more or less distorted form.

Let us stop to discuss the color picture as observed in three directions where it is especially expressive.

It is easy to verify that in the region of the sky where the "belt of Venus" is observed (see Sec. 2), deep twilight has already set in at the corresponding instant of time and that γ is very large in this region. This means that the function T(y) is projected on the line of sight ($\eta = \gamma y$) in an extremely exaggerated form, and the more or less dense layers of the atmosphere are illuminated exclusively by rays with very small y_n, whereas rays with large y_n illuminate only the highly rarefied layers of the air (Fig. 49). This explains the so clearly pronounced purple coloring of the "belt," as well as its small angular dimensions. With increasing ζ this effect rapidly attenuates and the "belt" spreads out into a broad hardly noticeable band.

It is furthermore easy to see that the maximum reddening of the sky (that is, the border between the semitwilight and total twilight) at $\zeta = 94—95°$ is located in the vicinity of the sun's vertical at $z \cong 65—75°$. These are precisely the values of ζ and z which correspond to the maximum development of the "purple light" (see Sec. 2), so that there are all grounds for regarding the "purple light" as a unique projection of $CE_{\lambda_2}^{\lambda_1}(\bar{H})$ on the sky. Thus, the "purple light" should be observed in a purely molecular atmosphere and it must not be related at all, as is done by many authors, with the existence of an aerosol layer near 20—25 km, although the presence of the latter may intensify the effect. Apparently it is this phenomenon that was erroneously taken by F. Volz and R. Goody [82] to be evidence for the existence of such an aerosol layer. We note that owing to the indicatrix effect, the maximum reddening should then be noticeably shifted toward the horizon. Yet the presence of aerosol layers in the region of the terminator should affect strongly the character and degree of development of the "purple light" in the stratosphere, owing to the changes in the spectral dependence of y_n.

Finally, in the region of the sunset segment, the sharp increase in m(z) begins to leave its imprint on the color and brightness of the sky, and this intensifies the influence of the optical state of the lower layers of the atmosphere. A consequence of this is the displacement of the brightness maximum from the horizon by a certain z_m (see Figs. 6, 7, 8, 9), which depends strongly on τ^*. The dependence of $m(z_m)$ on τ^* for ζ close to 90°, that is, when the sunset segment is still on the daytime hemisphere, is determined by the following approximate relation, which is the result of (36),

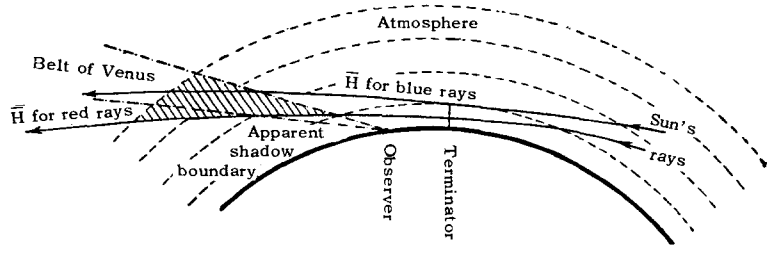

FIG. 49. Concerning the origin of the "Belt of Venus."

$$\tau^* = \frac{1}{m(z_m)}\left[1 - \frac{\frac{2KR}{m(z_m)\,m(\zeta)}}{\left(1+\frac{KR}{m(z)\,m(\zeta)}\right)+\left(1+\frac{KR}{m(z_m)\,m(\zeta)}\right)^3}\right]. \quad (65)$$

Figure 50 shows the corresponding dependence on τ^* for $\zeta = 90°$ and K = 0.15, and is in qualitative agreement with Fig. 9b. If ζ noticeably exceeds 90°, so that total twilight is already established in the region on the sunset segment, Eq. (65) is replaced by another relation, also approximate,

$$\tau^* \cong \frac{1}{m(z_m)} + Q(\overline{H})\,\frac{\overline{H}\xi}{(1+m(z_m)\,\xi)^2}, \quad (66)$$

where $\xi = \zeta - \pi/2$ as before. The corresponding plots of z_m vs. ξ for different τ^* and y_n are shown in Fig. 51, which is in good qualitative agreement with Fig. 8b. We note that in (66) the values of τ^* and $\overline{H}$ (that is, y_n) must be regarded as independent functions of the wavelength, for as a rule there is no correlation between the horizontal and vertical transparencies of the atmosphere [26]. Nonetheless, the decrease in wavelength should generally speaking lead to an increase in z_m. It is precisely this circumstance that determines, in final analysis, the coloring of the sunset segment and its dependence on the state of the weather.

10. THE PROBLEM OF MULTIPLE SCATTERING: DEEP TWILIGHT AND THE TRANSITION TO NIGHTTIME.

It was shown above that a study of the attenuation and single scattering of light under twilight conditions leads, at least qualitatively and in many respects even quantitatively, to a correct picture of the fundamental twilight phenomena. At the same time we are able to verify that the notion of the effective height of the earth's shadow enables us to clarify the analysis of the twilight phenomena, without loss of accuracy in their description. However, even Lambert [176] has called attention to the fact that an appreciable role can be played in the formation of the twilight (at least in the region of the sky covered by the projection of the earth's shadow) by self-illumination of the atmosphere, that is, multiple scattering of the light from the sun in the atmosphere. Therefore a reliable estimate and account of multiple scattering as it affects the brightness of the twilight sky are essential both for an estimate of the degree of correctness of the considerations developed above and for a reliable utilization of twilight sounding for investigations of the upper layers of the atmosphere, as already noted by V. G. Fesenkov in his first paper on this problem [4].

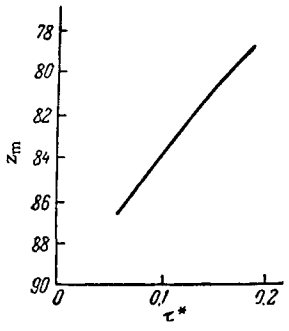

FIG. 50. Approximate τ^*-dependence of the position of the maximum brightness of the dawn or sunset segment at the instant of sunrise or sunset.

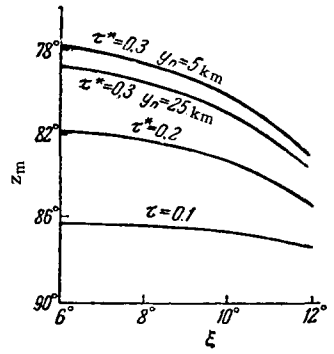

FIG. 51. Approximate plots of the position of the maximum of the brightness of the sunset segment vs. ξ for large ξ and different τ^* and y_n.

However, theoretical investigations of the contribution of multiple (predominantly double) scattering to the brightness and polarization of the twilight sky, undertaken by many authors [4,11,45,50,59,132,172,173,177–188] unavoidably encounter difficulties that have not yet been overcome. Even under daytime conditions, when the curvature of the earth's surface can be neglected and when only the lower layers of the atmosphere, for which the optical properties of air and their altitude variation are more or less known, need be taken into account, the problem of calculating the brightness and polarization of multiply scattered light from the sky entails serious difficulties and has been realized for the time being only for a few strongly idealized models (see, for example, [189–199]). During the time of twilight one can no longer neglect the curvature of the atmosphere, and this radically complicates the mathematics since the one-dimensional problem becomes three-dimensional. The corresponding methods of solving the radiation transport equation have not yet been sufficiently developed, so that the only way for solving the problem is the exceedingly laborious process of tracing the fate of each ray as it wanders through the atmosphere. It is necessary to start here with some assumptions, as yet unfounded, concerning the altitude variation of the scattering indicatrix and coefficient of the air, assumptions that influence the computational results quite strongly. A special analysis [50,179,180] has shown that the brightness of doubly scattered light I_2 varies relatively little with the choice of the model of the atmosphere, whereas the brightness of the singly scattered light I_1 is completely determined by this choice; and since I_1 and I_2 vary during the course of the twilight by at least a factor 10^7, even insignificant changes in the assumed form of $\tau'_p(h)$ change radically not only the value of I_2/I_1 but also its variation with ζ. By way

Table I

ζ	92°	94°	96°	98°	100°	101°	102°	103°	104°	105°	107°
"Twilight" atmosphere [180]	0.20	0.23	0.33	0.62	0.63	—	—	—	—	—	—
"Standard" atmosphere from data for 1948 [181]	—	0.30	0 49	0.76	0.78	—	0.87	0,97	1,16	1,68	2,40
Isothermal atmosphere [180]	0,20	0,23	0.53	3.65	97.5	—	—	—	—	—	—
Isothermal atmosphere [45]	—	0.01	0,11	1,3	20	85	$2\cdot10^4$	$3\cdot10^5$	—	—	—

of an example we give some of the calculated data on the dependence of I_2/I_1 on ζ for z = 0, obtained under different assumptions concerning the altitude variation of $\tau'_p(h)$ (Table I).

Thus, theoretical calculations do not give grounds as yet for any reliable estimates of the value of I_2/I_1 and its dependence on ζ and λ. Nevertheless we can conclude from them that under reasonable (from the point of view of present-day knowledge) assumptions concerning the altitude variation of the scattering ability of the atmosphere, the relative role of the double scattering during the semitwilight and total twilight periods should be not too large, although not small, so that it cannot change the picture of the sky appreciably, unlike the stage of deep twilight, when double scattering begins to predominate over single scattering.

Another important result of the theoretical analysis is the conclusion [45,180,184] that the main source of the doubly scattered light observed on earth is a layer of the atmosphere covering a relatively small altitude interval extending over about 20 km, whereas the maximum brightness of this layer, for ζ close to 90°, is located near the earth's surface and rises gradually with increasing ζ, reaching an altitude of about 20—30 km by the end of the total twilight. During the period of total twilight the main source of its illumination by singly scattered light becomes the sunrise segment.

With the theory in this state, it is obvious that observational data remain the only reliable source for judging the role of multiple scattering during the twilight period. However, before we proceed to consider them, we must stop on some considerations without which such an analysis would be impossible.

According to Rayleigh's theory, the coefficient of scattering of light by gases, outside the selective-absorption bands, is proportional to λ^{-4}. Since a factor of the same form for each new scattering event, is added it might be expected that the spectral dependence of k-fold scattering of light should be determined by a factor λ^{-4k}. These considerations are universally accepted, and many attempts were made to use them to determine the fraction of double scattering both during daylight and twilight conditions, starting from data concerning the color of the sky. In particular, F. Link [172,173] and F. F. Yudalevich [188] concluded on the basis of this assumption that I_2/I_1 should decrease rapidly with increasing wavelength and should amount to only several per cent in the near-infrared region of the spectrum. The fact that the sky turns blue with increasing ζ during total twilight was also usually attributed to an increase in the role of double scattering. The only difficulty was seen in the fact that in the presence of an aerosol the λ^{-4} law is replaced by a weaker dependence λ^{-n}, where $n < 4$.

However, the statement that the color of k-fold scattered light is determined by a factor λ^{-kn} does not correspond to reality, since it does not take into account the very strong extinction effect. As applied to the color of the twilight sky, this was pointed out by E. Ashburn [59] and G. V. Rozenberg [86]. A rigorous account of extinction for the doubly scattered light is indeed the main difficulty in the calculation of its brightness. It is therefore necessary for the time being to confine oneself to general considerations and to tentative estimates.

It has been long known, first, that a sufficiently thick layer of nonabsorbing scattering medium (for example, milk, clouds, snow, whitewash, paper) appears white in reflected light independently of the spectral variation of the scattering coefficient. Theory shows (see, for example, [157,200]) that this is the direct consequence of the fact that the main contribution to the brightness of the light reflected by the layer is made precisely by multiple-scattering effects. In transmitted light, if the layer is sufficiently thick so that the direct and in practice singly-scattered light does not reach the bottom of the layer at all, theory predicts [157] that the brightness I of scattered light is proportional to $(\tau^*)^{-1}$, that is, in the case of molecular scattering ($\tau^* \sim \lambda^{-4}$) we have $I \sim \lambda^4$ or, in other words, multiply-scattered light turns out to be much "redder" not only than singly scattered light, but even than direct light.

Further, using the results of Secs. 6, 8, and 9, we can calculate the color exponents $CE_{\lambda_2}^{\lambda_1}$ for light singly scattered by the atmosphere and coming from the zenith at $\zeta = 98°$, and for light initially scattered by the high layers of the atmosphere in the region of the maximum brightness of the sunset segment and doubly scattered in the lower layers of the atmos-

phere (for the same value of ζ). Direct calculation for $\lambda_1 = 0.46$ and $\lambda_2 = 0.54$ leads to an approximate relation

$$\left(\frac{I(\lambda_2)}{I(\lambda_1)}\right)_{\text{double}} \cong 2{,}3\left(\frac{I(\lambda_2)}{I(\lambda_1)}\right)_{\text{single}},$$

that is, in the doubly scattered light the green part of the spectrum turns out to be much more intensified relative to the blue part, compared with the singly scattered light.

The foregoing estimate must be regarded only as a qualitative illustration. Nonetheless, there are all reasons for stating that if the doubly scattered light of the twilight sky does differ in color from the singly scattered one at all, it is only in that the longer wavelengths predominate. From this it follows, incidentally, that the observed bluer color of the sky with increasing ζ during total twilight is evidence of the relatively insignificant role of multiple scattering during that period. We note that doubly scattered light, being "redder" than singly scattered light, nevertheless remains "bluer" than the direct light, that is, the brightness of doubly scattered light should increase monotonically with decreasing λ.

Finally, using the results of the preceding sections, we can roughly estimate the change in brightness of the secondarily scattered light as a function of z in the sun's meridian. Neglecting the indicatrix effect, such an estimate leads for not too large values of z to

$$I_2(z) \cong I_2(z=0)(1 + c\cdot 5\cdot 10^{-2}\tan z)\sec z, \quad (67)$$

where $c < 1$ and z is assumed positive in the vertical and negative in the counter-vertical of the sun, so that the minimum brightness of the secondarily scattered light turns out to be shifted away from the zenith in the side opposite the sun by not more than 2°.

Let us turn now to qualitative considerations, dictated by the general picture of the twilight sky. It is impossible to disagree with Lambert [176], that the very fact that the region of projection of the earth's shadow on the counter-sun horizon has a noticeable brightness, comparable with the brightness of the sky illuminated by the sun's direct ray, is evidence of the considerable contribution made by multiple scattering to the total brightness of the sky. This is also evidenced by the existence of a pronounced minimum in the brightness of the sky in the vicinity of the zenith [7,16,27,35] (see Figs. 5, 6, and 10). At the same time, starting with the contrast sensitivity of the eye and with the fact that the brightness of multiply-scattered light should not depend strongly on the sighting direction, it follows that for small ζ the ratio I_2/I_1 in the counter-vertical of the sun should be on the order of 10–20 per cent (compare Figs. 6 and 10) (we recall that in daytime conditions I_2/I_1 has the same order of magnitude [194-198]). In particular, the very existence of a more or less sharp boundary of the earth's shadow and the good observability of the "belt of Venus" allow us to state that even during total twilight I_2 cannot exceed I_1 by more than several times.

In exactly the same way, the noticeable displacement of the minimum of brightness relative to the zenith [207], exceeding by many times the above-mentioned approximate value of 2°, is evidence that in this region of the sky the secondary scattering does not have a decisive significance. For a quantitative estimate of this effect we can use relations (51) and (67) and take account of the fact that $I_2 \sim P^m$ m, just as I_1. The condition for the brightness of the sky to have the minimum $d(I_1 + I_2)/dz = 0$ for $|z| \ll 1$ leads then to the approximate relation

$$z_{\min} \cong -\frac{Q(\overline{H}_{\min})\,\overline{H}_{\min}\xi + c\cdot 5\cdot 10^{-2}\,[I_2(z_{\min})/I_1(z_{\min})]}{(1+\ln P)\left[1+\frac{I_2(z_{\min})}{I_1(z_{\min})}\right]}, \quad (68)$$

where account is taken of the fact that during total twilight

$$\frac{d\ln\tau'_p(\overline{H})}{dz} \cong \frac{d\ln\tau'_p(\overline{H})}{d\overline{H}}\,\overline{H}\,\frac{d\gamma}{dz} \cong Q(\overline{H})\,\overline{H}\xi, \quad (69)$$

hence, taking (46), (91), and (92) into account we find

$$\frac{I_2(z_{\min})}{I_1(z_{\min})} \cong \left[\frac{G[H(\xi)]\,\xi}{|z_{\min}|(1+\ln P)\int_{H(\xi)}^{\infty}\frac{G(H)}{H+\bar{y}}\,dH} - 1\right] \times\left[1-\frac{c\cdot 5\cdot 10^{-2}}{|z_m|(1+\ln P)}\right]^{-1}, \quad (70)$$

which enables us to obtain a tentative estimate of I_2/I_1, with

$$\frac{I_2(z=0)}{I_1(z=0)} \cong \frac{I_2(z_{\min})}{I_1(z_{\min})}\,\frac{1-Q(\overline{H})\,\overline{H}\xi\,|z_{\min}|}{1-c\cdot 5\cdot 10^{-2}\,|z_{\min}|}. \quad (71)$$

Among the attempts of determining experimentally the contribution of the secondary scattering to the brightness of the twilight sky, the greatest objections have been evoked by the work of R. Robley [138]. The idea underlying this work is that if the scattering in the high layers of the atmosphere has a purely molecular character, that is, it obeys Rayleigh's law with the Cabannes correction, and if the doubly scattered light is completely depolarized, then we can determine I_2/I_1 from the observed polarization defect. However, these two initial premises are known to be in error, so that Robley's estimates are not reliable. First, there is no longer any doubt at present that at all altitudes there are noticeable quantities of aerosol, which change radially the degree of polarization of the scattered light (see for example [3,26]), and not necessarily always on the down side. Second, under twilight conditions the degree of polarization of the doubly scattered light is

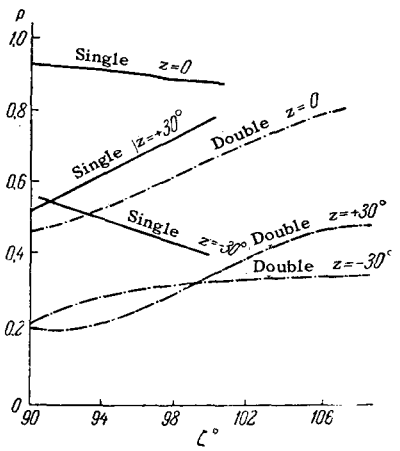

FIG. 52. Plot of the degree of polarization of singly and doubly scattered light of the twilight sky against ζ for different z in the case of a molecular atmosphere.

quite high and may reach 80 per cent and more [50, 132,183,184]. Figure 52 shows the ζ-dependences of the degree of polarization of singly and doubly scattered light for z = 0° and ±30°, as calculated by J. Dave [94] for an isothermal molecular atmosphere. Comparison with the experimental data [67] shows that in all cases the really observed degree of polarization is smaller than the calculated one, but the character of the dependence of $p(\zeta)$ turned out to be similar. We clearly see here, first, a relative displacement of the experimental and theoretical curves along the abscissa axis, indicating that the role of secondary scattering has been overestimated in the calculations, and second, that the sharp decrease in the degree of polarization for $\zeta \gtrsim 102°$ (see Sec. 4) can be attributed to the progressing visibility of the night sky through the veil of scattered light.

The first sufficiently well-founded empirical estimates of the role of double scattering was obtained in 1934 by V. G. Fesenkov [37]. They were based on measurements of the sky brightness at two points of the sky, with coordinates z = 67° and A = 0 and π. Supported by these data and using the concept of the twilight layer, Fesenkov consistently calculated the brightnesses of the singly and doubly scattered light for both points. He obtained for the ratios $I(A = \pi)/I(A = 0)$ the following values:

ζ	92°	94°	96°	98°
$\frac{I_1(\pi)}{I_1(0)}$	0.64	0.26	0.054	0.01
$\frac{I_2(\pi)}{I_2(0)}$	0.67	0.50	0.42	0.16

Thus, the ratio $I_2(\pi)/I_2(0)$ varies with changing ζ incomparably more slowly than $I_1(\pi)/I_1(0)$.

Simultaneously, Fesenkov obtained the following values of the ratio I_2/I_1 (this ratio is arbitrarily taken as 1 for ζ = 92 for the point z = 67°, A = 0):

ζ	92°	94°	95°	98°
$A=0$	1	0.82	0.90	0.99
$A=\pi$	0.01	1.54	6.8	14

The data of the last table show unambiguously that whereas for A = 0 and z = 67° the role of secondary scattering remains almost unchanged (as we have seen, semitwilight and the bright part of total twilight still predominate in this region of the sky for the indicated values of ζ), for A = π and the same value of z the role of double scattering increases rapidly, and when ζ = 96° it already decisively predominates over single scattering (we note that this interval of variation of ζ in this region of the sky encompasses the dark part of the total twilight and essentially the deep twilight).

The most important result of this investigation of V. G. Fesenkov is the conclusion that when the sun lies sufficiently far below the horizon (say at ζ = 96°) the brightness of the sky at the point with coordinates z = 57° and A = π is determined almost completely by the intensity of the doubly scattered light and that its intensity differs relatively little from its intensity at the analogous point of the sun's vertical (A = 0), whereas the brightness of singly scattered light at this point is incomparably higher. From this follows directly a method for estimating the brightness of the secondarily scattered light at the point z = 67° at A = 0, consisting of the simple procedure of multiplying $I(A = \pi)$ for the same value of ζ by the little-varying ratio $I_2(A = 0)/I_2(A = \pi)$. This method of eliminating the contribution of the secondary scattering from the results of the measurements of the twilight-sky brightness has been used many times by various authors (for example, [65]), but has been subjected in recent times to an appreciable improvement by V. G. Fesenkov [201].

Making use of the results of the preceding sections, we can also propose some modification of this method, starting from the fact that the brightness of the singly scattered light at a point (A = π, z) with the sun having a zenith distance ζ should be equal to its brightness at the point (A = 0, z) for ζ', if $\overline{H}(\zeta, -z) = \overline{H}(\zeta', +z)$, which leads to the equality $I_2(\zeta, -z) \cong I(\zeta, -z) - I(\zeta', +z)$, where I is the measured brightness of the sky, and where a relatively small quantity, equal to $I_2(\zeta', +z)$ has been left out (Fig. 10). Since ζ and ζ' are related by the equation

$$\frac{R(1-\sin\zeta)+\bar{y}}{\sin(\zeta+z)} = \frac{R(1-\sin\zeta')+\bar{y}}{\sin(\zeta'-z)},$$

the main difficulty consists in determining $\bar{y}$. How-

ever, when $I(\zeta, -z) \gg I(\zeta, +z)$, that is, after the occurrence of deep twilight in the region of the sun's counter-vertical, the uncertainty in $\bar{\gamma}$ does not introduce an appreciable error as compared with neglecting the indicatrix effect.

Mention should further be made of the semi-empirical work of G. V. Rozenberg [86] and N. B. Divari [73], who have shown by various means that calculations of $CE_{\lambda_2}^{\lambda_1}$, based on an account of single scattering only, are in good agreement with the observations only until the end of total twilight, and disagree completely with the results when the sky no longer turns blue but again reddens. N. B. Divari proposes that the reddening is already due to the beginning transition to nighttime, that is, to the fact that the atmosphere's own illumination, which is more intense in the red region of the spectrum enters into play. However, as we have already seen, this can also be due to the increasing role of double scattering (which by all accounts is of little importance during the total twilight period), all the more since the reddening process usually begins for smaller values of ζ than expected from the assumption of N. B. Divari (see Figs. 11—13).

Finally, T. G. Megrelishvili and I. A. Khvostnikov [65,202] obtained independent and very weighty proof of the relative smallness of the role of multiple scattering during total twilight and the increase of this role on going to deep twilight. The gist of their result is that data on the density and pressure of the atmosphere, extracted from observations of the twilight sky, are in good agreement with the data obtained by other methods (including rocket methods), so long as total twilight governs in the region of observation, and depart decisively from them when deep twilight sets in, unless corrections for double scattering are introduced. On the other hand, if such corrections are introduced by using the method of V. G. Fesenkov employed above, then the agreement extends also to larger heights (at least to 120—130 km) (Fig. 53). The estimates of I_2/I_1 turn out to be then close to those calculated by F. F. Yudalevich and N. M. Shtaude (for the "twilight" atmosphere) (see above).

Let us turn to the color exponent $CE_{\lambda_2}^{\lambda_1}$ and let us again trace its dependence on ζ for a given region of the sky (z, A), for example for the zenith. Under daytime conditions ($\zeta \ll 90°$) we have $CE_{\lambda_2}^{\lambda_1} = C_{\lambda_2}^{\lambda_1}$, where $C_{\lambda_2}^{\lambda_1}$ is given by (63). As the sun approaches the horizon, a progressing dispersion of the effective heights of the earth's shadow occurs and causes an increase in $CE_{\lambda_2}^{\lambda_1}$, that is, a reddening of the sky, which corresponds to the semitwilight or sunset phase (Fig. 54). At a certain value of ζ,

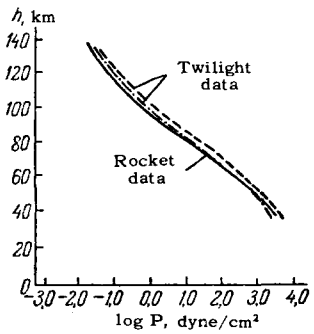

FIG. 53. Comparison of the altitude dependence of the air pressure as determined by rocket measurements and from twilight data after introducing corrections for double scattering.

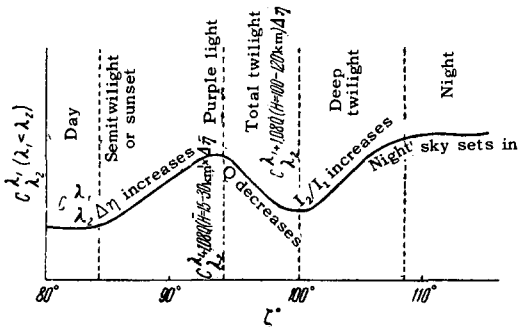

FIG. 54. Diagram showing the change in the phases of the twilights for the region of the sky close to the zenith ($\eta - \bar{\eta}$). The ordinates represent $CE_{\lambda_2}^{\lambda_1}$.

the increase in $\Delta\bar{\eta}$ stops, and the principal role is assumed by the altitude dependence of $Q = d \ln \tau'_p/dh$, which is usually manifest in the sky turning progressively bluer and corresponds to the total twilight phase. Further, when the height of the geometrical shadow reaches approximately 100 km, the role of the doubly scattered light begins to increase rapidly, and this causes a new reddening of the twilight sky and contributes to the occurrence of the deep twilight phase. Soon after its occurrence, the night sky begins to be visible through the veil of the scattered light from the sun, and the deep twilight phase ends with transition to night. The instants at which the phases changes, and the durations of the latter, depend on the choice of the wavelength interval and on the sighting direction. Attention must be called to the fact that during the entire period of the twilight the sky is redder than in the day and is usually bluer than at night.

Since the polarization of the doubly scattered light is sufficiently large, but is smaller than the singly scattered light, the occurrence of deep twilight should manifest itself also in the course of the $p(\zeta)$ curves, but to a lesser extent than in the $CE_{\lambda_2}^{\lambda_1}(\zeta)$ curve. This is precisely how R. Robley [183], J. Dave [94], and N. B. Divari [70] explain the "ledge" or minimum of polarization in the angle region $\zeta = 96—100°$ (see Figs. 22—24 and 26). However, there are two kinds of objections to this explanation.

First, the aggregate of the data makes it necessary to recognize that the role of the double scattering greatly increases for large ζ, and second, the larger λ, the smaller the values of ζ at which the influence of the doubly scattered light, which is

"redder" than the singly scattered light, should manifest itself, whereas actually the opposite takes place (see Fig. 26). For the same reason, this ledge cannot be ascribed to the contribution of the unpolarized light from the night sky. At the same time, if the polarization is due to the presence of an aerosol layer at altitudes 80—100 km, that is, in the region of the silver clouds and the sharply pronounced temperature inversion, it should manifest itself at smaller ζ the larger the value of λ, owing to the dispersion of $\overline{H}(\lambda)$, as is actually the case. One must add to this that in the entire height interval the real degree of polarization is smaller than the degree of polarization of the doubly scattered light, that is, the scattering has an essentially aerosol character in the entire altitude interval. But then the correlation between the degree of depolarization of the critical frequency of the reflection of radiowaves from the E layer becomes understandable, since the reflection frequency, as is well known, increases with increasing falling of meteors, and consequently, with increasing turbidity of the mesopause region. Additional arguments in favor of such a conclusion are obtained from the polarization measurements of G. Dietze [80] and also from the fact that with further increase of ζ there frequently occurs an increase in the degree of polarization (see Figs. 22 and 23), which is perfectly understandable if one starts from the hypothesis that the role of double scattering or of the glow of the atmosphere increases.

However, when $\zeta \cong 102—104°$, that is, when $H \cong 200—250$ km, a sharp change is observed in the $p(H)$ or $p(\zeta)$ curves (see Figs. 22, 24, 26), obviously due to the progressively increasing role of the glow from the night sky, as is clear also from the calculations of J. Dave [184] and from the character of the dependence $q = -d \ln I/dH$ on ζ [50], as well as from a simple comparison of the brightness of the sky at corresponding ζ with the brightness of the night sky (see Figs. 3, 4, 25). This again explains the correlation of the degree of depolarization of the light from the sky in the corresponding region of angles ζ with the critical frequency of reflection of the radiowaves from the F layer, since the brightness of the night sky is closely related with the state of the ionosphere. In conclusion we add that V. L. Ginzburg [203] has demonstrated the inconsistency of I. A. Khvostnikov's initial idea, according to which the depolarization was attributed to features of the scattering of light by ions. G. V. Rozenberg [50] has also shown that it likewise cannot be due to peculiarities in the scattering by the molecules located in the earth's force field.

11. THE INVERSE PROBLEM OF TWILIGHT THEORY AND TWILIGHT SOUNDING OF THE ATMOSPHERE

We have concluded above that during the time of semitwilight and total twilight the main factor causing the brightness of the sky is the single scattering of the sun's direct rays over the level of the effective boundary of the earth's shadow. In this case, although the role of double scattering is noticeable it is not so considerable. On the other hand, during deep twilight the mechanism governing the luminosity of the sky changes twice: first the dominant role is assumed by the multiply scattered light, and then by the glow from the night sky. Therefore, from the point of view of extracting information on the structure of the atmosphere from twilight observations, only semitwilight, total twilight, and in part the bright part of the deep twilight (to the extent to which the effects of multiple scattering can be taken into account) are of interest.

We have seen further that during the period of semitwilight the main phenomena occur in the lower relatively well investigated layers of the atmosphere, and are furthermore highly complicated by the effect of refraction on $\overline{H}$. Therefore the interpretation of data pertaining to semitwilight becomes unreliable on the one hand and less interesting on the other. To the contrary, during the period of total twilight, particularly in the short-wave part of the visible range of the spectrum, the role of refraction becomes little noticeable, and the main significance is assumed by the conditions under which light is scattered in the altitude interval approximately between 20—30 and 100—120 km, that is, in a region of the mesosphere and lower ionosphere which has been relatively little investigated and is not readily accessible.

For these reasons, the most promising to twilight sounding of the atmosphere is the stage of total twilight, predominantly in the region of the sky near the zenith, where the interference caused by the variability of the lower layers of the atmosphere is reduced to a minimum. We must add that in order to interpret the twilight phenomena it is usually sufficient (except for a special case) to confine oneself to the solar meridian (where the picture is simpler), since the remaining regions of the sky do not contain additional information concerning the state of the upper layers of the atmosphere. Finally, the brightness of the singly scattered light changes over the extent of the total twilight by a factor of approximately 10^5, whereas the contribution of the double scattering changes this quantity by not more than a

factor of 2. This gives grounds for neglecting, for the time being, the double scattering (in the next section we shall fill this gap).

Taking the foregoing qualifications into account, we can rewrite (44) in the form

$$I(z, A, \zeta, \lambda) = I_0(\lambda)\omega_0 P^{m(z)}(\lambda) m(z) \times \int_0^\infty D(h, \zeta - z, \lambda) T\left[\frac{h - H(\zeta, \lambda)}{\gamma(\zeta, \lambda)} - y_n(\lambda)\right] dh. \quad (72)$$

If we regard it as a function of ζ for z = const or as a function of z for ζ = const, then from the mathematical point of view (72) represents with respect to D a Volterra integral equation of the first kind with kernel T, and if the function T were known, the equation could be solved by usual methods of integral-equation theory. The difficulty of the inverse problem of twilight theory lies precisely in the fact that the kernel T is unknown and depends on the atmospheric conditions, that is, it must be determined, like D, from observations of the twilight sky. (Direct methods of determining T, for example with the aid of rockets and satellites or by observation of silver clouds, which are perfectly essential for the development of twilight theory, can be useful only if the places and times of the measurements coincide.) This possibility arises because of a combination of two circumstances. First, during total twilight D is determined by the state of the mesosphere, whereas T is determined by the state of the troposphere and the lower stratosphere, making these functions independent. Second, the tracing of the variation of $I(\zeta, z)$ can be regarded a scanning of the function D with the aid of an apparatus function T, but, unlike in laboratory problems, the apparatus function varies regularly during the scanning process. The scanning is carried out here independently in two directions (ζ and z). Inasmuch as the variation of the apparatus function with ζ differs from the variation with z, and since these variations are known, the analysis of the dependence of I on the coordinates in the ζ, z plane makes it possible to determine both D(h) and D(y) (see Sec. 12 for more details). Another way is to specify a certain averaged function T, starting from our information concerning the structure of the lower layers of the atmosphere, and accordingly neglecting its variability.

A consistent solution of the inverse problem of twilight theory with T(y) specified beforehand was first undertaken by V. G. Fesenkov [4], who started from his own measurements of the brightness of the twilight sky in the zenith. Assuming that $D \sim \rho$ (where ρ is the air density) and that $\rho(h) = \rho_0(h)[\alpha + \beta h + \gamma h^2]$ (where $\rho_0(h)$ is a specified function while α, β, and γ are unknown constants), Fesenkov determined these constants by the method of least squares. As shown by N. M. Shtaude [39], the specific $\rho(h)$ dependence obtained in [4] cannot be regarded as corresponding to reality, since the solution contained many arbitrary assumptions. However, the analysis carried out by V. G. Fesenkov was of primary significance and served as the basis for further development of twilight theory, leading, in particular, to the formulation of the concept of the twilight layer (see Sec. 7).

Referring the reader to the original papers [31,37, 39,54,167-170] for details, we shall touch upon only a few basic premises connected with the use of this concept for the solution of the inverse problem.

Assuming that within the limits of the twilight layer we have

$$\varrho(h) = \varrho(H) e^{-K(h-H)},$$

where K is a constant, and choosing on the basis of calculations carried out in [5] the function T(y) in the form

$$T(y) = \exp[-\alpha + \beta\sqrt{y} + \gamma y],$$

where β = 3.83 and γ = 0.352, Fesenkov [31] substitutes these expressions in (72) and arrives at the approximate relation

$$\frac{d \ln I}{d\zeta} = \frac{\cos\zeta}{\sin^2\zeta} RK, \quad (73)$$

which connects K with d ln I/dζ. (A more exact solution obtained in [31] was never used for an analysis of twilight, because of its complexity.) As shown by N. M. Shtaude [39], the same expression is obtained directly from the concept of twilight layer, if it is assumed that its illumination does not depend on either h or ζ. Later on the same expression was obtained in a somewhat different manner by F. Link [141,171] (see also [116,117]). It is easy to show that under these assumptions (73) is equivalent to stipulating that

$$I(\zeta) = \text{const} \cdot \varrho(h_m),$$

that is, that the brightness of the sky must be proportional to the air density at the level h_m of the maximum brightness of the twilight layer.

Were the scattering actually to have a molecular character in the region of the mesosphere, that is, were there no aerosol at the corresponding altitudes then, assuming further that the atmosphere is in static equilibrium, it is easy to arrive at the relation

$$K = \frac{gM}{R_0 T(h)} + \frac{d \ln \tau(h)}{dh},$$

where R_0 is the gas constant, M is the molecular weight, g the gravitational acceleration, and T(h) the temperature. Thus, measurements of $I(\zeta)$ and consequently of K have yielded directly the altitude variation of the temperature in the mesophere. We add that the use of the more correct relation $I(\zeta)$

$\sim \tau'_p(h_m)$, which follows from the more refined concept of twilight layer [84], instead of (73), leads in this case to the expressions

$$\frac{d \ln I}{d\zeta} = \frac{gM}{R_0 T(h)} \frac{\cos\zeta}{\sin^2\zeta} R, \tag{74}$$

where R is as before the earth's radius,

$$\frac{dI}{d\zeta} = I_0 \omega_0 P \sigma_0^{mol} \frac{\cos\zeta}{\sin^2\zeta} R \frac{\varrho(h_m)}{\varrho_0} \tag{75}$$

and

$$I = I_0 \omega_0 P \sigma_0^{mol} \frac{R_0 T_0}{gM} \frac{p(h)}{p_0}, \tag{76}$$

where σ_0^{mol}, ρ_0 are the scattering coefficient, density, and pressure of pure air at sea level, while $\rho(h_m)$ is the density of the air at an altitude h_m; from these we can obtain the functions T(h), ρ(h), and p(h).

Actually, the scattering of light at all levels, including the mesosphere, has essentially an aerosol character and, strictly speaking, the assumption $\sigma \sim \rho$ is unfounded. However, this should not manifest itself appreciably on the determination of ρ and T if, of course, one excludes cases where clearly pronounced aerosol layers exist [26]. First, the role of the aerosol scattering decreases rapidly with decreasing λ, making it possible in principle to separate the effects of the aerosol and molecular scattering. Second, if we exclude cases where aerosol layers are present (for example, mother-of-pearl or silver clouds), then the relative concentration of the aerosol changes relatively little with altitude (see [26] and [195], part II), so that the assumption $\sigma \sim \rho$ is not far from reality. The variations of the aerosol lead, as a rule, to variations of σ by not more than two or three times [26]. At the same time, in the height interval of interest to us, σ varies at least by four orders of magnitude, and within the limits of the half-thickness of the twilight layer, over which one actually averages the data of the twilight sounding, it changes by almost half an order. In other words, the uncertainty due to variations of the aerosol contents turns out to be less than the uncertainty due to the unreliability of the value of h_m, that is, the height to which the measurement results pertain. We note incidentally that the errors in rocket measurements of ρ and T are for the time being not much less, than the errors connected with failure to take the role of the aerosol into account.

In this connection let us dwell on three investigations which are the most significant, both with respect to observational material on which they are based and with respect to the deductions obtained. In 1948 a paper was published by T. G. Megrelishvili and I. A. Khvostnikov [202], in which the first summaries of the reduction of prolonged and quite thorough measurements of the brightness of the twilight sky were published, from the point of view of obtaining data on the density and pressure of the air in the high layers of the atmosphere. Results of the processing of the individual sporadic measurements were reported earlier by many authors. The feature of the cited paper was precisely the large quantity of initial data, which encompassed 250 individual $I(\zeta)$ curves, enhancing the reliability of their averages. By eliminating from the observational data the background of the night sky and by using relations (74)—(76), the authors have determined the average "climatic" altitude variation of the pressure, density, and the so-called height of the homogeneous atmosphere R_0T/gM, comparing them with data obtained by other methods (Fig. 55). It is easy to see that up to heights on the order of 100 km, there is satisfactory agreement, and the noise due to double scattering is not eliminated from the twilight data.

The second paper was published by T. G. Megrelishvili [65] in 1956, and was devoted to a special analysis of the reconciliation of the data obtained by the method of twilight sounding with those obtained by other methods. In particular, satisfac-

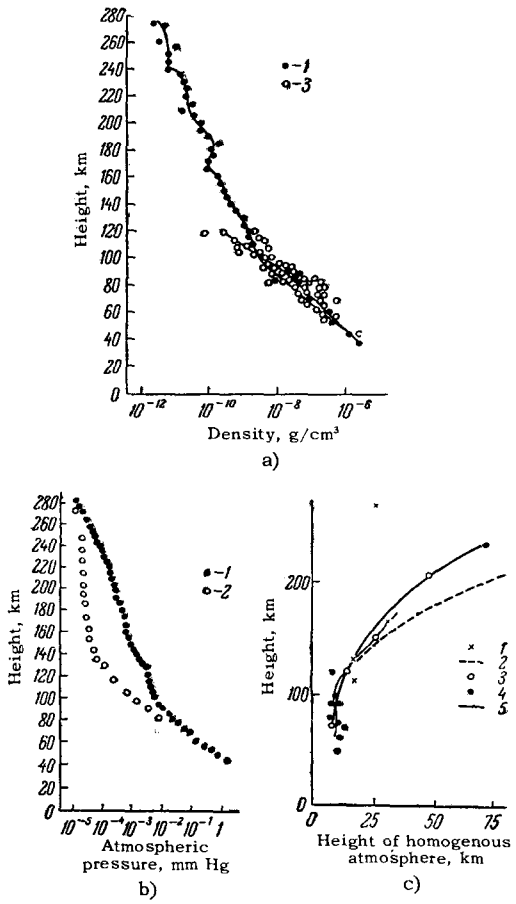

FIG. 55. Average altitude dependence of the density ρ, pressure p, and height of the homogenous atmosphere H: from data of twilight sounding – curves 1, from durations of auroras – curves 2, from meteor observations – curves 3, from data on ionospheric measurements – curves 4, and (Fig. 55a) average – curve 5.

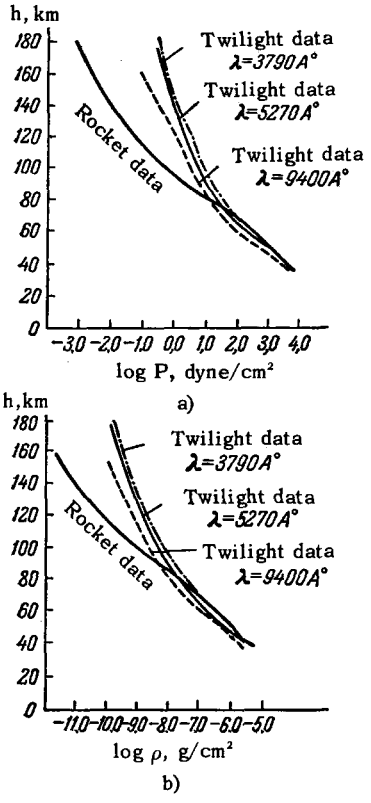

FIG. 56. Comparison of altitude dependences of the pressure and air density as obtained by twilight and rocket measurements.

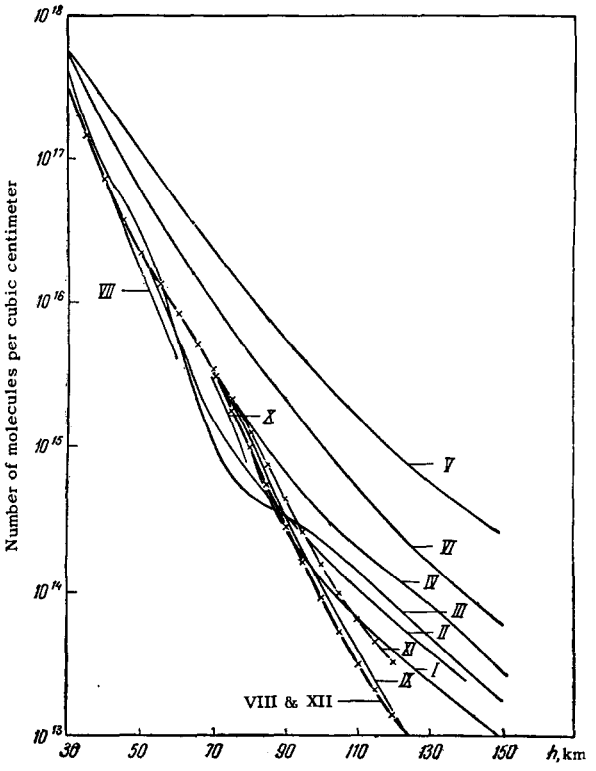

FIG. 57. Comparison of data on the altitude variation of the atmospheric density as obtained from twilight and rocket measments. I – Megrelishvili and Khvostnikov[202]; II – Link[173]; III – Fesenkov[4]; IV – Ljunghall[16]; V – Link[131]; VI – Chiplenkar[62]; VII – Hulbert[45]; VIII – standard NACA atmosphere; IX – Grimminger; X – Heavens et al (V-2 rockets); XI – Ashburn (first approximation); XII – Ashburn (second approximation).

tory agreement is observed between the data extracted from measurements of the brightness of the twilight sky without corrections for double scattering, and data of rocket measurements as summarized by H. Kahlmann [204] up to heights on the order of 90 km, along with a sharp disparity with these data for greater altitudes (Fig. 56). However, this discrepancy disappears if one takes into account the corrections necessitated by the background of the double scattering (see Fig. 53).

The third investigation was carried out in 1952 by E. Ashburn [59]. On the basis of thorough measurements of the brightness and polarization of the light of the twilight sky at the zenith and in the sunset segment, and with allowance for many factors, which were not always taken into account by other investigators, Ashburn, by means of a procedure which is not quite clear from the description, has obtained the brightness of the doubly scattered light as a function of ζ and, after introducing corresponding corrections, obtained the altitude variation of the molecule concentration (molecular scattering was assumed). In Fig. 57 the data of E. Ashburn are compared with the results of many other twilight measurements, and also rocket measurements as well as with the standard NACA atmosphere. Again, the agreement extends to altitudes on the order of 120 km, if secondary scattering is taken into account, and again the agreement disappears above 80–90 km, if they are not taken into account, while account of the secondary scattering does not make any essential changes below 80 km. Thus, there are all grounds for assuming that upon suitable formulation and reduction of the twilight observations, they are capable of yielding reliable data on the high layers of the atmosphere.

In the next section we shall see that the possibilities of the twilight method have not yet been exhausted and that the data obtained with its aid admit of appreciable refinement.

12. DIFFERENTIAL METHOD OF SOLVING THE INVERSE PROBLEM AND THE METHOD OF EFFECTIVE HEIGHT OF THE EARTH'S SHADOW

An approximate solution of the inverse problem of twilight theory, starting from the concept of the twilight layer, is based on the requirement of a rapid decrease of the scattering coefficient with altitude. At high altitudes, however, this drop slows down rapidly, and the twilight layer extends over many tens of kilometers, which leads to an increase in the uncertainty of its height, that is, to a decrease in the resolving power of the method of the twilight

sounding. Moreover, this method in its initial variant cannot be applied to twilight luminescence (say of sodium), since the concentration of the luminescent substance has an entirely different altitude variation. It is therefore more rational to use a different approximate solution of the inverse problem, proposed in 1946 by G. V. Rozenberg [50,137] This solution has, in particular, the advantage that the constant component of the brightness of the twilight sky, that is, the contribution of the glow of the night sky and the illumination from terrestrial sources are automatically eliminated from the calculations.

If we differentiate (72) with respect to ζ with z constant and recognize that

$$\left(\frac{dy}{d\zeta}\right)_h \cong -\frac{1}{\gamma}\frac{dH}{d\zeta} \cong R\cos\zeta,$$

we obtain

$$\frac{dI}{d\zeta} - I_0\omega P^m mR\cos\zeta \int_0^\infty D(h)\frac{dT}{dy}\left(\frac{h-H}{\gamma}\right)dh. \qquad (77)$$

Using further the approximation (43) and the theorem of the mean, we can readily arrive at the relation

$$D(\tilde{H}) = \frac{\left(\frac{dI}{d\zeta}\right)_z}{I_0\omega_0 P^m m k\zeta\gamma}, \qquad (78)$$

where $\tilde{H} = H + \gamma\tilde{y}$ is a certain height lying between H + a and H + a + b, and $\tilde{y} \cong \tilde{y}_n$ under sensible assumptions concerning the altitude variation of D and the absence of selective absorption (y differs from y_n by not more than ±5 km). It is easy to see that the transition from (72) to (78) corresponds to a transition from scanning with an apparatus function T, of the type shown in Fig. 32, to scanning with approximately symmetrical apparatus function dT/dy of the type of Fig. 58, while the transition to the approximation (43) corresponds to a transition from the continuous curve on Fig. 58 to the dashed curve. From the general theory of the apparatus function (see, for example, [205]) it follows that the spatial frequencies with period smaller than $\Delta y = b$ are suppressed upon scanning. However, whereas the higher spatial frequencies are lost without trace, the first harmonic can be reconstituted to some degree.

As applied to (78), if we retain the approximation (43) with b = e/K and put $\tilde{y} = y_n$, that is, $\tilde{H} = \overline{H}$, then the theory leads to the following expression (cf. [205])

$$D(\overline{H}) = \frac{\left(\frac{dI}{d\zeta}\right)_H + \frac{1}{3}\left\{\left(\frac{dI}{d\zeta}\right)_H - \frac{1}{2}\left[\left(\frac{dI}{d\zeta}\right)_{H+\gamma\frac{\Delta y}{2}} + \left(\frac{dI}{d\zeta}\right)_{H-\gamma\frac{\Delta y}{2}}\right]\right\}}{I_0\omega_0 P^m m\cos\zeta\cdot\gamma}. \qquad (79)$$

The first term coincides here with (78), while the second takes into account a correction which can be readily obtained graphically.

In fact, if we plot $dI/d\zeta$ as a function of H (or $\overline{H}$) and draw a chord joining the points at $H + \gamma\Delta y/2$ and $H - \gamma\Delta y/2$, then the distance between the $dI/d\zeta$ curve at the point H and the middle of the chord will correspond to the square brackets. Figure 59 shows an example of introducing such a correction by the chord method [117], as applied to the twilight flash of sodium. By specifying the altitude dependence of the concentration of N of the sodium, that is, D(h) (continuous curve) and by specifying the function T(y), D. Hunten calculated $dI/d\zeta$ as a function of $\tilde{h}$ (dashed curve), and then used the method of chords, that is, formula (79), to reconstitute from it the altitude curve of N (crosses). Such a correction turns out to be quite effective and almost doubles the resolving power of the method.

A modification of the differential method described above for the solution of the inverse problem of twilight theory is the method of effective height of the earth's shadow, developed by the author and having, from our point of view, major advantagee both in the sense of further increasing the resolving power and because it makes it possible to exclude

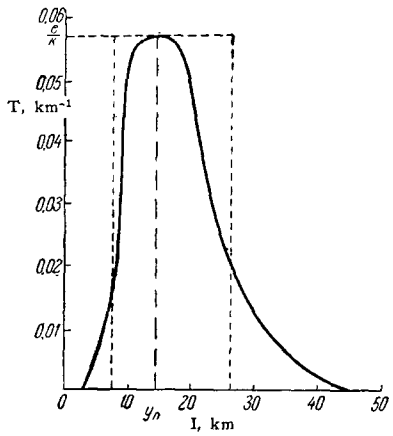

FIG. 58. Typical plot of dT/dy against y outside of the region of selective absorption (it corresponds to the case of Fig. 32).

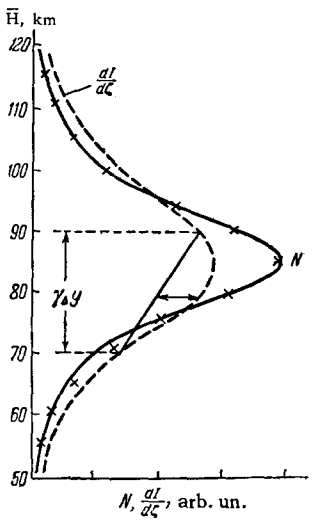

FIG. 59. Illustration of the use of the chord method for the refinement of the altitude dependence of D(h).

automatically the effects of double scattering, which are not taken into account at all in the methods described above (when the latter are used it is necessary first to get rid of the contribution of the double scattering, for example by the method of V. G. Fesenkov; see Sec. 10). The starting point of this method is relation (51), which with account of the brightness I_2 of the secondarily scattered light assumes the form

$$I\left(z, \zeta, \frac{A}{\lambda}\right) = I_0(\lambda)\omega_0 P^{m(z)}(\lambda) m(z) \tau'_p(\overline{H}) + I_2. \quad (80)$$

Inasmuch as P is subject to appreciable variations and cannot be measured accurately with any degree of reliability, it becomes necessary to reduce its influence on the result as much as possible. This can be done, for example, on high mountains or in the near-zenith region of the sky (m is then close to 1). The latter requirement improves also the accuracy with which the air mass is determined (see Sec. 5). In addition to this, since P can vary over the sky [26], it is desirable to concentrate the observations in a relatively small area of the latter.

The contribution of the doubly scattered light to (73) depends strongly on ζ and λ, but its dependence on z and A is relatively small, particularly in the near-zenith region (compare with Sec. 10). At the same time, for small z, when the double-scattering angle is close to 90°, the indicatrix effect should also be relatively small. Therefore the near-zenith region of the sky is most favorable for the measurements.

Further, since the double scattering during the period of total twilight occurs essentially in a layer which is already quite high above the earth's surface, we can assume with sufficiently good approximation that the brightness of the doubly-scattered light I_2, like the brightness of the singly scattered light, is proportional to mP^m, that is,

$$I_2(\zeta, z, A, \lambda) = I_0(\lambda)\omega_0 P^m m b(\zeta, z, A, \lambda), \quad (81)$$

where b is now weakly dependent on the sighting direction, at any rate in the near-zenith region of the sky. Therefore expression (73) can be rewritten in the form

$$I(z, \zeta, A, \lambda) = I_0(\lambda)\omega_0 P^{m(z)}(\lambda) m(z)[\tau'_p(\overline{H}, \lambda) + b(\zeta, z, A, \lambda)]. \quad (82)$$

Let us consider first the conditions existing in the verticals $A = \pm\pi/2$, that is, perpendicular to the solar meridian. According to (13), (10), (7), and (8) we have in the near-zenith region of these verticals

$$\overline{H} = \frac{R(1-\sin\zeta)+\bar{y}}{\sin\zeta},$$

that is, $\overline{H}$ does not depend on z, and the dependence of $\tau'_p(\overline{H})$ on z is determined exclusively by the indicatrix effect, and the scattering angle φ (for which, according to (16), $\cos\varphi = \cos z \cos\zeta$) is also practically independent of z. The conditions for the occurrence of the double scattering are identical at all points of the verticals $A = \pm\pi/2$, that is, b does not depend on z. In other words, when $A = \pm\pi/2$ the quantities contained in the square brackets of (82) can be considered to be independent of m. This means that I(z) does not contain in this case any more information on $\tau'_p(\overline{H})$, $\overline{H}$, or b than I(z = 0). It does contain, however, additional information concerning the value of P and can be used for its measurement. In fact, it follows from (82) that

$$\tau^* = \frac{\ln\sec z + \ln I(z=0, \zeta, \lambda) - \ln I(z, A=\pm\pi/2, \zeta, \lambda)}{\sec z - 1}, \quad (83)$$

where for the near-zenith region of the sky we have assumed m = sec z, it being desirable to have sec z − 1 small (see $z \lesssim 1.5$–2) and to make the measurements in both verticals.

Let us turn now to the solar meridian, again confining ourselves to the near-zenith region of the sky. We introduce the notation

$$B = \frac{I}{I_0\omega_0 P^m m}. \quad (84)$$

Then from (82) we have $B = \tau'_p + b$ and, taking (50) into account,

$$\frac{dB}{d\zeta} = -D\frac{d\overline{H}}{d\zeta} + \frac{db}{d\zeta}, \quad (85)$$

where according to (9), (7), and (8) we have

$$\frac{d\overline{H}}{d\zeta} = -\frac{R\cos\zeta\cos z}{\sin(\zeta-z)} - \frac{\overline{H}\cos(\zeta-z)}{\sin(\zeta-z)}, \quad (86)$$

and

$$\frac{dB}{dz} = -D\frac{d\overline{H}}{dz} + \frac{db}{dz}, \quad (87)$$

where

$$\frac{d\overline{H}}{dz} = \frac{H\cos\zeta}{\sin(\zeta-z)\cos z}. \quad (88)$$

In the near-zenith region of the sky, the second term in (86) is much smaller than the first, and can be neglected. If furthermore we neglect $db/d\zeta$, then (85) assumes a form equivalent to (78). We have already seen that this expression is essentially the basis of the methods used to solve the inverse problem, and in the best case one first introduces a correction for the secondary scattering (say by the method of V. G. Fesenkov or on the basis of theoretical estimates). Therefore the quantity $db/d\zeta$ is not small, and the error of the method is essentially determined in exactly the way allowance is made for this quantity.

We note incidentally that if the contribution of the secondary scattering is small or accounted for, then relations (85) and (88) can be used to determine $\overline{H}(\zeta, \lambda)$. In fact, putting $db/d\zeta = db/dz = 0$ and dividing (87) by (85) we obtain with account of (86) and (88)

$$\overline{H} = -R\cos^2 z \frac{dB/dz}{dB/d\zeta}. \quad (89)$$

However, if the role of the secondary scattering is not known beforehand and if it is not small, a more effective method is one based on the smallness of db/dz as compared with $Dd\overline{H}/dz$, particularly in the vicinity of the zenith.

Let us consider two points of the solar meridian with $z = \pm\delta$, where $\delta \ll 1$. Expanding $B(z)$ in powers of z and using (87), in which we neglect db/dz, we obtain without difficulty

$$D(\overline{H})\,\overline{H} = \frac{I(-\delta) - I(+\delta)}{2I_0\omega_0\delta P}\tan\zeta. \qquad (90)$$

Starting from the foregoing considerations, the value of δ should not exceed approximately 20°. Excessively small values of δ are likewise not very useful, owing to the weak dependence of $\overline{H}$ on z, and can be chosen only if specialized apparatus is used, such as described in [64,116].

If we disregard the investigations of Rundle, Hunten, and Chamberlain [116], which pertain especially to the twilight flash of sodium, the only measurements carried out in accordance with the corresponding procedure are those of R. Karandikar [64], who published, unfortunately, only one of the experimental relations he obtained (Fig. 60). The measurements were carried out with the aid of a special differential photometer, which directly yielded the intensity difference $\Delta I = I(+\delta) - I(-\delta)$ as a function of ζ for $\delta = 6°$. The corresponding values of ΔI (in W/m^2sr) referred to a spectral interval of 1μ (the measurements were made with interference optical filters), are plotted along the ordinate axis of Fig. 60.

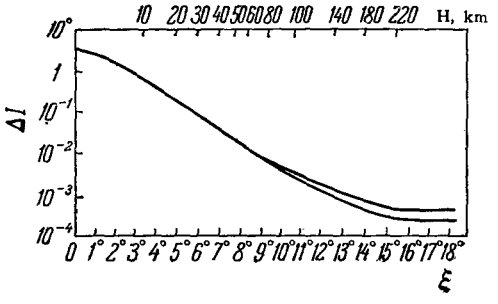

FIG. 60. Example of the dependence of $\Delta I = I(+\delta) - I(-\delta)$ on ξ.

Unfortunately, the author, who identified the effective height of the earth's shadow $\overline{H}$ with the height of the geometrical shadow H, does not present the details necessary to use calculations by means of (90), but the relative course of $\overline{H}$ for the sensible assumption $y_n \cong 25$—30 km is in good agreement with the rocket data shown in Fig. 57. (When $\overline{H}$ is replaced by H no agreement is obtained, this being apparently the reason why Karandikar refrained from interpreting his data.) The splitting of the curves for different λ at $\zeta \gtrsim 100°$ is due in all probability to the glow of the night sky, which begins to pass through the veil of the scattered light and which was not taken into account by Karandikar.

The main source of errors in the determination of

$$G(\overline{H}) = D(\overline{H})\,\overline{H} \qquad (91)$$

is nevertheless the neglect of the contribution of the double scattering. An estimate shows that this error can in some cases reach 25—30 percent.

Were the value of $\overline{H}$ to be known, then (90) would solve the inverse problem completely. Actually, however, $\overline{H}$ can vary (to be sure, in rather narrow limits, see Sec. 8), and the need arises for refining it in each specific case. In this method, the error in the determination of $\overline{H}$ not as a factor but as an argument of the function $D(\overline{H})$ becomes particularly significant, since the dependence of D on $\overline{H}$ is quite strong. From general considerations, connected with the theory of the apparatus function, one cannot expect beforehand the value of $\overline{H}$, which depends in particular in the form of the function $D(\overline{H})$, to be determined with an error less than approximately ±3 km, which corresponds to an uncertainty in the determination of D at the given geometrical height on the order of a factor close to 2. Better accuracy can not be expected in general from the twilight sounding of the atmosphere. This estimate, however, pertains to the absolute value of D(h), but not to the character of the altitude variation of D(h), which can be determined, as we have seen, with an error on the order of 25—30 per cent.

Knowledge of $G(\overline{H})$ as a function of H enables us to find also the value of b(H). It is easy to see that

$$G(\overline{H})\,d\ln\overline{H} = d\tau'_p(\overline{H}),$$

and since

$$d\ln\overline{H} \cong \frac{dH}{\overline{H}} = \frac{dH}{H+\bar{y}},$$

the optical density of the atmosphere above the level $\overline{H}$ is equal to

$$\tau'_p(H+\bar{y}) = \int_H^\infty \frac{G(H)}{H+\bar{y}}\,dH, \qquad (92)$$

where G is already considered as a function of the height of the geometrical shadow H. Since $b(H) = B(H) - \tau'_p(H+\bar{y})$, we have according to (84), for $z = 0$,

$$b(H,\lambda) = \frac{I(H,\lambda)}{I_0\omega_0 P} - \int_H^\infty \frac{G(H)}{H+\bar{y}}\,dH, \qquad (93)$$

or

$$\frac{I_2(H,\lambda)}{I_1(H,\lambda)} = \frac{b(H)}{\tau'_p(H+\bar{y})} = \frac{I(H,\lambda)}{I_0\omega_0 P\tau'_p(\overline{H}+y)} - 1. \qquad (94)$$

During the period of total twilight $\bar{y}$ has the same order of magnitude as H, particularly in the short-wave region of the spectrum. It is therefore not permissible to neglect $\bar{y}$ in the denominator. How-

ever, the easily obtainable estimate of $\bar{y}$ accurate to about 5 km is generally speaking sufficient. Inasmuch as $\tau'_p(H+\bar{y})$ is determined in this case with an error on the order of 30—40 per cent, the error in the determination of I_2/I_1 will reach 60—80 per cent which, incidentally, is sufficient to determine the interval of heights within which formula (90) remains valid. We note also that the error in determining the quantity $db/d\zeta$ will in this case be much less. This enables us to use the thus obtained value of $db/d\zeta$ to take into account the role of secondary scattering in formulas (89) and (78)—(79), which leads to a more accurate value of $\bar{H}$ and to an independent check on $D(\bar{H})$ against the temporal variation of the sky brightness.

Relations (51), (78), (79), (89), (90), (93), and (94) remain in force also if we operate not with the intensities I but with the Stokes parameters S_i [3,206], by merely replacing I with S_i. Inasmuch as the brightness I, the degree of polarization p, the degree of ellipticity q, and the angle ψ_0 of rotation of the plane of predominant polarization are connected with S_i by the relations

$$I=S_1,\ p=\frac{\sqrt{S_2^2+S_3^2}}{S_1},\quad q=\frac{S_4}{S_1},\quad \tan 2\psi_0=\frac{S_3}{S_2}, \tag{95}$$

the formulas (92) and (93) enable us to determine separately the polarization of the singly and doubly scattered light as a function of the height $\bar{H}$, while formulas (78), (79) and (90) yield the first column of the scattering matrix [3,26,206] of the air at the altitude $\bar{H}$.

In conclusion we note that the use of the results of Sec. 8 enables us also to propose several methods for determining the height of the effective shadow of the earth $\bar{H}$ or the value of $\bar{y}$ by comparing plots of $G(\zeta)$ for different z but identical ζ, or G(H) for different z but identical H.

The analysis presented above has shown that most twilight phenomena can be qualitatively explained by taking only single scattering of light into account, and that double scattering plays a role of an appreciable but accountable correction.

At the same time the analysis has shown that if the necessary type and amount of information is obtained regarding the brightness and polarization of the twilight sky, it becomes possible to extract, with sufficient degree of reliability, many important data on the state and structure of the high layers of the atmosphere in the altitude interval from approximately 20 to approximately 120 km. By the same token, there is a possibility of investigating not only the "climate," but also the "weather," of the high layers of the atmosphere by measurements carried out from the earth's surface. In this case the reliability and the accuracy of the obtained data are practically no worse than what is attainable with modern methods of rocket sounding. This makes timely the development of an extensive regularly operating twilight service network, with a unified operating program, as well as direct comparison of the data of twilight sounding of the atmosphere with data of rocket sounding, obtained at the same geographical point and at the same time.

[1] See, e.g., F. Rozenberger, Istoriya fiziki (History of Physics), p. I, ONTI, 1933.
[2] Bezold, Pogg. Ann. 123, 240 (1863).
[3] G. V. Rozenberg, UFN 71, 173 (1960), Soviet Phys. Uspekhi 3, 346 (1960).
[4] V. G. Fesenkov, Tr. Gl. Rossiĭskoĭ astrofiz. observatorii (Trans. Main Russ. Astrophys. Observ) 2, 7 (1923).
[5] P. P. Feofilov, Izv. AN SSSR, ser. geogr. i geofiz. 6, 290 (1942).
[6] N. B. Divari, ibid. 3 (3), 242 (1949).
[7] W. Brunner, Publ. d Eidgenössischen Sternwarte in Zürich, Bd. 6, 1935.
[8] V. V. Sharonov, Tablitsy dlya rascheta prirodnoĭ osveshchennosti i vidimosti (Tables for the Calculation of Natural Illumination and Visibility), AN SSSR, 1945.
[9] P. Kalaja, Die Zeiten von Sonnenscheinen, Dämmerung und Dunkelheit in verschiedenen Breiten, Helsinki, 1958.
[10] V. V. Sharonov, DAN SSSR 42, 310 (1947); Trudy, Jubilee Science Session, Leningrad State Univ., 1948, p. 47.
[11] H. Kimball, Moth. Wether Rev. 42, 650 (1914); 44, 12, 614 (1916); Trans. Illumin. Eng. Soc. Cleveland, 1961.
[12] F. Schmid, Sirius 55, 95 (1921); 56, 1 (1922).
[13] K. Kahler, Meteorol Zs. 44, 212 (1927).
[14] N. N. Kalitin, Gerl. Beitr. Geophys. 24 (1930).
[15] I. N. Yaroslavtsev, Zh. geofiz. 3, (2), 222 (1933); Gerl. Beitr. Geophys. 29 (1931).
[16] A. Ljunghall, The Intensity of Twilight and Its Connection with the Density of the Atmosphere, Meddelande Från Lunds Astronom. Observ., Sec. 11, No. 175, Hälsingborg, 1949.
[17] N. N. Kalitin, Meteor. i gidrol. (Meteorology and Hydrology) No 11, 93 (1940).
[18] I. N. Yaroslavtsev, J. Geophys. and Meteor. 5 (1), 1 (1928); 6 (2), 143 (1929).
[19] F. Schembor, Gerl. Beitr. Geophys. 28, 279 (1930).
[20] P. Grunner und H. Kleinert, Die Dammerungerscheinungen, Hamburg, 1927.
[21] J. M. Pertner, F. M. Exner, Meteorologische Optik, Wien, 1910.
[22] P. Brounow. Atmospheric Optics, Gostekhizdat, 1924.
[23] N. I. Kucherov, Izv. AN SSSR, ser. geogr. i geofiz. 11 (6), 465 (1947).

[24] M. Minnaert, The Nature of Light and Colour in the Open Air, Dover, N. Y., 1954.
[25] A. D. Zamorskiĭ, in coll. Aktinometriya i atmosfernaya optika (Actinometry and Atmospheric Optics), Gidrometeoizdat, 1961, p. 107.
[26] Georgievskiĭ, Driving, Zolotavina, Rozenberg, Feĭgel'son, and Khazanov, Prozhektornyĭ luch v atmosfere (Projector Beam in the Atmosphere), edited by Prof. G. V. Rozenberg, AN SSSR, 1960.
[27] C. Dorno, Himmelshelligkeit, Himmelspolarisation und Sonnenintensität in Davos 1911 bis 1918. Veroffent d. Preuss. Meteorolog. Inst., No. 303, 1919.
[28] Bauer, Donjon, Langevin, Compt. rend. **178**, 2115 (1924).
[29] J. Dufay, Bull. Observ. Lyons **10**, No. 9 (1928).
[30] R. J. Rayleigh, Proc. Roy. Soc. **A124** (795), 395 (1929).
[31] V. G. Fesenkov, Astron. zhur. **7** (2), 100 (1930).
[32] F. Schembor, Gerl. Beitr. Geophys. **29**, 69 (1931).
[33] K. Graff, Sitz. Ber. Acad. Wiss. Wien **140** (11a), 513 (1931).
[34] K. Graff, Sitz. Ber. Acad. Wiss. Wien **141** (11a), 509 (1932).
[35] K. Graff, Sitz. Ber. Acad. Wiss. Wien **141** (11a), 509 (1932).
[36] W. M. Smart, Mont. Not. Roy. Astron. Soc. **93** (6), 441 (1933).
[37] V. G. Fesenkov, Izv. AN SSSR, OMEN, 1501 (1934).
[38] F. Link, J. Observateurs **17**, 161 (1934).
[39] N. M. Shtaude, Photometric Observations of Twilight as a Method of Studying the Upper Atmosphere, Trudy, Commission on the Study of the Stratosphere, USSR Adad. Sci., vol. 1, 1936.
[40] V. I. Chernyaev and M. F. Vuks, DAN SSSR **14**, 77 (1937).
[41] Wirz, Ann. Hydrogr. **63**, 66, 170, 442 (1935); **64**, 33, 473 (1936); **65**, 130, 269 (1937).
[42] W. Smosarsky, Gerl. Beitr. Geophys. 50, 252 (1937).
[43] F. Schmid, Meteorol. Zs. **54**, 10 (1937).
[44] R. Grandmontagne, Compt. rend. **207**, (26), 1436 (1938).
[45] E. O. Hulburt, J. Opt. Soc. Amer. 28 (7), 227 (1938).
[46] A. V. Mironov, Izv. AN SSSR, ser. geogr. i geofiz. No 6, 843 (1940).
[47] Khvostikov, Magid, and Zhubin, ibid. No. 5 (1940).
[48] R. Grandmontagne, Ann. de phys. **16**, 253 (1941).
[49] G. V. Rozenberg, DAN SSSR **36** (9), 288 (1942).
[50] V. V. Rozenberg, Features of the Polarization of Light Scattered by the Atmosphere under Twilight Illumination Conditions, Dissertation (Moscow, 1946).
[51] F. Link, Meteorol. Zs. **61**, 87 (1944).
[52] F. Link, Compt. rend. **222**, 333 (1946).
[53] T. G. Megrelishvili, DAN SSSR 43 (2), 127 (1946).
[54] N. M. Shtaude, Izv. AN Kazakh SSR, ser. astron. i fiz., No 2, 108 (1946).
[55] N. M. Shtaude, DAN SSSR 55 (1), 27 (1947).
[56] N. M. Kopylov, Meteorol. i gidrol. No 2, 3 (1947).
[57] T. G. Megrelishvili, Bull. Abastumani Astrophys. Obs. No 9, 1 (1948).
[58] G. Vaucouleurs, Compt. rend. 232 (4) 342 (1951).
[59] E. V. Ashburn, J. Geophys. Res. 57 (1), 85 (1952).
[60] Koomen, Lock, Packer, Scolnik, Tousey and Hulburt, J. Opt. Soc. Amer. 42, 352 (1952).
[61] N. B. Divari, Izv. AN SSSR, ser. geofiz. No 1, 79 (1952).
[62] M. W. Chiplonkar and J. D. Ranade, Proc. Ind. Acad. Sci. **A18**, 121 (1953).
[63] E. D. Sholokhova and M. S. Frish, DAN SSSR 105 (6), 1213 (1956).
[64] R. V. Karandikar, J. Opt. Soc. Amer. 45 (5), 389 (1955).
[65] T. G. Megrelishvili, Izv. AN SSSR, ser. geofiz., No 8, 976 (1956).
[66] I. Zacharov, Bull. Astr. Inst. Czechosl. 8 (26), 135 (1956).
[67] J. V. Dave and K. R. Romanathan, Proc. Ind. Acad. Sci. **A43** (12), **67** (1956).
[68] E. K. Bigg, Nature **177** (4498), 77 (1956); J. Meteorol. **13** (3), 262 (1956).
[69] T. G. Megrelishvili, DAN SSSR **116**(5), 766 (1957).
[70] B. N. Divari, DAN SSSR **112** (2), 217 (1957).
[71] M. Gadsden, J. Atm. Terr. Phys. **10** (3), 176 (1957).
[72] T. G. Megrelishvili, Izv. AN SSSR, ser Geofiz. No 4, 560 (1958).
[73] N. B. Divari, DAN SSSR **122** (5), 795 (1958).
[74] F. Link, L. Neužil and I. Zacharov, Astron. Inst. Czechosl. Acad. Sci., Publ. No. 38, 1958.
[75] O. D. Barteneva and A. N. Boyarova, Trudy, Main Geophys. Observatory, No 100, 133 (1960).
[76] K. Ya. Kondrat'ev and O. A. Zigel', Vestnik, Leningrad State Univ. No 10, Phys. and Chem. Ser., Issue 2, 45 (1960).
[77] A. Kh. Darchiya, Izvestiya, Main Astronom. Obs. Acad. Sci. USSR, No. 165 (1960).
[78] T. G. Megrelishvili, op. cit. [25], p. 105.
[79] Driving, Rozenberg, and Turikova, ibid. p. 104.
[80] G. Dietze, Paper at the All-union Meteorological Conference, Leningrad, 1961.
[81] F. Volz and R. M. Goody, Twilight Intensity of 20° Elevation, Blue Hill Meteorolog. Observ. Scient. Rep. No. 1, on Contract AF-10-604 (4546), Harvard University, 1960.
[82] F. E. Volz and R. M. Goody, The Intensity of Twilight and Upper Atmospheric Dust, J. Atmosph. Sci. **19** (5), 385 (1962).

[83] W. Smosarsky, Gerl. Beitr. Geophys. 48, 213 (1936).
[84] N. M. Shtaude, Izv. AN SSSR, ser geogr. i geofiz. 13 (4), 307 (1949).
[85] O. V. Vasil'ev, Trudy, Sixth Conf. on Silver Clouds, Riga, 1961, p. 105.
[86] G. V. Rozenberg, op. cit. [25], p. 105.
[87] Chapuis, Compt. rend. 91, 522 (1880).
[88] J. Gauzit, Ann. de phys. 4, 460 (1935).
[89] E. O. Hulburt, J. Opt. Soc. Amer. 43 (2), 113 (1953).
[90] J. Dufay et J. Gauzit, Ann. d'astrophys. 9, 135 (1946).
[91] K. Ya. Kondrat'ev, Luchistaya énergiya Solntsa (Radiant Energy of the Sun), Leningrad, 1954.
[92] V. M. Slipher, Mon. Not. Roy. Astr. Soc. 93, 666 (1933).
[93] H. Garrigue, Compt. rend. 202, 1807 (1936).
[94] G. Courtes, Compt. rend. 231, 62 (1950); M. Dufay, Compt. rend. 233, 413 (1953); Ann. de phys. 8, 813 (1953).
[95] A. B. Meinel, Repts. Progr. Phys. 14, 21 (1951).
[96] P. Berthier, Compt. rend. 236, 1808 (1953); Ann. Geophys. 12, 113 (1956).
[97] A. V. Jones, Nature 178, 276 (1956).
[98] J. Delannoy and G. Weill, Compt. rend. 247, 806 (1958).
[99] J. W. Chamberlain, Ann. Geophys. 14 (2), 196 (1958).
[100] I. A. Khvostikov, Sechenie nochnogo neba (Cross Section of the Night Sky), AN SSSR, 1948.
[101] J. Bricard et A. Kastler, Ann. Geophys. 1 (1), 1 (1944).
[102] J. Blamont et A. Kastler, Ann. Geophys. 7 (2), 73 (1951).
[103] D. M. Hunten, J. Atm. Terr. Phys. 5, 44 (1954).
[104] D. H. Hunten and G. G. Shepherd, J. Atm. Terr. Phys. 5 (1954).
[105] T. M. Donahue and R. Resnick, Phys. Rev. 98 (6), 1622 (1956).
[106] T. M. Donahue and A. Foderare, J. Geophys. Rev. 60 (1), 75 (1955).
[107] J. E. Blamont, T. M. Donahue and Stull, Ann. Geophys. 14 (3), 253 (1958).
[108] J. E. Blamont, T. M. Donahue and W. Weber, Ann. Geophys. 14 (3), 282 (1958).
[109] J. W. Chamberlain, J. Atm. Terr. Phys. 9, 75 (1956).
[110] J. W. Chamberlain and B. J. Negaard, J. Atm. Terr. Phys. 9, 169 (1956).
[111] D. M. Hunten, J. Atm. Terr. Phys. 9 (4), 179 (1956).
[112] J. W. Chamberlain, D. M. Hunten and J. E. Mack, J. Atm. Terr. Phys. 12 (2), 153 (1958).
[113] J. C. Brandt and J. W. Chamberlain, J. Atm. Terr. Phys. 13, 90 (1958).
[114] T. M. Donahue and D. M. Hunten, J. Atm. Terr. Phys. 14, 165 (1958).
[115] E. A. Lyttle and D. M. Hunten, J. Atm. Terr. Phys. 16, 236 (1959).
[116] H. N. Rundle, D. M. Hunten and J. W. Chamberlain, J. Atm. Terr. Phys. 17, 205 (1960).
[117] D. M. Hunten, J. Atm. Terr. Phys. 17, 295 (1960).
[118] T. M. Donahue and J. E. Blamont, Symposium on Astronomy, Copenhagen, 1960.
[119] S. V. Venkateswaran, J. S. Moore, A. T. Krueger, J. Geophys. Res. 66 (6), 1751.
[120] See, e.g., N. A. Prokof'eva, Atmosfernyĭ ozon (Atmospheric Ozone), AN SSSR, 1951.
[121] F. W. Götz, Gerl, Beitr. Geophys. 31, 119 (1931).
[122] Rodionov, Pavlova, and Stupnikov, DAN SSSR 19, 43 (1938).
[123] C. Dorno, Physik d. Sonnen- und Himmelstrahlung, Braunschwieg, 1919.
[124] F. Roggenkamp, Meteorolog. Zs. 50, 111 (1933).
[125] Knopf, Beitr. Phys. frei. Atmosph. 8, 57 (1919).
[126] A. Wegener, Optik d. Atmosphäre, Miller-Poullets Lehrbuch d. Phys., Bd. 5, Physik d. Erde, Braunschweig, 1928.
[127] Ch. Jensen, Gerl. Beitr. Geophys. 35, 166 (1932).
[128] Ch. Jensen, Meteorol. Zs. 54, 90 (1937).
[129] F. Busch und Ch. Jensen, Tatsachen und Theorien der atmosphärischen Polarisation, 1911.
[130] Ch. Jensen, Himmelstrahlung, Handb. d. Physik, 1928.
[131] Z. Sekera, Advances Geophys 3 (4), 43, (1956).
[132] G. V. Rozenberg, Izv. AN SSSR, ser. geogr. i geofiz. 13, 154 (1949).
[133] I. A. Khvostikov and A. I. Sevchenko, DAN SSSR 4 (8), 347 (1936).
[134] I. A. Khvostikov, UFN 19, 49 (1938).
[135] Bovsheverov, Mironov, Mikhaĭlin, Morozov, Ponizovskiĭ, Sokolov, and Khvostikov, Izv. AN SSSR, ser. geogr. i geofiz. No 5, 657 (1940).
[136] Z. L. Ponizovskiĭ and G. V. Rozenberg, DAN SSSR 37, 249 (1942).
[137] G. V. Rozenberg, Trudy, Geophys. Inst. Acad. Sci. USSR, No 12 (130), 35 (1948).
[138] R. Robley, Ann. d. geophys. 6 (3), 191 (1950).
[139] P. Grunner, Beitr. z. Phys. frei. Atmosph. 8, 120 (1919).
[140] F. Link, Compt. rend. 196, 251 (1933).
[141] F. Link, Compt. rend. 199, 303 (1934).
[142] F. Link, J. Observateurs 17, 41 (1934).
[143] F. Link, Mem. Inst. Nat. Meteorol. Pologne, No. 5, 55 (1935).
[144] J. Sweer, J. Opt. Soc. Amer. 28, 327 (1938).
[145] F. Link, Z. Sekera, Publ. Pražské statni Hvésdárny 14, 1 (1940).
[146] F. Link, Mitteilungen und Beobachtungen d. Tschechischen Astron. Ges., Praha, No. 6, 1 (1941).
[147] F. Link, Publ. Pražské statni Hvésdárny 18, 1 (1947).
[148] V. G. Fesenkov, Astron. zh. 32 (3) 265 (1955).
[149] V. G. Fesenkov, DAN SSSR 101 (5), 845 (1955).

[150] V. G. Fesenkov, Astron. zh. 36 (2), 201 (1959), Soviet Astronomy 3, 207 (1959).
[151] Lugeon, Tables crepuculaires, Warszawa, 1934, p. 438.
[152] G. V. Rozenberg, Izv. AN SSSR, ser. geogr. i geofiz. 13 (5), 383 (1949).
[153] K. W. Allen, Astrophysical Quantities (Transl.) IL, 1960.
[154] N. M. Shtaude, Izv. AN Kazakh SSR No 32, Astron. and Phys. Series, Issue 2, 22 (1946).
[155] N. M. Shtaude, Izvestiya, Lesgaft Science Inst. 15, Nos. 1 and 2, (1929).
[156] F Link, L. Neuzil, Publ. Astron. Inst. Czechosl. 9 (1), 28 (1957).
[157] G. V. Rozenberg, DAN SSSR 145 (4), 775 (1962), Soviet Phys. Doklady 7, 706 (1962).
[158] D. O. Connell, Endeavoure 20 (79), 131 (1961).
[159] G. V. Rozenberg, DAN SSSR 145 (6), 1269 (1962).
[160] G. P. Gushchin, Izv. AN SSSR, ser geofiz. No. 8, 1113 (1962).
[161] S. F. Rodionov, Izv. AN SSSR, ser. geograf. i geofiz. 14 (4), 334 (1950).
[162] Rodionov, Pavlova, Rdultovskaya, and Reĭnov, ibid. No 4, 135 (1942).
[163] E. A. Polyakova, Trudy, Main Geophys. Obs. No 19, 185 (1950).
[164] J. Dufay, Compt. rend. 222, 691 (1947).
[165] E. A. Polyakov, Izv. AN SSSR, ser. geogr. i geofiz. 3 (3), 247 (1949).
[166] D. Deirmendjian, Arch. Meteorol. Geophys. Biokl 6, 452 (1956).
[167] N. M. Shtaude, Izv. AN Kazakh SSR, ser astron. i fiz. No 2, 97 (1946).
[168] N. M. Shtaude, Izv. AN SSSR, ser. geogr. i geofiz. 11 (4), 349, (1947).
[169] V. G. Fesenkov, Trudy, All-Union Acad. Sci. Conference on the Study of the Stratosphere, vol. 1, 1960.
[170] N. M. Shtaude, ibid.
[171] F. Link, Compt. rend. 200, 78 (1935).
[172] F. Link, Meteorol. Zs. 59 (1), 7 (1942).
[173] F. Link, Bull. Astron. Inst. Czechosl. 1 (9), 135 (1949).
[174] F. Link, Mem. Soc. Roy. Scei. Liege 12 (1—2), 151, 155 (1952).
[175] R. P. Gruner, Ergebn. d. kosm. Phys. 3, 113 (1938); Gerl. Beitr. Geophys. 46, 202 (1935); 50, 143 (1937); 51, 174 (1937).
[176] J. Lambert, Photometrie (1760), Zweites Heft, Teil III, IV, V (Ostwald's Klassiker, No. 3, Leipzig, 1892), p. 96-112.
[177] C. Raman, Molecular Scattering of Light, 1922.
[178] V. L. Ginzburg and N. N. Sobolev, DAN SSSR 40 (6), 316 (1943).
[179] Rozenberg, Khvostikov, and Yudalevich, DAN SSSR 59 (7), (1948).
[180] N. M. Shtaude, Izv. AN SSSR, ser. geogr. i geofiz. 12 (5), 387 (1948); DAN SSSR 59 (7), 1281 (1958) and 64 (6), (1949).
[181] F. F. Yudalevich, DAN SSSR 75 (6), (1950); Izv. AN SSSR, ser. geogr. if geofiz. No 6 (1950).
[182] F. F. Yudalevich, DAN SSSR 44 (8), (1947).
[183] R. Robley, Ann. Geophys. 8, 1 (1952).
[184] J. V. Dave, Proc. Ind. Acad. Sci. 43 (1956).
[185] T. Sato, Sci. Rep. Tohoku Univ., Ser. 5, Geophys. 3 (3), 114 (1951); J. Meteorol. Soc. Japan 30 (1), 1 (1952); J. Meteorol. Soc. 39 (3) (1961).
[186] F. F. Yudalevich, Izv. AN SSSR, ser. geofiz. No 8, 1199 (1961).
[187] V. G. Fesenkov, Astronom. zh. 33 (5), 708 (1956).
[188] F. F. Yudalevich, Izv. AN SSSR, ser. geofiz. No 7, 862 (1956).
[189] J. L. Soret, Ann. chim. et phys. 503 (1888); Arch. Sci. phys. et nature 20, 439 (1958).
[190] F. Ahlegrimm. Jahrb. d. Hamburg, Wiss. Austalten 32 (1914).
[191] I. I. Tikhanovskiĭ, Phys. Z. 28, 252 (1927).
[192] S. Chandrasekhar, Transport of Radiant Energy (Russ. Transl.), IIL, 1953.
[193] V. V. Sobolev, Perenos luchistoĭ energii v atmosferakh zvezd i planet (Transport of Radiant Energy in Atmospheres of Stars and Planets) Gostekhizdat, 1956.
[194] E. S. Kuznetsov, Izv. AN SSSR, ser. geograf. i geofiz. 9 (3), 204 (1945).
[195] Feigel'son, Malkevich, Kogan, Astroshenko, et al. Raschet yarkosti sveta v atmosfere pri anizotropnom rasseyanii (Calculation of the Brightness of Light in the Atmosphere in Anisotropic Scattering) AN SSSR, part I, 1958, part II, 1961.
[196] K. S. Shifrin and N. P. Pyatovskaya, Tablitsy naklonnoĭ dal'nosti vidimosti i yarkosti dnevnego neba (Tables of Slant Range Visibility, and Brightness of the Daytime Sky), Gidrometeoizdat, 1959.
[197] M. S. Chandrasekhar and D. Elbert, Trans. Amer. Phil. Soc. 44, 643 (1958).
[198] K. L. Coulson, J. V. Dave, Z. Sekera, Tables Related to Radiation Emerging from a Planetary Atmosphere with Rayleigh Scattering, Univ. of Cal California, 1960.
[199] S. I. Sivkov, op. cit. [25],.
[200] G. V. Rozenberg, UFN 69, 57 (1959), Soviet Phys. Uspekhi 2, 666 (1960).
[201] V. G. Fesenkov, in collection: Rasseyanie i polyarizatsiya sveta v atmosfere (Scattering and Polarization of Light in the Atmosphere), Alma-Ata 1962, p. 214.
[202] T. G. Megrelishvili and I. A. Khvostikov, DAN SSSR 59 (7), 1283 (1948).
[203] V. L. Ginzburg, DAN SSSR 38 (9), 251 (1954).
[204] H. Kahlmann, in coll. Problemy Sovremennoi fiziki (Problems of Modern Physics), No 4, 1954.
[205] Bracewell, JOSA 45, 873 (1955), Austral. J. Phys. 7, 615 (1954).
[206] G. V. Rozenberg, UFN 56 (1), 77 (1955).
[207] N. B. Divari, op. cit. [201], p. 188.

Translated by J. G. Adashko